

Tesi doctoral presentada per En/Na

Yolanda CÁMARA NAVARRO

amb el títol

**"Estudio funcional de la proteína desacopladora
mitocondrial UCP3 en relación con la apoptosis y
las especies reactivas de oxígeno"**

per a l'obtenció del títol de Doctor/a en

BIOLOGIA

Barcelona, 25 de juliol de 2005.

Facultat de Biologia
Departament de Bioquímica i Biología Molecular



UNIVERSITAT DE BARCELONA



Uncoupling Protein-3 Sensitizes Cells to Mitochondrial-Dependent Stimulus of Apoptosis

LAURENT DEJEAN,¹ YOLANDA CÁMARA,¹ BRIGITTE SIBILLE,² GEMMA SOLANES,¹
AND FRANCESC VILLARROYA^{1*}

¹*Departament de Bioquímica i Biologia Molecular, Universitat de Barcelona, Barcelona, Spain*

²*Laboratoire de Physiologie et Régulations Energétiques, Cellulaires et Moléculaires, Université Claude Bernard-Lyon I, Villeurbanne, France*

The mitochondrial uncoupling protein-3 is a member of the mitochondrial carrier protein family. As a homologue of the thermogenic brown fat uncoupling protein-1, it possesses a mitochondrial uncoupling activity and thus can influence cell energy metabolism but its exact biological function remains unclear. In the present study, uncoupling protein-3 was expressed in 293 cells using the tetracycline-inducible system and its impact on cell bioenergetics and responsiveness to the apoptotic stimulus was determined. The induction of uncoupling protein-3 expression in mitochondria did not lead to uncontrolled respiratory uncoupling in intact cells. However, it caused a GDP-inhibition of state 4 respiration and a GDP-induced repolarization of the inner mitochondrial membrane in the presence of fatty acids, in agreement with its expected physiological behavior as an uncoupling protein (UCP). Uncoupling protein-3 expression did not cause apoptosis per se but increased the responsiveness of the cells to a mitochondrial apoptotic stimulus (i.e., addition of staurosporine in the culture medium). It enhanced caspase 3 and caspase 9 activation and favored cytochrome c release. Moreover, cells in which uncoupling protein-3 expression had been induced showed a higher mitochondrial Bax/Bcl-2 ratio essentially due to enhanced translocation of Bax from cytosol to mitochondria. Finally, the induction of uncoupling protein-3 also increased the sensitivity of mitochondria to open the permeability transition pore in response to calcium. It is concluded that the presence of uncoupling protein-3 in mitochondria sensitizes cells to apoptotic stimuli involving mitochondrial pathways. *J. Cell. Physiol.* 201: 294–304, 2004. © 2004 Wiley-Liss, Inc.

In addition to their established function in energy metabolism, mitochondria have a key role in the control of cell death. Several events are important for signaling apoptotic pathway stimuli from mitochondria, especially the release to the cytosol of proapoptotic factors such as cytochrome c, apoptosis-inducing factor, and Smac/Diablo (Ravagnan et al., 2002). In cytosol, these factors collaborate to induce the caspase cascade and nuclear endonuclease activation, which lead to cell death. Caspase 9 is mainly activated by apoptotic factors of mitochondrial origin, which causes caspase 3 activation, an end-point in the caspase activation cascade (Kuida, 2000). A complex interplay of anti-apoptotic and pro-apoptotic proteins is involved in the mitochondrial control of the activation of apoptotic pathways. Thus, members of the Bcl-2 family modulate apoptosis signaling by acting on mitochondria. For instance, Bcl-2, which interacts with the mitochondrial outer membrane, behaves as an anti-apoptotic factor, whereas Bax acts as a pro-apoptotic factor when it translocates from the cytosol to mitochondria (Antonsson, 2001). The opening of the permeability transition pore (PTP) is another mitochondrial event involved in the commitment to cell death activation. PTP activation brings

about collapse of the proton-motive force and mitochondrial swelling. The pore appears to be formed by a multiprotein channel with components located both in the inner and the outer mitochondrial membranes (Kroemer and Reed, 2000). The bioenergetic status of mitochondria can also alter the activity of the

Laurent Dejean and Yolanda Cámara contributed equally to this work.

Contract grant sponsor: Ministerio de Ciencia y Tecnología. Spain; Contract grant number: SAF2002-03648; Contract grant sponsor: Fundació la Marató de TV3; Contract grant number: 991910; Contract grant sponsor: Instituto de Salud Carlos III, FIS. Ministerio de Sanidad y Consumo; Contract grant number: C03/08.

*Correspondence to: Francesc Villarroya, Departament de Bioquímica i Biologia Molecular, Universitat de Barcelona, Avda Diagonal 645, Barcelona E-08028, Spain.
E-mail: gombau@bio.ub.es

Received 18 June 2003; Accepted 12 January 2004

DOI: 10.1002/jcp.20048

mitochondrial-dependent signaling pathways of apoptosis. For instance, a reduction in the mitochondrial inner membrane potential, elicited by chemical uncouplers, can promote apoptosis (Dispersyn et al., 1999; Armstrong et al., 2001) whereas low doses of chemical uncouplers enhance or protect cells from apoptosis depending on the inducing agent and cell type (Linsinger et al., 1999; Stoetzer et al., 2002). Moreover, also according to the cell type and apoptotic stimulus, respiratory activity can be required (Huang et al., 2001; Nishimura et al., 2001) or not (Jiang et al., 1999) for cytochrome c release upon apoptotic stimuli. Finally, the PTP opening sensitivity is also modulated by the electron flux through the respiratory chain (Fontaine et al., 1998).

The uncoupling proteins (UCPs) are a family of proteins present in the inner mitochondrial membrane that belongs to the super-family of mitochondrial carriers, together with the adenine nucleotide translocase and the phosphate carrier among others (Ricquier and Bouillaud, 2000). UCP1 is preferentially expressed in brown adipocytes and behaves as a natural uncoupler of oxidative phosphorylation. It increases the proton conductance of the mitochondrial inner membrane; its activity requiring fatty acids and being specifically inhibited by GDP (Nicholls et al., 1989). The physiological role of UCP1 is heat production and, by the way, non-shivering thermogenesis in rodents in response to cold environments (Enerback et al., 1997). UCP2 is expressed ubiquitously and appears to be involved in pancreatic beta cell function and sensitivity to infections (Arsenijevic et al., 2000; Zhang et al., 2001). UCP3 is expressed preferentially in skeletal muscle cells and to a minor extent in cardiomyocytes, brown and white adipocytes (Boss et al., 1997; Vidal-Puig et al., 1997). Its expression is dramatically induced in response to metabolic signals related to stress such as an increase of the concentration of free fatty acids in blood (Brun et al., 1999) or due to the action of TNF α (Masaki et al., 1999), as well as in cancer cachexia (Bing et al., 2000) or sepsis (Sun et al., 2003). However, up-regulation of UCP3 in human muscle in response to a high-fat diet is not associated to significant changes in mitochondrial bioenergetics (Hesselink et al., 2003). Although the precise role of UCP2 and UCP3 in mitochondria is still a matter of debate (Schrauwen, 2002; Nedergaard and Cannon, 2003), it is well established that both proteins can act as natural uncouplers of oxidative phosphorylation upon the influence of intracellular activators (e.g., fatty acids and reactive oxygen species) or inhibitors (e.g., GDP and ADP) (Echtay et al., 2001, 2002). However, the possibility that these proteins influence the control of cell death elicited by mitochondria has been poorly explored. According to a micro-array analysis, UCP2 expression is dramatically increased during UV-induced apoptosis in an apoptosis-sensitive murine B lymphoma cell line, but unaffected in a non-sensitive cell line (Voehringer et al., 2000). Recently, the over-expression of UCP2 in HeLa cells has been reported to lead to a form of cell death that is not inhibited by the anti-apoptotic gene product Bcl-2 and that morphologically resembles cellular oncosis (Mills et al., 2002). Other recent reports have indicated that UCP2 over-expression prevents neuronal cell death (Diano et al., 2003; Mattiasson

et al., 2003). However, the potential role of UCP3 in the apoptotic process has not been studied.

We report in this study, the development of a cellular system allowing a conditional expression of functional UCP3 protein in mitochondria. We establish that the induction of UCP3 expression, at a level compatible with a functional physiological behavior, does not lead by itself to apoptosis but sensitizes cells to apoptotic stimuli involving mitochondrial pathways.

MATERIALS AND METHODS

Establishment of doxycycline-regulated UCP3-expressing 293 cell lines

Human UCP3L cDNA (Vidal-Puig et al., 1997) was subcloned into a tetracycline-inducible vector, pTRE (BD Biosciences, San Diego, CA) to obtain pTRE-UCP3. A *HindIII* fragment encoding the full-length long form of human UCP3 was ligated into *EcoRI*-linearized pTRE. 293 Tet-On cells (Clontech), which stably express reverse tetracycline-controlled transactivator, were cotransfected with linearized pTRE-UCP3 and pTK-Hyg (hygromycin-resistant plasmid) using the calcium phosphate procedure. One day after transfection, cells were grown in a medium containing 200 μ g/ml hygromycin. After 14 days, hygromycin-resistant clones were isolated, individually grown, aliquoted, and frozen for storage. To test for doxycycline inducibility of UCP3 expression, cells were expanded in Dulbecco's modified Eagle's medium (DMEM) containing 10% tetracycline-free fetal bovine serum (Clontech) in the presence of 90 μ g/ml hygromycin. Cells were left untreated or treated with various amounts of doxycycline for 48 h. The content of NADH in cells under different treatments was assessed as already reported (Klingenberg, 1974) and the content of ATP was determined using a bioluminescence-based assay and following the instructions of the supplier (ATP Bioluminescence Assay Kit HSII, Roche Diagnostics, St. Cugat del Valles, Spain).

When needed, mitochondrial-dependent apoptosis induction in these cell lines was induced by adding 0.5 μ M staurosporine in the culture medium for 6 h.

Oxygen consumption assays

Cells ($5-15 \times 10^6$) were rinsed with phosphate buffered saline (PBS) and dissociated from the plates by incubation at room temperature with a buffer containing 7.5 mM tri-sodium citrate 2-hydrate, 7 mM KCl, pH 7.4. After centrifugation (2 min, 400g), they were resuspended in 1 ml of DMEM supplemented with 5 mM HEPES, pH 7.4 (respiration medium). Oxygen consumption rates were continuously measured polarographically at 37°C using a Clark oxygen electrode (Rank Brothers, Ltd., Cambridge, UK) connected to a micro-computer giving an on-line display of oxygen concentration in the medium (PicoLog Recorder, Pico Technology, Interworld Electronics, Point Roberts, UK). First, the basal oxygen consumption rate was measured. Thereafter, oxygen uptake was monitored, either in the presence of the protonophoric uncoupler, carbonyl cyanide *m*-chlorophenylhydrazine (CCCP) (0.25–1 μ M), or in the presence of the F₁F₀-ATP synthase inhibitor, oligomycin (10 μ g/ml). In all conditions, single measurement did not exceed 20 min and cell viability, assessed

by the trypan blue exclusion assay, was not significantly changed for incubation times up to 1 h (about 90–95%).

Permeabilization of the cells and determination of cytochrome c oxidase activity

Cells were collected as described above and resuspended in a permeabilization medium (250 mM sucrose, 1 mM EDTA, 50 mM KCl, 2 mM KH_2PO_4 , 25 mM Tris-HCl, pH 7.4). Digitonin, interacting with the cholesterol of the cytoplasmic membrane, was used to permeabilize the cells. To determine the minimal amount required for the complete permeabilization of cells, oxygen consumption with 6 mM succinate and 1 mM ADP was recorded, and the increase in state 3 respiration after the addition of small amounts of digitonin was followed as described elsewhere (Ouhabi et al., 1998). The optimal digitonin concentration for 293 cells and 293-UCP3 clones was established as 25 $\mu\text{g}/\text{ml}$ after 5 min of incubation of the cell suspensions with the detergent. These modalities of permeabilization were used throughout all the study.

For cytochrome c oxidase activity measurements, cells were first permeabilized as described above in the presence of antimycin A (0.25 $\mu\text{g}/\text{ml}$), CCCP (0.25 μM), and ascorbate (1 mM). The reaction was then started by the adding of 0.5 mM of *N,N,N,N'*-tetramethyl-*p*-phenylenediamine (TMPD) and monitored polarographically at 37°C using a Clark oxygen electrode (Rank Brothers, Ltd.) connected to a micro-computer giving an on-line display of oxygen concentration in the medium (PicoLog Recorder, Pico Technology).

Determination of mitochondrial $\Delta\Psi$ variation and state 4 respiration in permeabilized cells

Mitochondrial $\Delta\Psi$ variations of permeabilized cells were estimated by the changes in fluorescence emission of rhodamine 123 (Sigma). 293 cells or 293-UCP3 clones (12×10^6 in 1.5 ml of permeabilization medium) were first permeabilized in the presence of 6 mM succinate and 10 $\mu\text{g}/\text{ml}$ oligomycin. They were then incubated with 0.5 $\mu\text{g}/\text{ml}$ of rhodamine 123 and fluorescence emission changes were continuously monitored at room temperature with a Shimadzu RF-5001PC fluorimeter at 525 nm, the excitation wavelength being 485 nm.

State 4 respiratory rates were determined polarographically in cells permeabilized in the presence of 6 mM succinate and 10 $\mu\text{g}/\text{ml}$ oligomycin in the same conditions than for the mitochondrial $\Delta\Psi$ variation assays except that rhodamine 123 was omitted.

Determination of the Ca^{2+} sensitivity of the mitochondrial transition pore (PTP)

PTP was assayed in digitonin-permeabilized cells, essentially as described elsewhere (Chauvin et al., 2001). Briefly, uptake and release of Ca^{2+} were assessed by loading cells with a train of 15 μM Ca^{2+} pulses at 2-min intervals. Permeabilized cells took up and retained Ca^{2+} ; and the Ca^{2+} retention capacity for every cell type and culture condition was determined. Free Ca^{2+} was measured fluorimetrically in the presence of 0.5 μM Calcium Green-5N with excitation and emission wavelengths set at 506 and 532 nm, respectively. To confirm that Ca^{2+} release was due to PTP opening,

parallel assays were performed in the presence of 0.5 μM of the PTP inhibitor cyclosporin A.

Caspase 3 activity

Caspase activity was measured using the fluorimetric CaspACE Assay System (Promega) based on the fluorimetric detection of amino-4-trifluoromethyl coumarin after proteolytic cleavage of the synthetic substrate DEVD-amino-4-trifluoromethyl coumarin. Cells were exposed to staurosporine as described above and lysed by three cycles of freezing/thawing in "lysis buffer" (25 mM HEPES, 5 mM MgCl_2 , 5 mM EDTA, 5 mM DTT, 2 mM PMSF, 10 $\mu\text{g}/\text{ml}$ pepstatin A, 10 $\mu\text{g}/\text{ml}$ leupeptin) and cytosolic extracts to be assayed were collected after 10,000g centrifugation for 20 min. Protein (0.4 mg), as determined by the Bradford Assay Kit (Bio-Rad, Hercules, USA), was used for the assay, which was performed as indicated by the supplier (Promega). Specificity of the assay was assessed by the use of CPP32 inhibitor Ac-DEVD-CHO (Promega). Pre-incubation of the cell extracts with 50 μM CPP32 inhibitor led in all the assays to a residual activity of less than 5% of the total activity detected.

Cell fractionation

Cells were harvested with a buffer containing 7.5 mM tri-sodium citrate 2-hydrate, 7 mM KCl, pH 7.4, and centrifuged at 400g for 2 min. The cell pellets were washed once with PBS and then resuspended in 1 ml of homogenization buffer (250 mM Sucrose, 1 mM EGTA, 10 mM HEPES, pH 7.4, 1 mM PMSF, 1 mM DTT, Complete-Mini Protease Inhibitor cocktail tablets (Roche)). After chilling on ice for 1 min, cells were disrupted by 50 strokes in a glass homogenizer. The homogenate was centrifuged once at 1,500g for 10 min at 4°C to remove unbroken cells, plasmatic membranes, and nuclei. The mitochondria-enriched fraction (heavy membrane fraction) was then pelleted by centrifugation at 10,000g for 10 min. The supernatant was subjected to further ultracentrifugation at 100,000g for 60 min at 4°C with the resultant supernatant being used as the cytosolic fraction. For controls using mitochondria from tissue, mitochondria-enriched extracts were prepared from gastrocnemius muscles obtained from fed or 24 h-fasted Swiss mice and Wistar rats fed a regular chow or a high-fat diet (80% fat/20% protein) for 3 months, as described elsewhere (Pedraza et al., 2000). Protein concentration of subcellular fractions was measured using the BCA Protein Assay kit (Pierce) in the presence of 0.1% TritonX-100 (Boehringer Mannheim).

Western blot analysis

For UCP3, cytochrome c, Bax, and Bcl-2 analysis, samples of homogenates, mitochondria, or cytosolic fractions were separated by SDS-PAGE on either 12.8 or 15% acrylamide gels, and transferred to polyvinylidene fluoride membranes (PVDF membranes) (Immobilon-P, Millipore). These were further incubated with antibodies against UCP3 (Chemicon AB3046 (1:1,000)), cytochrome c (Pharmingen clone 7H8.2C12 (1:500)), Bax (Santa Cruz N-20 sc-493 (1:350)), and Bcl-2 (Santa Cruz sc-509 (1:500)). For caspase-9 analysis, cytosolic extracts (obtained by freezing/thawing cycles as described above for caspase-3 assays) were separated

by SDS-PAGE on 12.8% gels, transferred to PVDF membranes, and incubated with a polyclonal antibody against cleaved caspase-9 (New England Biolabs 9505 (1:1,000)). Antibodies against β -Actin (Sigma clone AC-15 (1:10,000)), voltage-dependent anion carrier or porin (VDAC) (Calbiochem Anti-Porin 31HL (1:1000)), or cytochrome oxidase subunit I (CO I) (Molecular Probes A-6403 (1:500)), were used to ensure equal protein loading and correct cell fractionation. The binding of antibodies was detected with a horseradish peroxidase-coupled anti-mouse (Bio-Rad 170-6516 (1:3,000)) or anti-rabbit (Santa Cruz sc-2004 (1:3,000)) secondary antibody, and an enhanced chemiluminescence (ECL) detection kit (Amersham). When required, densitometric analysis of immunoblot signals was performed (Phoretix, Millipore, Bedford, USA).

Statistical analysis

Data, shown as means \pm SEM, were analyzed with Student's *t*-test for determination of the significance of differences, which were considered to be significant at a *P* value of less than 0.05.

RESULTS

Induction of the expression of UCP3 in 293 cells

To investigate how UCP3 influences mitochondrial activity and apoptotic pathways, human UCP3 cDNA was stably transfected into 293 cells. The transcription of UCP3 cDNA was under the control of doxycycline addition in the medium in a tetracycline-inducible system. Twelve cell clones were obtained, all of them expressing UCP3 after the induction of the tetracycline inducible system. At least two independent clones, 293-UCP3A and 293-UCP3B, were used for further studies to rule out that the effects further observed were of clonal origin. In the absence of doxycycline, UCP3 was hardly expressed in total cell lysates or in mitochondria-enriched preparations of these clones. Overexposure of Western blots showed a faint band in the absence of doxycycline in the 293-UCP3 clones, which was not detected in parental cells, and surely corresponded to a minor leaking of the doxycycline dependency of the promoter driving UCP3 expression (not shown). The levels of UCP3 expression in mitochondria were tightly regulated by the doses of doxycycline (Fig. 1A, left). Moreover, when doxycycline was withdrawn from the medium after 48 h exposure, UCP3 remained present at similar levels for at least 24 h (Fig. 1A, right). Therefore, to minimize interferences on the functional studies of 293 and 293-UCP3 cells, doxycycline was always withdrawn from the culture medium after cells had been treated for 48 h.

Figure 1B shows Western blot analyses of mitochondrial-enriched and cytosolic fractions of cell lysates from a representative 293-UCP3 clone after doxycycline treatment. UCP3 expression induced by doxycycline was detected in the mitochondrial fraction but not in the cytosol. Correct separation of the mitochondrial fraction was ensured by the parallel analysis of the expression of subunit I of cytochrome c oxidase (COI) and porin (VDAC), as representatives of mitochondrial inner membrane and outer membrane components, respectively (Fig. 1B). Thus, doxycycline-induced UCP3 was correctly delivered to mitochondria. The dose-

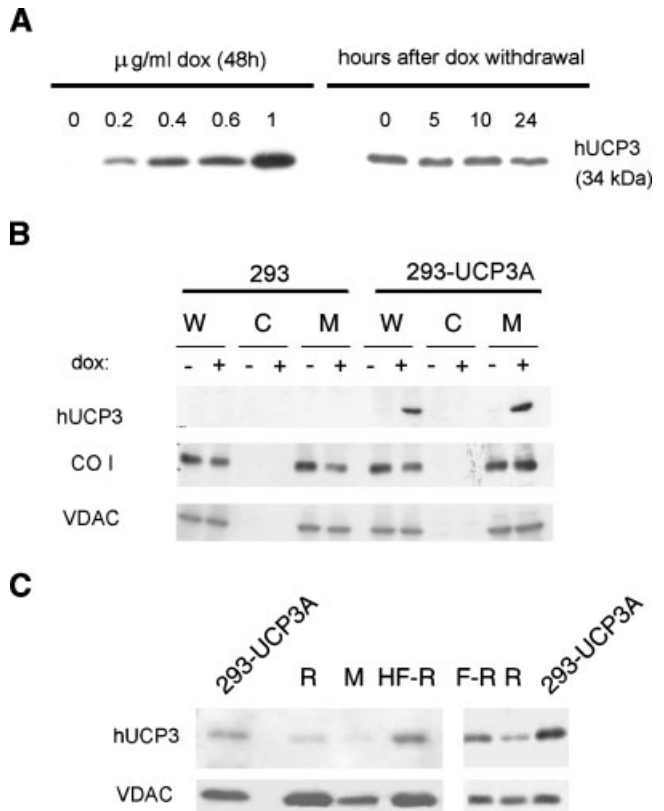


Fig. 1. Characterization of doxycycline-dependent induction of UCP3 expression. **A:** Dose-response analysis of UCP3 protein expression induced by doxycycline (dox) (left) and time-course analysis of UCP3 levels after doxycycline withdrawal (right) in the 293-UCP3A clone. Immunodetections were performed on 12 μg of mitochondrial protein. **B:** Cell fractionation analysis of UCP3 induction. In this case, 25 μg protein of whole cells homogenate (W), cytosol (C), and mitochondrial (M) fractions from 293 or 293-UCP3A cells, exposed or not to 1 $\mu\text{g/ml}$ doxycycline (dox), were probed with antibodies against UCP3, COI, and VDAC. **C:** Comparison of mitochondrial UCP3 levels in the doxycycline-treated 293-UCP3A mitochondrial fractions versus mitochondrial fractions of gastrocnemius muscle of mice (M), rats (R), rats fed with a high-fat diet (HF-R), or 24 h-fasted rats (F-R). Immunodetections of UCP3 and VDAC were performed on 20 μg mitochondrial protein (see Materials and Methods).

response to doxycycline, stability after doxycycline withdrawal and correct delivery of the doxycycline-induced expression of UCP3 into mitochondria occurred equally for at least the two independent 293-UCP3 clones studied. The induction of UCP3 did neither alter the mRNA levels of UCP2 nor the abundance of the mRNA encoding for proteins of the respiratory chain such as cytochrome c oxidase subunit IV (not shown).

To estimate the amounts of UCP3 induced in 293-UCP3 clones in relation to the UCP3 protein levels *in vivo*, mitochondrial protein extracts from doxycycline-induced clones and skeletal muscle of mice and rats in various physiological situations were analyzed. The levels of expression of mitochondrial UCP3 attained in the clones after exposure to 1 $\mu\text{g/ml}$ doxycycline were higher than those in mouse or rats fed a regular diet and still higher than in 24 h-fasted rats but in the range of those attained in rats chronically fed a high-fat diet, a known nutritional activator of UCP3 gene expression in skeletal muscle (Pedraza et al., 2000). Hence, the

induction dose of 1 $\mu\text{g/ml}$ doxycycline was selected and used for further studies.

UCP3 allows in situ GDP-dependent re-polarization of the mitochondrial inner membrane and a GDP-dependent reduction of state 4 respiration in the presence of fatty acids

Changes in mitochondrial membrane potential were determined in cells permeabilized in the presence of succinate and oligomycin (i.e., state 4, a functional condition in which the mitochondrial membrane potential is maximal) using the fluorescent lipophilic cation rhodamine 123. The upper trace of Figure 2 illustrates a representative experiment in control 293 cells that were exposed to doxycycline identically to 293-UCP3 clones. Low concentrations of palmitic acid added to the medium caused a slight reduction in mitochondrial $\Delta\Psi$. No effect on the mitochondrial membrane potential was observed when GDP was added. Mitochondrial $\Delta\Psi$ collapsed upon addition of the protonophoric uncoupler CCCP. Addition of palmitic acid to permeabilized cells 293-UCP3 (293-UCP3A clone), in which UCP3 had been induced, caused a similar depolarization of the mito-

chondrial inner membrane. However, in contrast to 293 cells, GDP increased the mitochondrial membrane potential in 293-UCP3 cells induced to express UCP3 ($5.7 \pm 1.5\%$ with respect to the total signal intensity in the presence of CCCP in 293-UCP3A cells treated with doxycycline versus $0.9 \pm 1\%$ in 293 cells treated with doxycycline, $n=3$ and $P \leq 0.05$; compare upper and lower traces in Fig. 2). Re-polarization caused by GDP was only observed upon prior addition of palmitic acid to the medium and was in the range of that elicited by GDP in other models of expression of UCP proteins (Fink et al., 2002). Similar results were obtained for an independent UCP3-expressing clone (293-UCP3B) (not shown).

To determine the effects of fatty acids and GDP on state 4 mitochondrial respiratory rates, cells were permeabilized in the presence of succinate and oligomycin, and oxygen consumption was recorded in basal conditions and after the addition of palmitate alone or palmitate plus GDP. Results are shown in Figure 3. In 293 cells, palmitate elicited a small but significant rise in oligomycin insensitive respiration, which was unaffected by GDP, regardless of pre-treatment with doxycycline. 293-UCP3 respiratory rates showed the same pattern of response to palmitate and palmitate plus GDP in the absence of doxycycline. However, when UCP3 had been induced, the rise in state 4 respiration elicited by palmitate was enhanced and addition of GDP blocked this effect. These results demonstrate that UCP3 confers a GDP-dependent sensitivity to fatty acid of mitochondrial state 4 respiration.

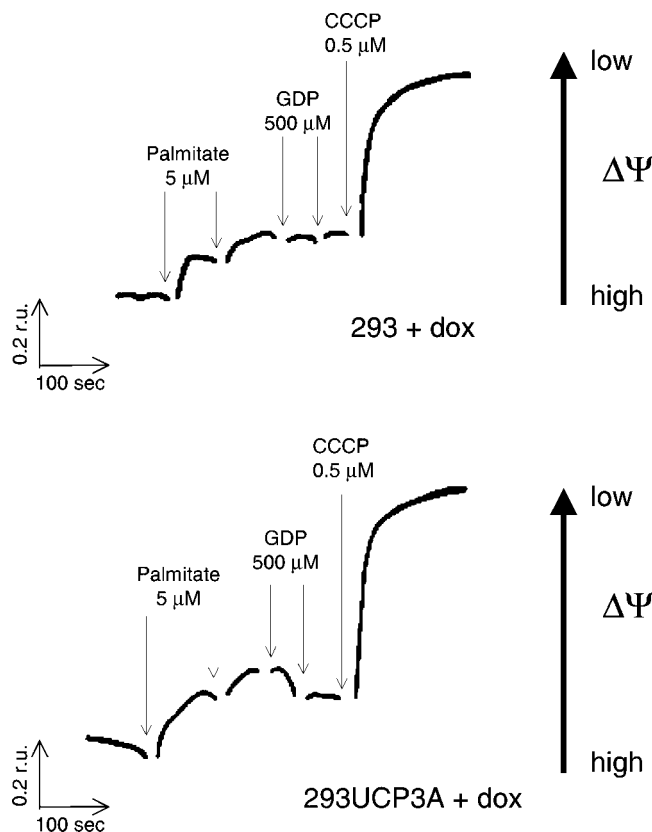


Fig. 2. Influence of UCP3 on mitochondrial $\Delta\Psi$ variations of permeabilized cells. Effects of palmitate and GDP. 293 and 293-UCP3 cells were cultivated, exposed to 1 $\mu\text{g/ml}$ doxycycline for 48 h (dox) and subjected to digitonin treatment as described in "Materials and Methods." This figure shows representative recordings of the mitochondrial membrane potential evolution estimated from the $\Delta\Psi$ -dependent red shift and fluorescence quenching of rhodamine 123. r.u.: fluorescence relative unit.

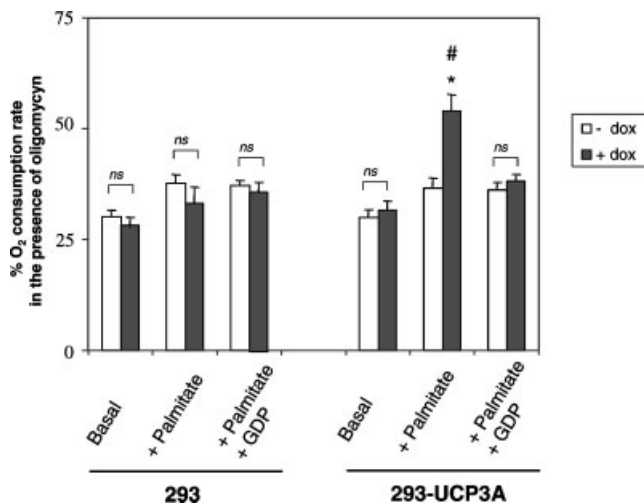


Fig. 3. State 4 respiratory activities in permeabilized 293 and 293-UCP3 cells. Effects of palmitate and GDP. The respiratory rates of 293 and 293-UCP3A cells were determined after a treatment or not with 1 $\mu\text{g/ml}$ doxycycline during 48 h and permeabilization with digitonin, as described in Materials and Methods. Cells were incubated in permeabilization medium in the presence of 6 mM succinate and 10 $\mu\text{g/ml}$ oligomycin. The effects of addition of 10 μM palmitate and subsequent addition of 1 mM GDP was determined. The respiratory activities of 293 and 293-UCP3A cells are shown as the ratio between their oxygen consumption rates and their respective cytochrome c oxidase activities ($n=3$ for each activity measured in each condition). Statistically significant differences ($P \leq 0.05$) due to doxycycline for every experimental situation are shown as *, and those obtained by comparing 293-UCP3A respect to 293 by #. ns: non-statistically significant.

These results indicate that UCP3 induction in 293 cells caused a fatty acid-dependent, GDP-regulated proton, and/or ionic transport(s) throughout the inner mitochondrial membrane and that fatty acids are required for this regulation, in agreement with the expected behavior of physiological UCP3 activity in mitochondria (Echtay et al., 2001).

UCP3 induction does not cause uncontrolled, uncoupled cellular respiration

The degree of coupling of the mitochondrial respiratory chain was estimated in intact, non-permeabilized 293 and 293-UCP3 cells cultivated either in the presence or absence of doxycycline. First, basal oxygen consumption was determined (JO_{basal}) and the part of oxygen uptake not coupled to ATP synthesis was then assessed by addition of oligomycin to the respiration medium ($JO_{\text{oligomycin}}$). The maximal respiratory activity of the cells in conditions of complete uncoupling was then measured using the protonophoric uncoupler CCCP, which dissipates the proton electrochemical gradient across the inner mitochondrial membrane and thereby stimulates the respiratory rate to its maximal value (JO_{CCCP}). All of these respiratory activities were completely inhibited when antimycin A 0.25 $\mu\text{g/ml}$, an inhibitor of the respiratory chain complex III, was added to the respiration medium. Finally, as cytochrome c oxidase has been shown to be the principal respiratory control step in several cell lines (Villani et al., 1998), we also measured cytochrome c oxidase activity in all the clones tested; and the respiratory activities measured were expressed as their percentage with respect to complex IV activity (Fig. 4). Measurement of cytochrome c oxidase activities in permeabilized 293 cells was

performed with 0.5 mM TMPD and 1 mM ascorbate in the presence of antimycin A (0.25 $\mu\text{g/ml}$) and CCCP (0.5 μM) as described in the Methods section. These activities were 76.0 ± 2.5 , 70.0 ± 2.0 , 90.0 ± 4.0 , and 78.0 ± 3.0 $\text{nat.O/min}/10^7$ cells for 293 cells, 293 cells treated with doxycycline, 293-UCP3A cells and 293-UCP3A cells treated with doxycycline, respectively ($n = 3$ for each condition).

There was no difference in basal oxygen consumption between 293 and 293-UCP3A cells (Fig. 4). Moreover, exposure of control 293 cells or 293-UCP3A clones to doxycycline, and subsequent induction of UCP3 in the latter case, did not modify basal oxygen consumption. Neither oligomycin-insensitive residual oxygen uptake nor the uncoupled respiration was affected by doxycycline in intact 293 cells or intact 293-UCP3A cells (Fig. 4). The same results were obtained with 293-UCP3B cells (not shown). This indicates that UCP3 expression: (i) does not enhance the amount of uncoupled mitochondrial respiration of 293 cells; and (ii) did not induce an uncontrolled uncoupling of oxidative phosphorylation in mitochondria of 293 cells due to a misfolding of this protein in the inner mitochondrial membrane, in contrast to reports in rat L6 cells (Guerini et al., 2002).

Further evidence that the induction of UCP3 did not modify the overall basal energetic status of cells was obtained by measurements of cellular ATP, which was not significantly changed by doxycycline pre-treatment of either parental 293 cells or 293-UCP3 clones (14.4 ± 1.3 nmol/mg protein in 293 cells, 12.9 ± 1.0 nmol/mg protein in 293 cells plus doxycycline; 12.1 ± 1.1 nmol/mg protein in 293-UCP3A cells, 15.0 ± 1.7 nmol/mg protein in 293-UCP3A cells plus doxycycline, $n = 5$). Moreover, cellular NADH was not significantly changed in the same conditions (8.3 ± 1.6 nmol/mg protein in 293 cells, 10.3 ± 1.8 nmol/mg protein in 293 cells plus doxycycline; 9.5 ± 1.3 nmol/mg protein in 293-UCP3A cells, 7.8 ± 2.3 nmol/mg protein in 293-UCP3A cells plus doxycycline, $n = 5$).

UCP3 enhances the induction of caspase-3 activity in response to staurosporine

To determine how the presence of UCP3 affects the responsiveness to an apoptotic stimulus involving mitochondrial pathways, cells were exposed to staurosporine, a specific mitochondrion-mediated pro-apoptotic reagent. This treatment was performed either before or after UCP3 expression had been induced, and the activity of caspase-3 was determined in cytosolic extracts (see Materials and Methods). Preliminary experiments were performed to determine a dose and time of exposure to staurosporine that elicited sub-maximal induction of caspase-3 activity in control 293 cells (see Materials and Methods). Staurosporine treatment increased caspase-3 activity, whereas pre-treatment with doxycycline before staurosporine exposure slightly reduced this increase (Fig. 5). The induction of UCP3 expression by doxycycline treatment of 293-UCP3 clones did not enhance basal caspase-3 activity, even after a longer (96 h) incubation of these cells with this drug (data not shown). However, prior doxycycline-induced UCP3 expression in 293-UCP3 cells significantly increased the extent of staurosporine-induced

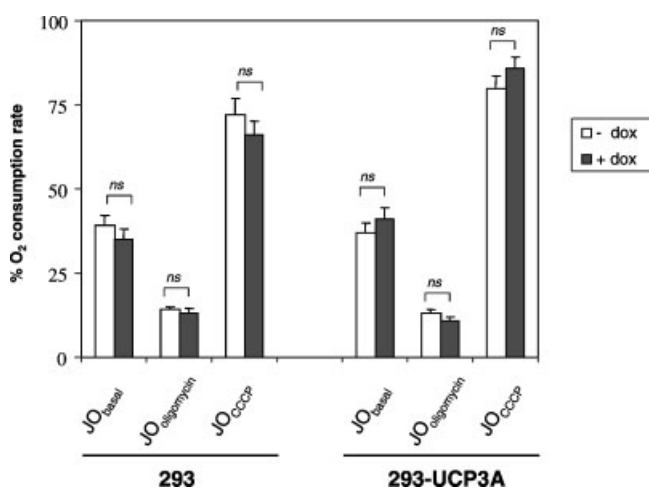


Fig. 4. Respiratory activities of 293 and 293-UCP3 cells. The respiratory rates of 293 and 293-UCP3A cells were determined after a treatment or not with 1 $\mu\text{g/ml}$ doxycycline during 48 h. Cells were incubated in DMEM supplemented with 5 mM HEPES without any addition (JO_{basal}) or either in the presence of 1 μM of the protonophoric uncoupler CCCP (JO_{CCCP}) or 10 $\mu\text{g/ml}$ of the F1F0-ATP synthase inhibitor oligomycin ($JO_{\text{oligomycin}}$) as described in Materials and Methods. The respiratory activities of 293 and 293-UCP3A cells are shown as the ratio between their oxygen consumption rates and their respective cytochrome c oxidase activities ($n = 3$ for each activity measured in each condition). ns: non statistically significant.

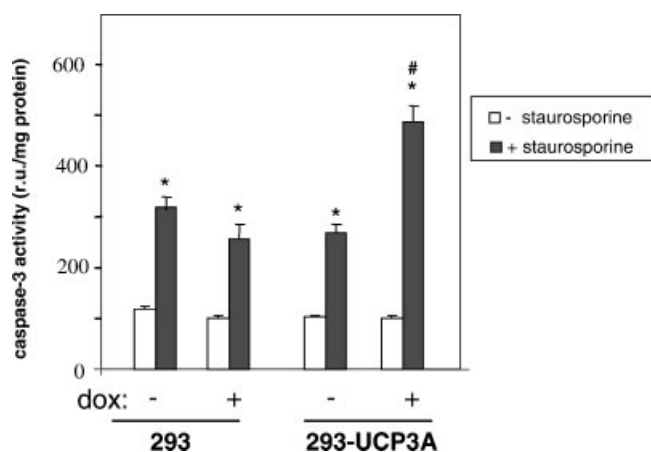


Fig. 5. Effects of UCP3 on caspase-3 activity in response to staurosporine. 293 controls and 293-UCP3 cells, previously treated or untreated with 1 μ g/ml doxycycline, were exposed to 0.5 μ M staurosporine for 6 h. Cytosolic extracts were prepared after freezing/thawing cycles and caspase-3 activity was measured fluorimetrically as described in "Materials and Methods." Bars show the caspase-3 activity (r.u.: fluorescence relative unit/mg protein) and are means \pm SEM of 5 to 7 independent experiments performed in duplicate. Statistically significant differences due to staurosporine for every situation are shown by *, and those between the 293-UCP3A clone and 293 control cells were shown by #.

caspase-3 activity compared with that observed for similarly treated 293 cells.

The induction of UCP3 enhances cytochrome c release from mitochondria and cleavage of caspase-9 in response to staurosporine

As caspase-3 activation is considered an end-point in the apoptotic cascade involving either mitochondrial-dependent or independent pathways, we next determined whether UCP3 induction affected the responsiveness of cells to two apoptotic events more closely related to mitochondrial pathways: caspase-9 activation and cytochrome c release. Exposure of 293 cells to staurosporine induced the release of cytochrome c from the mitochondrial to the cytosolic fraction. This effect was significantly reduced in the presence of doxycycline. In contrast, the extent of cytochrome c release to the cytosol in 293-UCP3 cells exposed to staurosporine was not reduced and was even slightly enhanced by pre-treatment with doxycycline (Fig. 6). Thus, in the presence of doxycycline, the amount of cytochrome c released to the cytosol was significantly higher in 293-UCP3A cells, in which UCP3 is induced, than in the parental 293 cells (Fig. 6B).

A parallel analysis was performed for caspase-9 activity by assessing the cleavage of pro-caspase-9. Exposure of 293 cells to staurosporine enhanced the appearance of the cleaved, 37 kDa active form, of caspase-9 in cell lysates, as shown by Western blot analysis, and the action of staurosporine was not affected by doxycycline treatment (Fig. 7). Exposure of 293-UCP3 clones to doxycycline and induction of UCP3 in mitochondria significantly increased the abundance of cleaved caspase-9 in response to staurosporine (Fig. 7B).

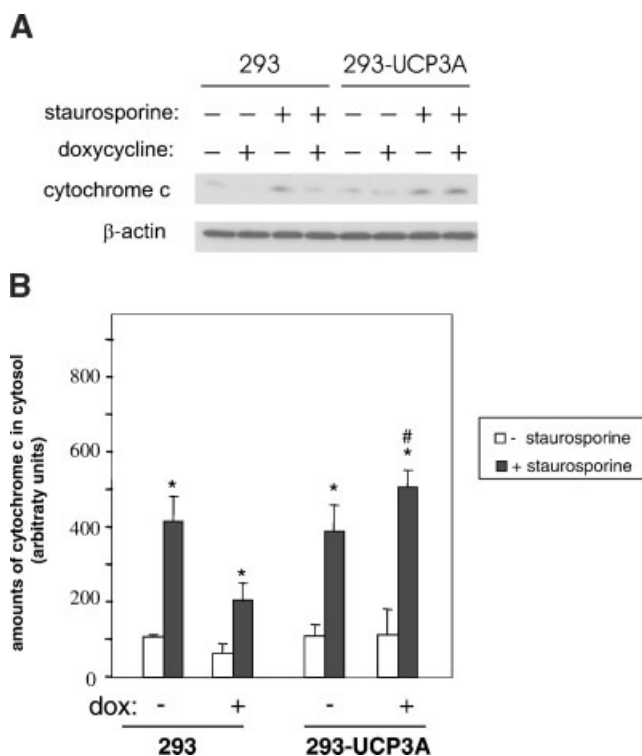


Fig. 6. Effects of UCP3 on cytochrome c release to cytosol in response to staurosporine. 293 controls and 293-UCP3 cells, previously treated or untreated with doxycycline (dox), were exposed to 0.5 μ M staurosporine for 6 h. Cytosolic fractions were prepared after cell homogenization, centrifugation and ultracentrifugation as described in "Materials and Methods." **A**: example of immunodetection performed on 50 μ g protein from cytosolic extracts with antibodies against cytochrome c and β -actin; **B**: bars are means \pm SEM (3–4 independent experiments) of densitometric scanning of cytochrome c immunodetected signals in cytosol, corrected for loading variability by the use of the β -actin signal. Statistically significant differences due to staurosporine for every situation are shown by *, and those between the 293-UCP3A clone and 293 control cells were shown by #.

UCP3 expression favors Bax translocation to mitochondria

Since the expression and localization of anti-apoptotic and pro-apoptotic mitochondrial proteins of the Bcl-2 family favors or represses apoptosis, we assessed the effects of UCP3 expression on Bax and Bcl-2 expression as well as on the extent of Bax translocation from the cytosol to mitochondria. When corrected for gel loading using β -actin (whole cell homogenates) or VDAC (mitochondria) immunoblot signals, no significant differences were detected in basal levels of Bcl-2 when 293 cells and 293-UCP3A cells were compared, either in whole cell homogenates ($89 \pm 14\%$ in 293-UCP3A cells with respect to 293 cells, $n = 4$) or in the mitochondrial fraction ($107 \pm 18\%$ in 293-UCP3A cells with respect to 293 cells, $n = 4$). Moreover, doxycycline treatment did not significantly modify Bcl-2 levels in the mitochondrial fractions from either 293 cells ($93 \pm 15\%$ in 293 + doxycycline, with respect to 293, $n = 3$) or 293-UCP3A cells ($114 \pm 17\%$ in 293-UCP3A + doxycycline, with respect to 293-UCP3A, $n = 4$).

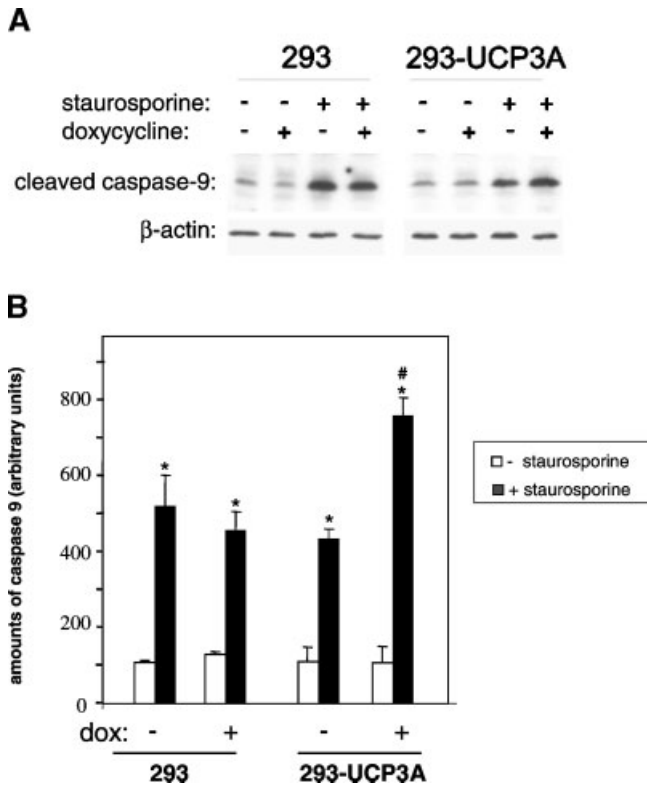


Fig. 7. Effects of UCP3 on caspase-9 activation in response to staurosporine. 293 controls and 293-UCP3 cells, previously treated or untreated with doxycycline (dox), were exposed to 0.5 μ M staurosporine for 6 h. Cytosolic fractions were prepared as in Figure 6. **A:** Example of immunodetection performed on 75 μ g protein from cytosolic extracts with antibodies against the active, cleaved-form, of caspase-9, and β -actin. **B:** Bars are means \pm SEM (3–4 independent experiments) of densitometric scanning of cleaved caspase 9 signal corrected for loading variability by the use of the β -actin signal, and expressed as percents respect to basal activity in 293 untreated cells. Statistically significant differences due to staurosporine for every situation are shown by *, and those between the 293-UCP3A clone and 293 control cells were shown by #.

Neither doxycycline treatment of 293 cells nor UCP3 induction by doxycycline in the 293-UCP3A clone significantly modified the expression of Bax in whole cell homogenates. However, UCP3 induction by doxycycline in 293-UCP3A cells significantly increased the presence of Bax in the mitochondrial fraction as well as significantly lowered the levels of Bax in the cytosolic fraction (Fig. 8). This effect was not observed when parental 293 cells were treated with doxycycline. This resulted in a higher Bax/Bcl-2 ratio in mitochondria in which UCP3 had been induced with respect to controls (4.3-fold increase in the mitochondrial Bax/Bcl-2 ratio in 293-UCP3A cells + doxycycline with respect to 293 cells + doxycycline). As for the other parameters, parallel testing of at least two assays in an independent 293-UCP3 clone led to the same conclusions.

UCP3 sensitizes mitochondria to Ca²⁺-induced mitochondrial permeability transition

The effect of UCP3 induction on the sensitivity of cells to mitochondrial permeability transition in response to an increase in extramitochondrial Ca²⁺ was determined

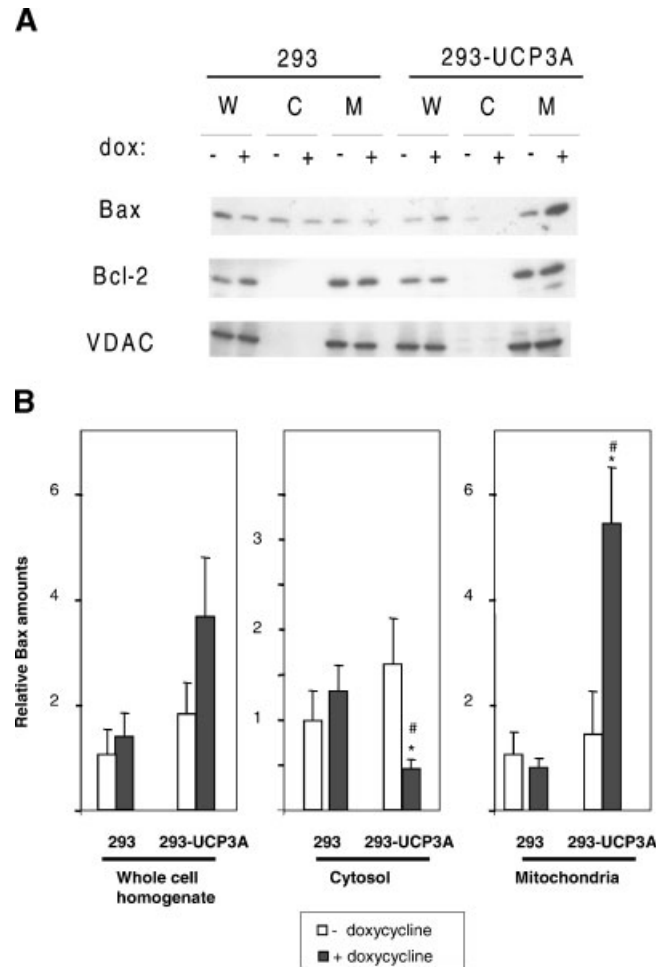


Fig. 8. Effects of UCP3 on Bax levels in cells and mitochondria. 293 controls and 293-UCP3 cells, previously treated or untreated with doxycycline (dox) were analyzed. Cells were homogenized and mitochondrial and cytosolic fractions were prepared by centrifugation and ultracentrifugation, as described in “Materials and Methods.” **A:** Example of immunodetections performed on 30 μ g protein of whole cell homogenates (W), cytosolic extracts (C), and mitochondrial extracts (M) with antibodies against Bcl-2, Bax, and VDAC proteins. **B:** Bars are means \pm SEM (3–4 independent experiments) of the fold-change in Bax content in every cell fraction respect to basal levels in 293 cells. Quantitative data were calculated on the basis of densitometric scanning of the Bax immunodetected signal corrected for loading variability by the use of the β -actin signal in W and C, and by the VDAC signal in M. Statistically significant differences ($P \leq 0.05$) between the 293-UCP3A clone and 293 controls for every cellular fraction are shown by #.

by using a recently developed technique to assess this parameter in permeabilized cells (Chauvin et al., 2001). Figure 9 shows a representative determination of the amount of Ca²⁺ pulses required to induce mitochondrial permeability transition in cells in which UCP3 expression had been induced with doxycycline. It also shows the same determination in 293 controls cells previously treated with doxycycline. The mean amount of Ca²⁺ required for permeability transition was of 100.5 + 9.9 μ M (n = 5) in doxycyclin-treated 293 control cells but only of 67.6 + 13.0 μ M (n = 6) in 293-UCP3 cells in which UCP3 expression had been induced. Addition

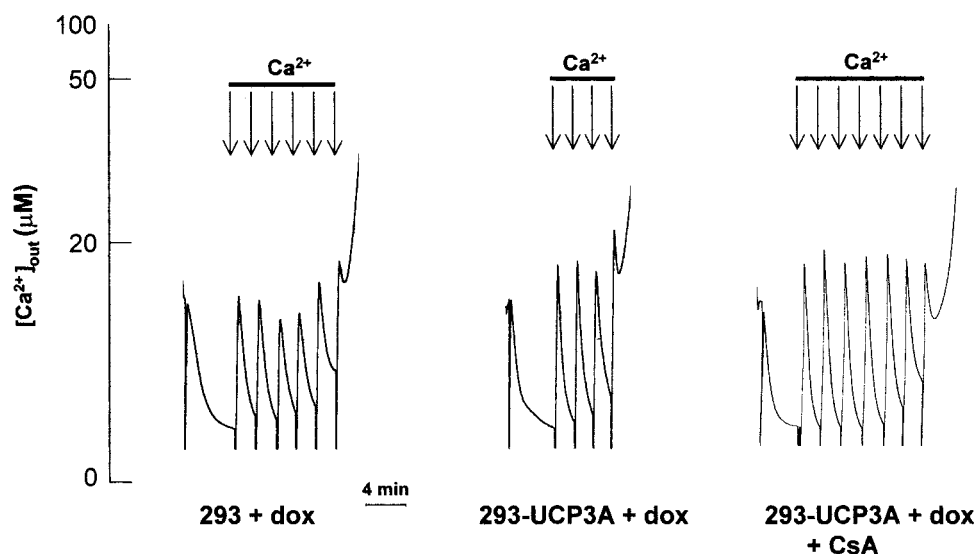


Fig. 9. Mitochondrial Ca^{2+} retention capacity in permeabilized UCP3-expressing cells. The incubation medium contained 250 mM sucrose, 50 mM KCl, 2 mM KH_2PO_4 , 25 mM Tris-HCl (pH 7.3), 1 mM MgCl_2 , and 0.5 μM Calcium Green-5N. Cells ($3 \times 10^6/2$ ml) were permeabilized by incubation for 5 min under stirring with 25 $\mu\text{g}/\text{ml}$ digitonin. Extra-mitochondrial Ca^{2+} concentration was continuously measured fluorimetrically with excitation and emission wavelengths

at 506 and 532 nm, respectively. After incubation for 48 h with doxycycline, Ca^{2+} retention capacity was determined in permeabilized 293 control cells (293 + dox, left part), permeabilized 293-UCP3A cells (293-UCP3A + dox, central part), and 293-UCP3A in the presence of 0.5 μM cyclosporine A (293-UCP3A + dox + CsA, right part). Each arrow indicates the addition of a 15 μM Ca^{2+} pulse.

of 0.5 μM cyclosporine A to the incubation medium dramatically increased the amounts of Ca^{2+} required for permeability transition, in agreement with the known role of cyclosporin A as a PTP inhibitor. The amounts of calcium required for PTP opening in 293 controls and 293-UCP3 cells without treatment with doxycycline did not differ significantly (data not shown).

DISCUSSION

We have established a novel model of inducible UCP3 gene expression in cultured cells. In this model, UCP3 expression in cell mitochondria, within similar amounts to those elicited in physiological situations of maximal induction of the endogenous gene, confers to mitochondria a GDP-regulated re-polarization of their inner membrane in the presence of fatty acids. Moreover, it caused an enhancement in fatty acid induction of state 4 respiration that could be inhibited by GDP. This behavior is similar to that observed in reconstituted systems (Echtay et al., 2001; Zackova et al., 2003) and confirms the properties of UCP3 as a fatty acid and GDP regulated UCP in mitochondria. Moreover, this model does not show any signs of uncontrolled uncoupling when UCP3 is expressed, in contrast with other models of high over-expression of the protein (Guerini et al., 2002). It is free of endogenous expression of UCP3, which allows a high sensitivity in the detection of specific effects driven by the presence of UCP3 in mitochondria.

The presence of UCP3 in mitochondria did not lead to apoptosis per se, but it sensitizes cells to apoptosis, as evidenced by the enhanced activation of caspase 3 activity, an end-point of the apoptotic signaling cascade, in response to the apoptotic inducer staurosporine. The induction of apoptosis elicited by this chemical is known to involve mitochondrial events such as enhanc-

ed cytochrome c release and activation of caspase-9. Our observations indicate that these events are over-stimulated upon exposure to staurosporine when cells contain UCP3 in their mitochondria. We also show that, in the absence of apoptotic stimuli, this apoptosis-sensitive status of cells due to UCP3 in mitochondria is associated with a higher mitochondrial versus cytosolic Bax content and with a higher sensitivity of the mitochondrial PTP to open in response to a cytosolic Ca^{2+} overload.

Massive Bax translocation to mitochondria and opening of the PTP are considered primary events eliciting the cascade of mitochondrial events leading to apoptosis (Ravagnan et al., 2002). However, the relationship between both phenomena and the precise sequence of activation of these and other events such as cytochrome c release remain unclear. Issues such as whether PTP opening is prior to cytochrome c release or not, or whether Bax translocation is the main event leading to PTP opening and cytochrome c release from mitochondria to the cytosol, are a matter of current debate concerning the understanding of the regulation of apoptotic pathways, and discrepancies are probably due to the diversity of cell systems and experimental models studied (Herrera et al., 2001; De Giorgi et al., 2002; Polster et al., 2003). In any case, whichever is primary, the presence of UCP3 in mitochondria increases all these pro-apoptotic parameters.

The effects of UCP3-sensitizing cells to apoptosis may be indirect and related to the impact of the presence of UCP3 in the mitochondrial inner membrane on the bioenergetic status of the cells. The parameters tested here in permeabilized cells indicate that UCP3 facilitates mitochondrial proton conductance but only in a regulated manner, requiring fatty acids and inhibited by purine nucleotides such as GDP. This result, together with the unchanged respiration rates in intact cells

induced to express UCP3, rules out the possibility that a non-specific collapse of mitochondrial $\Delta\Psi$ due to UCP3 acts as an apoptotic sensitizing mechanism. This is also consistent with the fact that UCP3 expression never caused the cells to undergo apoptosis in the absence of staurosporine. However, it has been reported that treatments with chemical uncouplers that do not lead to apoptosis by themselves can enhance sensitivity to Fas-induced apoptosis (Linsinger et al., 1999). Therefore, it cannot be ruled out that a mild reduction in the proton membrane potential, such as that elicited by UCPs under the physiological stimulus of intracellular metabolites, could alter the sensitivity of 293 cells to apoptosis.

UCP3 may also promote sensitivity to apoptosis by direct interaction with other mitochondrial proteins involved in the apoptotic machinery. To date, the only study that has addressed the issue of potential interactions of UCP3 with other proteins has established the interaction of UCP3 with 14.3.3 proteins (Pierrat et al., 2000). Although the exact function of 14.3.3 proteins is unknown, they are involved in multiple processes including the control of apoptosis (Van Hemert et al., 2001). These proteins act as anti-apoptotic factors through the binding and the resulting inhibition of the activity of pro-apoptotic proteins such as Bad (Subramanian et al., 2001) and Bax (Nomura et al., 2003). Whether the capacity of UCP3 to bind anti-apoptotic 14.3.3 proteins mediates the sensitization to apoptotic stimuli provided by UCP3 should deserve further research. Moreover, it should be considered that UCP3 is a member of the super-family of mitochondrial carriers that includes the adenine nucleotide translocase (Ricquier and Bouillaud, 2000). This protein, in addition with its function as an ADP/ATP translocator, appears to participate in the multi-protein complex that constitutes the PTP (Vieira et al., 2000). It cannot be ruled out that UCP3 could interact directly with this complex in a similar way and thus influence the behavior of the PTP reported here. Further research is under-way to explore these possibilities.

Recent studies on UCP2, a closely similar protein to UCP3, indicate that UCP2 can favor or prevent cell death depending on the cell type (Mills et al., 2002; Diano et al., 2003; Mattiasson et al., 2003). The cell-specific expression of UCP3 should be taken into account when considering the biological role of its apoptosis-sensitizing activity. Skeletal muscle cells are the major site for UCP3 expression in vivo although other cells types such as brown adipocytes, white adipocytes, or cardiomyocytes show substantial expression, at least in rodents (Vidal-Puig et al., 1997). UCP3 is up-regulated in most of these cells by stimuli related to metabolic stress signals, such as a rise in the concentration of free fatty acids (Brun et al., 1999) or by other agents related to cellular stress such as TNF α (Masaki et al., 1999). These factors are also known as activators of apoptosis in several cell types (Gupta, 2001; Penzo et al., 2002). Apoptosis has also been described in skeletal muscle in association with development, aging, and pathologies such as muscle dystrophies and atrophies (Sandri and Carraro, 1999; Dirks and Leeuwenburgh, 2002). Recently, UCP3 up-regulation in skeletal muscle has been reported as an early metabolic defect in amy-

otrophic lateral sclerosis and it has been proposed to contribute to skeletal muscle damage in this disease (Dupuis et al., 2003). Cardiomyocytes, another specialized cell type expressing UCP3, can also undergo apoptotic through intracellular pathways involving mitochondria (Bishopric et al., 2001).

In conclusion, our results indicate that UCP3 may act as a pro-apoptotic factor activated in response to physiological signals that can lead to apoptosis. The functional consequences of the sensitization to apoptosis due the presence of high levels of UCP3 in mitochondria and the specific mechanisms mediating the apoptotic sensitization by UCP3 should deserve further studies using specific cell-type models.

ACKNOWLEDGMENTS

L.D. is recipient of a research fellowship from Fondation pour la Recherche Médicale, France. G.S. is a researcher from the "Ramon y Cajal" program of Ministerio de Ciencia y Tecnología, Spain.

LITERATURE CITED

- Antonsson B. 2001. Bax and other pro-apoptotic Bcl-2 family "killer-proteins" and their victim the mitochondrion. *Cell Tissue Res* 306:347–361.
- Armstrong JS, Steinauer KK, French J, Killoran PL, Walleczek J, Kochanski J, Knox SJ. 2001. Bcl-2 inhibits apoptosis induced by mitochondrial uncoupling but does not prevent mitochondrial transmembrane depolarization. *Exp Cell Res* 262:170–179.
- Arsenijevic D, Onuma H, Pecqueur C, Raimbault S, Manning BS, Miroux B, Couplan E, Alves-Guerra MC, Gubern M, Surwit R, Bouillaud F, Richard D, Collins S, Ricquier D. 2000. Disruption of the uncoupling protein-2 gene in mice reveals a role in immunity and reactive oxygen species production. *Nat Genet* 26:435–439.
- Bing C, Brown M, King P, Collins P, Tisdale MJ, Williams G. 2000. Increased gene expression of brown fat uncoupling protein (UCP)1 and skeletal muscle UCP2 and UCP3 in MAC16-induced cancer cachexia. *Cancer Res* 60:2405–2410.
- Bishopric NH, Andreka P, Slepak T, Webster KA. 2001. Molecular mechanisms of apoptosis in the cardiac myocyte. *Curr Opin Pharmacol* 1:141–150.
- Boss O, Samec S, Paoloni-Giacobino A, Dossier C, Dulloo A, Seydoux J, Muzzin P, Giacobino JP. 1997. Uncoupling protein-3: A new member of the mitochondrial carrier family with tissue-specific expression. *FEBS Lett* 408:39–42.
- Brun S, Carmona MC, Mampel T, Vinas O, Giralt M, Iglesias R, Villarroya F. 1999. Uncoupling protein-3 gene expression in skeletal muscle during development is regulated by nutritional factors that alter circulating non-esterified fatty acids. *FEBS Lett* 453:205–209.
- Chauvin C, De Oliveira F, Ronot X, Mousseau M, Leverve X, Fontaine E. 2001. Rotenone inhibits the mitochondrial permeability transition-induced cell death in U937 and KB cells. *J Biol Chem* 276: 41394–41398.
- De Giorgi F, Lartigue L, Bauer MK, Schubert A, Grimm S, Hanson GT, Remington SJ, Youle RJ, Ichas F. 2002. The permeability transition pore signals apoptosis by directing Bax translocation and multimerization. *FASEB J* 16:607–609.
- Diano S, Matthews RT, Patrylo P, Yang L, Beal MF, Barnstable CJ, Horvath TL. 2003. Uncoupling protein 2 prevents neuronal death including that occurring during seizures. A mechanism for preconditioning. *Endocrinology* 144:5014–5021.
- Dirks A, Leeuwenburgh C. 2002. Apoptosis in skeletal muscle with aging. *Am J Physiol Regul Integr Comp Physiol* 282:R519–R527.
- Dispersyn G, Nuydens R, Connors R, Borgers M, Geerts H. 1999. Bcl-2 protects against FCCP-induced apoptosis and mitochondrial membrane potential depolarization in PC12 cells. *Biochim Biophys Acta* 1428:357–371.
- Dupuis L, di Scala F, Rene F, de Tapia M, Oudart H, Pradat PF, Meininger V, Loeffler JP. 2003. Up-regulation of mitochondrial uncoupling protein 3 reveals an early muscular metabolic defect in amyotrophic lateral sclerosis. *FASEB J* 17:2091–2093.
- Echtay KS, Winkler E, Frischmuth K, Klingenberg M. 2001. Uncoupling proteins 2 and 3 are highly active H(+) transporters

- and highly nucleotide sensitive when activated by coenzyme Q (ubiquinone). *Proc Natl Acad Sci USA* 98:1416–1421.
- Echtay KS, Roussel D, St-Pierre J, Jekabsons MB, Cadenas S, Stuart JA, Harper JA, Roeback SJ, Morrison A, Pickering S, Clapham JC, Brand MD. 2002. Superoxide activates mitochondrial uncoupling proteins. *Nature* 415:96–99.
- Enerback S, Jacobsson A, Simpson EM, Guerra C, Yamashita H, Harper ME, Kozak LP. 1997. Mice lacking mitochondrial uncoupling protein are cold-sensitive but not obese. *Nature* 387:90–94.
- Fink BD, Hong YS, Mathahs MM, Scholz TD, Dillon JS, Sivitz WI. 2002. UCP2-dependent proton leak in isolated mammalian mitochondria. *J Biol Chem* 277:3918–3925.
- Fontaine E, Eriksson O, Ichas F, Bernardi P. 1998. Regulation of the permeability transition pore in skeletal muscle mitochondria. Modulation by electron flow through the respiratory chain complex I. *J Biol Chem* 273:12662–12668.
- Guerini D, Prati E, Desai U, Nick HP, Flammer R, Gruninger S, Cumin F, Kaleko M, Connelly S, Chiesi M. 2002. Uncoupling of protein-3 induces an uncontrolled uncoupling of mitochondria after expression in muscle derived L6 cells. *Eur J Biochem* 269:1373–1381.
- Gupta S. 2001. Molecular steps of tumor necrosis factor receptor-mediated apoptosis. *Curr Mol Med* 1:317–324.
- Herrera B, Fernández M, Alvarez AM, Roncero C, Benito M, Gil J, Fabregat I. 2001. Activation of caspases occurs downstream from radical oxygen species production, Bcl-xL down-regulation, and early cytochrome C release in apoptosis induced by transforming growth factor beta in rat fetal hepatocytes. *Hepatology* 34:548–556.
- Hesselink MK, Greenhaff PL, Constantin-Teodosiu D, Hultman E, Saris WH, Nieuwlaar R, Schaart G, Kornips E, Schrauwen P. 2003. Increased uncoupling protein 3 content does not affect mitochondrial function in human skeletal muscle in vivo. *J Clin Invest* 111:479–486.
- Huang X, Zhai D, Huang Y. 2001. Dependence of permeability transition pore opening and cytochrome C release from mitochondria on mitochondria energetic status. *Mol Cell Biochem* 224:1–7.
- Jiang S, Cai J, Wallace DC, Jones DP. 1999. Cytochrome c-mediated apoptosis in cells lacking mitochondrial DNA. Signaling pathway involving release and caspase 3 activation is conserved. *J Biol Chem* 274:29905–29911.
- Klingenberg M. 1974. Nicotinamide adenine dinucleotides (NAD, NADP, NADH, NADPH) spectrophotometric and fluorimetric methods. In: Bergmeyer HU, editor. *Methods of enzymatic analysis*. New York, London: Academic Press. pp 2045–2059.
- Kroemer G, Reed JC. 2000. Mitochondrial control of cell death. *Nat Med* 6:513–519.
- Kuida K. 2000. Caspase-9. *Int J Biochem Cell Biol* 32:121–124.
- Linsinger G, Wilhelm S, Wagner H, Hacker G. 1999. Uncouplers of oxidative phosphorylation can enhance a Fas death signal. *Mol Cell Biol* 19:3299–3311.
- Masaki T, Yoshimatsu H, Chiba S, Hidaka S, Tajima D, Kakuma T, Kurokawa M, Sakata T. 1999. Tumor necrosis factor- α regulates in vivo expression of the rat UCP family differentially. *Biochim Biophys Acta* 1436:585–592.
- Mattiasson G, Shamloo M, Gido G, Mathi K, Tomasevic G, Yi S, Warden CH, Castilho RF, Melcher T, Gonzalez-Zulueta M, Nikolich K, Wieloch T. 2003. Uncoupling protein-2 prevents neuronal death and diminishes brain dysfunction after stroke and brain trauma. *Nat Med* 9:1062–1068.
- Mills EM, Xu D, Fergusson MM, Combs CA, Xu Y, Finkel T. 2002. Regulation of cellular necrosis by uncoupling protein 2. *J Biol Chem* 277:27385–27392.
- Nedergaard J, Cannon B. 2003. The 'novel' 'uncoupling' proteins UCP2 and UCP3: what do they really do? Pros and cons for suggested functions. *Exp Physiol* 88:65–84.
- Nicholls DG, Cunningham SA, Rial E. 1989. The bioenergetic mechanisms of brown adipose tissue mitochondria. In: Trayhurn P, Nicholls DG, editors. *Brown adipose tissue*. London: Edward Arnold. pp 55–85.
- Nishimura G, Prosk RJ, Doyama H, Higuchi M. 2001. Regulation of apoptosis by respiration: Cytochrome c release by respiratory substrates. *FEBS Lett* 505:399–404.
- Nomura M, Shimizu S, Sugiyama T, Narita M, Ito T, Matsuda H, Tsujimoto Y. 2003. 14-3-3 interacts directly with and negatively regulates pro-apoptotic Bax. *J Biol Chem* 278:2058–2065.
- Ouhabi R, Boue-Grabot M, Mazat JP. 1998. Mitochondrial ATP synthesis in permeabilized cells: Assessment of the ATP/O values in situ. *Anal Biochem* 263:169–175.
- Pedraza N, Solanes G, Carmona MC, Iglesias R, Vinas O, Mampel T, Vazquez M, Giral M, Villarroya F. 2000. Impaired expression of the uncoupling protein-3 gene in skeletal muscle during lactation: Fibrates and troglitazone reverse lactation-induced downregulation of the uncoupling protein-3 gene. *Diabetes* 49:1224–1230.
- Penzo D, Tagliapietra C, Colonia R, Petroni V, Bernardi P. 2002. Effects of fatty acids on mitochondria: Implications for cell death. *Biochim Biophys Acta* 1555:160–165.
- Pierrat B, Ito M, Hinz W, Simonen M, Erdmann D, Chiesi M, Heim J. 2000. Uncoupling proteins 2 and 3 interact with members of the 14.3.3 family. *Eur J Biochem* 267:2680–2687.
- Polster BM, Basanez G, Young M, Suzuki M, Fiskum G. 2003. Inhibition of Bax-induced cytochrome c release from neural cell and brain mitochondria by dibucaine and propranolol. *J Neuroscience* 23:2735–2743.
- Ravagnan L, Roumier T, Kroemer G. 2002. Mitochondria, the killer organelles and their weapons. *J Cell Physiol* 192:131–177.
- Ricquier D, Bouillaud F. 2000. The uncoupling protein homologues: UCP1, UCP2, UCP3, StUCP, and AtUCP. *Biochem J* 345:161–179.
- Sandri M, Carraro U. 1999. Apoptosis of skeletal muscles during development and disease. *Int J Biochem Cell Biol* 31:1373–1390.
- Schrauwen P. 2002. Skeletal muscle uncoupling protein 3 (UCP3): Mitochondrial uncoupling protein in search of a function. *Curr Opin Clin Nutr Metab Care* 5:265–270.
- Stoetzer OJ, Pogrebniak A, Pelka-Fleischer R, Hasmann M, Hidemann W, Nuessler V. 2002. Modulation of apoptosis by mitochondrial uncouplers: Apoptosis-delaying features despite intrinsic cytotoxicity. *Biochem Pharmacol* 63:471–483.
- Subramanian RR, Masters SC, Zhang H, Fu H. 2001. Functional conservation of 14-3-3 isoforms in inhibiting bad-induced apoptosis. *Exp Cell Res* 271:142–151.
- Sun X, Wray CC, Tian X, Hasselgren PO, Lu J. 2003. The expression of uncoupling protein-3 is upregulated in skeletal muscle during sepsis. *Am J Physiol Endocrinol Metab* 285:E512–E520.
- Van Hemert MJ, Steensma HY, Van Exuden GP. 2001. 14-3-3 proteins: Key regulators of cell division, signalling, and apoptosis. *Bioessays* 23:936–946.
- Vidal-Puig A, Solanes G, Grujic D, Flier JS, Lowell BB. 1997. UCP3: An uncoupling protein homologue expressed preferentially and abundantly in skeletal muscle and brown adipose tissue. *Biochem Biophys Res Commun* 235:79–82.
- Vieira HL, Haouzi D, El Hamel C, Jacotot E, Belzacq AS, Brenner C, Kroemer G. 2000. Permeabilization of the mitochondrial inner membrane during apoptosis: Impact of the adenine nucleotide translocator. *Cell Death Differ* 7:1146–1154.
- Villani G, Greco M, Papa S, Attardi G. 1998. Low reserve of cytochrome c oxidase capacity in vivo in the respiratory chain of a variety of human cell types. *J Biol Chem* 273:31829–31836.
- Voehringer DW, Hirschberg DL, Xiao J, Lu Q, Roederer M, Lock CB, Herzenberg LA, Steinman L, Herzenberg LA. 2000. Gene microarray identification of redox and mitochondrial elements that control resistance or sensitivity to apoptosis. *Proc Natl Acad Sci USA* 97:2680–2685.
- Zackova M, Skobisova E, Urbankova E, Jezek P. 2003. Activating omega-6 polyunsaturated fatty acids and inhibitory purine nucleotides are high affinity ligands for novel mitochondrial uncoupling proteins UCP2 and UCP3. *J Biol Chem* 278:20761–20769.
- Zhang CY, Baffy G, Pret P, Krauss S, Peroni O, Grujic D, Hagen T, Vidal-Puig AJ, Boss O, Kim YB, Zheng XX, Wheeler MB, Shulman GI, Chan CB, Lowell BB. 2001. Uncoupling protein-2 negatively regulates insulin secretion and is a major link between obesity, beta cell dysfunction, and type 2 diabetes. *Cell* 105:745–755.

Relationship between the regulation of reactive oxygen species production and mitochondrial-driven apoptosis in skeletal muscle cells. Effects of the mitochondrial uncoupling protein-3.

Yolanda Cámara*, Carine Duval*, Brigitte Sibille# and Francesc Villarroya⁺

From the Departament de Bioquímica i Biologia Molecular. Universitat de Barcelona, 08028-Barcelona. Spain.

Running title: Reactive oxygen species and apoptosis in muscle cells.

* These authors contributed equally to this work.

Present address: Laboratoire de Physiologie des Régulations Énergétiques, Cellulaires et Moléculaires, Centre National de la Recherche Scientifique-Université Claude Bernard Lyon 1, Unité Mixte de Recherches 5123, Villeurbanne, France.

⁺ To whom correspondence should be addressed: Department of Biochemistry and Molecular Biology. University of Barcelona, Diagonal 645, 08028-Barcelona, Spain. Tel: 34-3-4021525; Fax: 34-3-4021559, E-mail: gombau@porthos.bio.ub.es

ABSTRACT

Acquisition of an apoptosis-resistant status is a part of differentiation program of skeletal muscle cells. However, skeletal muscle can undergo apoptosis as a post-mitotic tissue both in response to specific physiological stimuli or in pathological processes. Whereas intracellular redox state and mitochondrial activity are closely related to apoptosis in most cell types, their relative role in apoptotic signalling in muscle cells is unclear. The responsiveness of myoblasts and myotubes of rat L6 to the induction of mitochondrial apoptotic pathways was studied. We show that staurosporine, a mitochondrial apoptotic inducer, promotes ROS generation in myoblasts and myotubes but in a larger extent in non-differentiated stage. This oxidative stress is not required for activation of staurosporine-induced apoptosis in skeletal muscle cells and it does not appear to be involved in the differential sensitivity of myoblasts and myotubes to the apoptotic stimuli. Moreover, the expression of the muscle uncoupling protein UCP3, in myotubes does not affect ROS production although it exerts a slightly sensitization to staurosporine-induced apoptosis, suggesting that this sensitization is achieved by ROS-independent mechanisms.

INTRODUCTION

Apoptosis is a genetically programmed process of cellular self-death that accounts for numerous destructive effects associated with pathological processes, but that is also necessary to ensure normal development and tissue homeostasis. Apoptotic pathways activation can be triggered in response to both external and internal stimuli, starting either in cell membrane death receptors, or in mitochondria. Indeed, In addition to their established function in energy metabolism, mitochondria have a key role in the control of the apoptotic cell death in response to certain stimuli. Several events are important for signalling apoptotic pathway stimuli from mitochondria, especially the release to the cytosol of proapoptotic factors such as cytochrome c, AIF (Apoptosis inducing factor), Smac/Diablo.... Once in the cytosol, these factors collaborate to induce the caspase cascade and nuclear endonuclease activation that together with the loss of mitochondrial functions, finally leads to cell death. Caspase-9 is mainly activated by apoptotic factors of mitochondrial origin, which causes caspase-3 activation, an end-point in the caspase activation cascade (1). Programmed cell death is indeed a process highly regulated by a complex interplay of factors, including anti-apoptotic and pro-apoptotic proteins (such as members of Bcl-2 family, IAPs, etc) that can modulate the process before commitment to cell death is reached.

Reactive oxygen species (ROS) which are major by-products of mitochondrial respiratory chain in non-phagocytic cells are among the factors considered to modulate cell death. Increases in ROS are associated with both the early and late stages of apoptosis regulation, often as side effects of other changes. Excessive ROS production results in oxidative stress, which usually damages cell function and may elicit apoptosis (2-7). However, ROS can also promote cell survival whenever they are not exceeding cellular detoxification capacities (8-10). These beneficial effects of ROS are essentially related to their capacity to act as signaling messengers inside the cell (11; 12) as is evidenced by their ability to induce survival signaling pathways as PI3 kinase, MAP kinases and transcription factors as NFkappa B activation (13). This transcription factor regulates the inducible expression of several genes involved in cell survival and execution (i.e. Bcl-2, Bax, p53, thioredoxin...) (14; 15).

Skeletal muscle is a unique tissue in terms of apoptosis, in particular as regards to differentiated myotubes. Muscle cells are multi-nucleated, and myonuclei can undergo apoptosis individually, maintaining cell integrity and function (16; 17). Moreover, myotubes contain variable mitochondrial content, dependent both on fiber type and the extent of training. However, despite of scarce data on apoptotic pathways in skeletal muscle, several mechanistic have been shown to be similar to those described for other cell types (18). On the other hand, differentiated muscle cells are particularly resistant to apoptosis. Acquisition

of apoptosis resistance occurs during normal skeletal muscle cell differentiation. During early stages of differentiation, myogenic precursor cells withdraw irreversibly from the cell cycle, conferring mature myotubes a resistance to apoptosis. In addition, skeletal muscle exhibits *in vivo* an unusually high concentration of apoptosis repressors (19-23). However, skeletal muscle can undergo apoptosis as a post-mitotic tissue, both in response to specific physiological stimuli or in pathological processes (24-26). Whereas intracellular redox state and mitochondrial activity are closely related to apoptosis in most cell types, their relative role in apoptotic signaling in muscle cells is unclear. Skeletal muscle is a highly specialized tissue in which mitochondrial ROS production is relevant to physiological (i.e. contraction, exercise) or pathological situations. Indeed, oxidative stress appears to be associated to myogenic cell death activation in conditions such as ageing (27), muscle dystrophy (28-30), ischemia/reperfusion (31) and others.

The uncoupling proteins (UCPs) belong to the super-family of mitochondrial anion carriers located in the inner mitochondrial membrane. UCP1 was the first member to be identified. It is exclusively expressed in brown adipose tissue where it behaves as a natural uncoupler of oxidative phosphorylation (32). It increases proton conductance of the mitochondrial inner membrane with the consequent production of heat. Its activity requires of the presence of free fatty acids and it is inhibited by purine nucleotides. New members of the family have been recently characterized. Among these ones, there is UCP3, which is preferentially expressed in skeletal muscle and in a minor extent also in heart, white adipose tissue, and neuronal cells (33). Whereas UCP1 role in the generation of heat is clearly established, the physiological function of UCP3 is still a matter of current debate. Although its ability for uncoupling has been proved *in vitro*, it is not clear that this activity is closely related to its actual function *in vivo*. Moreover, its expression is dramatically induced in response to metabolic stress signals such as an increase in free fatty acids concentration in blood, the action of TNF α , cancer cachexia or sepsis. Evidence suggests that it may not have a role in energy dissipation. Indeed, several data have recently suggested a possible role for UCP3 in the control of ROS production and cell death sensitivity. Maximal ROS production is associated with high membrane potential (34; 35). Therefore, it has been suggested that a UCP3-driven mild uncoupling could decrease membrane potential beneath a threshold that avoids ROS production. In this sense, the only observed modification in *ucp3*^{-/-} mice is that skeletal muscle mitochondria lacking UCP3 are more coupled and generate more ROS than mitochondria from wild type animals, according to a UCP3 induced-mild uncoupling (36). On the other hand, superoxide anion itself and lipid peroxidation products such as 4-hydroxy-nonenal have been shown to induce UCP3-mediated proton conductance (37; 38). There is a widespread consensus that one of the biological activities of mitochondrial UCPs (at least UCP2 and UCP3), in addition to its metabolic effects promoting substrate oxidation, is to

influence ROS production in mitochondria. Mild uncoupling, such as that originated by UCP activity, has long been known to reduce ROS production in association with reduction with mitochondrial proton-motive potential. Therefore, UCP3 amount and activity may control responsiveness of skeletal muscle cells to challenges involving mitochondrial activity, either by controlling ROS production or by other mechanisms that remain to be explored. While in neuronal cells UCP3 seems to have a protective role against pro-apoptotic stimuli such as hyperglycaemia (33; 39), we have previously reported that this protein sensitized human kidney cells to a mitochondrial dependent stimulus of apoptosis (40). This is in agreement with the observation that UCP3 expression is among the first events leading to muscle damage in amyotrophic lateral sclerosis (41). So it appears that UCP3 effects on ROS and cell death modulation strongly depend on type cell.

Little is known about ROS effects and their relationship to cell death in skeletal muscle. Besides high complexity of these studies due to special characteristics of differentiated muscle cells, it should be noted that this effects may depend on differentiation stage. In this study, we first have analysed basal redox state along myogenic differentiation of rat skeletal muscle cells: L6 cells. Then we have analyzed responsiveness of L6 myoblasts and myotubes to a pro-apoptotic stimuli known to involve mainly mitochondrial pathways, such as staurosporine (42-44), to determine possible ROS involvement in this process regulation. It is concluded that staurosporine promotes ROS generation in skeletal muscle cells; myoblasts as myotubes but in a larger extend in non-differentiated stages. However, this oxidative stress is not required for activation of staurosporine-induced apoptosis in skeletal muscle cells and it does not appear to be involved in the differential sensitivity of myoblasts and myotubes to the apoptotic stimuli. On the other hand, UCP3 over-expression on myotubes does not affect ROS production although it exerts a slightly sensitization to staurosporine-induced apoptosis, suggesting that this sensitization is achieved by mechanisms independent of ROS generation.

MATERIAL AND METHODS

Chemicals and reagents

DMEM with Glutamax[®], phenol red free RPMI-1640, and fetal bovine serum (FBS) were purchased from GIBCO (Grand Island, N.Y.). The ROS-sensitive fluorescent probe 6-carboxy-2', 7'-dichlorodihydrofluorescein diacetate, diacetoxymethyl-ester (H₂-DCFDA; DCF, 2', 7' -dichlorodihydrofluorescein) and monochlorobimane were purchased from Molecular Probes (Eugene, OR, U.S.A) and dissolved in DMSO and acetonitrile respectively.

Staurosporine was purchased from Sigma-Aldrich and dissolved in DMSO. Other reagents and chemicals were obtained from Sigma, Merck and Roche.

Cell culture

Rat L6 cells (ATCC Rockville, MD, USA) were grown in Dulbecco's minimal essential medium (DMEM) containing 10% fetal bovine serum (FBS). To induce differentiation, L6 cells at 80% confluence were placed in DMEM containing 2% FBS. L6 were then maintained for 5 days in these conditions of culture to acquire myotube morphology. Mouse C2C12 cells (ATCC Rockville, MD, USA) were grown in Dulbecco's minimal essential medium (DMEM) containing 10% fetal bovine serum (FBS). To induce differentiation, C2C12 cells at 80% confluence were placed in DMEM containing 2% Horse serum (HS). C2C12 were then maintained for 5 days in these conditions of culture to acquire myotube morphology.

Determination of intracellular ROS

The H₂-DCFDA probe was used to estimate the generation of intracellular ROS (45; 46). After incubation with 10 μ M H₂-DCFDA for 1 h, cells were washed twice with PBS and scraped into water. After sonication, the fluorescence of H₂-DCFDA stained cells was measured with a spectrofluorometer (excitation wavelength 493 nm, emission wavelength 527 nm).

Reduced glutathione determination

The intracellular content of reduced GSH was determined using monochlorobimane, a thiol-reactive probe. Total cellular extracts were labeled with 20 μ M of monochlorobimane. After 2h of incubation, fluorescence was quantified at excitation and emission wavelengths of 380 nm and 460 nm, respectively, using a spectrofluorimeter. A standard curve was generated with known amounts of reduced GSH to infer GSH concentration in samples.

Caspase 3 activity

Caspase 3 activity was measured using the fluorimetric CaspACE Assay System (Promega) based on the fluorimetric detection of amino-4-trifluoromethyl coumarin after proteolytic cleavage of the synthetic substrate DEVD-amino-4-trifluoromethyl coumarin. Cells were exposed to staurosporine and were homogenized by 15 strokes of a 22G syringe in cell "lysis buffer" (25 mM Hepes, 5 mM MgCl₂, 5mM EDTA, 5 mM DTT, 2mM PMSF, 10 µg/ml pepstatin A, 10 µg/ml leupeptin). To assure complete disruption of cellular homogenates, they were finally lysed by 3 cycles of freezing/thawing and cytosolic extracts to be assayed were collected after 10.000 x g centrifugation for 20 min. 100 µg protein, as determined by the Bradford Assay Kit (Bio-Rad), were used for the assays, which were performed as indicated by the supplier (Promega). Specificity of the assay was assessed by the use of CPP32 caspase 3 inhibitor, which led in all the assays to a residual activity of less of a 5% of the total activity detected (Promega).

Immunoblot analysis

Samples of homogenates or mitochondria were separated by SDS-PAGE on 12.8% and transferred to polyvinylidene fluoride membranes (PVDF membranes) (Immobilon-P, Millipore). They were incubated with antibodies against UCP3 (Chemicon AB3046 (1:1000)), caveolin-3 (BD Pharmingen 610421 (1:1000)) or VDAC (Calbiochem Anti-Porin 31HL (1:1000)). VDAC detection was used to ensure equal loading of mitochondria. The binding of antibodies was detected with a horseradish peroxidase-coupled anti-mouse (Bio-Rad 170-6516 (1:3000)) or anti-rabbit (Santa Cruz sc-2004 (1:3000)) secondary antibody, and an enhanced chemiluminescence (ECL) detection kit (Amersham).

Nuclear extract preparation

Extracts were prepared using a modified method from Zamora et al. (47). For the isolation of nuclear protein extracts of either L6 myoblasts or myotubes, cells were washed twice with ice-cold PBS and scrapped off the plates in buffer A (10 mM Hepes, pH 7.9, 10 mM KCl, 0.1 mM EDTA, 0.1 mM EGTA, 1 mM dithiothreitol, 0.5 mM PMSF, and protease inhibitors (5 µg/ml each of aprotinin, leupeptin, and pepstatin)). Cells were allowed to swell on ice for 15 min; then 25 µl of Nonidet P-40 (0.5%) was added, and the suspension was thoroughly mixed for 10 s. The homogenate was centrifuged (16.000 x g, 4°C, 60 s.), and the nuclear pellet was resuspended in 50 µl of ice-cold buffer C (20 mM Hepes, pH 7.9, 0.4 M NaCl, 1 mM EDTA, 1 mM EGTA, 1 mM dithiothreitol, 1 mM PMSF, and protease inhibitors (5 µg/ml each of aprotinin, leupeptin, and pepstatin)). Nuclear lysates were maintained on ice for 15 min with occasional mixing. The nuclear extract was cleared (16.000 x g, 4°C, 5 min),

and the supernatant containing the proteins from the nuclear extract was transferred to a fresh tube and stored at -80°C . Protein concentrations were determined by the Bradford assay (Bio-Rad).

Electrophoretic Mobility Shift Assay

Nuclear extracts from L6 myoblasts or myotubes were used in electrophoretic mobility shift assays. For gel retardation assays, a double stranded oligonucleotide containing a consensus NF κ B DNA binding site (5'-TCT AGA GTT GAG GGG ACT TTC CCA G-3', obtained from Roche Applied Science) was end-labeled using [α - ^{32}P]dCTP and Klenow enzyme. Nuclear protein extracts (10 μg) were incubated for 30 min at room temperature with binding buffer (25 mM Hepes, pH 7.6, 0.5 dithiothreitol, 12.5 mM ZnSO_4 , 50 mM KCl, 1 mg/ml bovine serum albumin, 5% glycerol, 0.1% Nonidet P-40, and 2.5 μg of poly(dI-dC) (deoxyinosinic-deoxycytidylic acid)). The DNA probe (30,000 cpm) was added and incubated for 20 min at room temperature. Samples were run on 5% non-denaturing polyacrilamide gels in 0.5 X Tris-borate-EDTA at 130 V and 4°C for 60 min. Specific NF κ B activity was assessed in competition tests. In these assays, random samples were pre-incubated with 100-fold molar excess of unlabeled doubled-stranded oligonucleotides before the addition of the DNA probe to compete specific NF κ B binding.

Real time PCR

Total RNA was extracted from cells using the method of the Tripure Isolation Reagent (Boehringer Mannheim). Quantitative mRNA expression analysis was done in a two-step reaction: first, 1 μg of total RNA was transcribed into cDNA by means of RT-PCR (real time reverse transcriptase chain reaction) on the GeneAmp PCR system 2400 (Applied Biosystems, USA), and then, a Real-Time PCR was performed on the ABI PRISM 7700HT sequence detection (Applied Biosystems, U.S.A). The RT-PCR was done in a final volume of 50 μl using TaqMan[®] Reverse Transcription Reagents (Applied Biosystems, U.S.A), which contains MultiScribe[™] Reverse Transcriptase, RNase inhibitor, dNTP Mixture, Random Hexamers, 10X RT buffer, and MgCl_2 solution. TaqMan[®] Real-Time PCR reaction was performed in a final volume of 25 μl using TaqMan[®] Universal PCR Master Mix, and gene expression probes (Applied Biosystems, U.S.A) for rat L6 cell samples: 18S ribosomal RNA (Hs99999901_s1), glutathione peroxidase-1 (Rn00577994_g1), uncoupling protein-2 (Rn00571166_m1), uncoupling protein-3 (Rn00565874_m1), superoxide dismutase-2 (Rn00566942_g1), and superoxide dismutase-1 (Rn00584772_m1), and gene expression probes for mouse C2C12 cell samples: uncoupling protein 3 (Mm00494074_m1), uncoupling protein 2 (Mm00495907_g1), myogenin (Mm00446194_m1), PGC-1 α (Mm00447183_m1),

glutathione peroxidase 1 (Mm00656767_g1), glutathione peroxidase 4 (Mm00515041_m1), heme oxygenase 1 (Mm00516004_m1), superoxide dismutase 2 (Mm00449726-m1), sequestosome 1 (Mm00448091_m1), c-fos (Mm00487425_m1), c-jun (Mm00495062_s1), Transformation relation protein 53 (Mm00441964_g1), Nfkb1 (p105) (Mm00476361_m1), carnitine palmitoyltransferase 1 (Mm00487200_m1), acetyl-Coenzyme A dehydrogenase, medium chain (Mm00431611_m1). Appropriate controls with no RNA, primers, or reverse transcriptase were included in each set of experiments. Each sample was run in duplicate, and the mean value of the duplicate was used to calculate the mRNA expression of the gene of interest. The quantity of the gene of interest in each sample was normalized to that of the endogenous control using comparative ($2^{-\Delta CT}$) method according to manufacturer's instructions (Applied Biosystems, U.S.A). 18S was used as endogenous control gene.

Statistical analysis

Data, shown as means \pm SEM, were analyzed with Student's t-test for determination of the significance of differences, which were considered to be significant at a P value of less than 0.05.

RESULTS

Changes in ROS production, glutathione content, NFkappaB activity and oxidative-stress related gene expression in differentiating myogenic L6 cells.

We studied changes in oxidative stress related parameters in differentiating myogenic L6 cells. First, intracellular ROS content was measured using the H₂-DCFDA probe (for details, see material and methods). The profile of intracellular ROS level along the myogenic differentiation is shown figure 1 A. The initiation of differentiation (day 1) is linked to a decrease in intracellular ROS of about 60% compared to the value obtained in myoblasts (day 0). From day 2 to day 5 of differentiation, intracellular ROS level increases to about 60% (day 2) or even up to 115 % (day 5) of myoblasts content. It is concluded that although no significant difference is observed in intracellular ROS generation between myoblasts and differentiated myotubes at day 5, the process of myogenic cells differentiation is associated with a transient decrease in intracellular ROS. The intracellular GSH is also modified along L6 differentiation being 82 ± 6 % in myotubes respected to myoblasts ($p \leq 0.05$). L6 differentiation is associated with a progressive decrease of basal NFkappa B activation starting from first day of differentiation (Fig 1C). As changes in ROS content could be due to differential antioxidant capacity along myogenic differentiation, we studied the gene expression of three main antioxidant enzymes: the cytosolic superoxide dismutase (SOD1), the mitochondrial superoxide dismutase (SOD2), and the cytosolic glutathione peroxidase (Gpx1) (Fig 1D). For the three mRNA, there was a progressive decrease during differentiation although the intensity of the decrease was variable. A significant decrease was reached in day 2 of differentiation for SOD1 mRNA, in day 4 of differentiation for SOD2 mRNA and in day 1 of differentiation for Gpx1 mRNA. For the three genes, mRNA expression in day 5 myotubes was less than 50% that in myoblasts.

Concerning UCPs, UCP2 mRNA was progressively down-regulated throughout the myogenic differentiation process, similarly to the observations for mRNA expression of the oxidative-stress related genes. Conversely, UCP3 mRNA was induced in association with the differentiation process, in parallel with the induction of expression of marker genes of myogenesis (myogenin), as expected.

Differential responsiveness to the apoptotic inducer staurosporine in myoblasts and myotubes.

In order to compare the responsiveness of myogenic differentiating L6 cells to an apoptotic stimulus involving mitochondrial pathways, myoblasts and myotubes (day 5 of differentiation) were exposed to staurosporine, a pro-apoptotic reagent acting through

mitochondrial dependent mechanisms. For this purpose, we studied the activation of caspases. A dose-response analysis of the effect of staurosporine treatment during 4 hours on caspase-3 activity in myoblasts and myotubes is shown figure 2A. Staurosporine induces a significant increase in caspase-3 activity in a dose dependent manner, in myoblasts and myotubes but the extent of induction was completely different depending on differentiation stage. In myoblasts, a two-fold increase in caspase-3 activity is observed after exposing cells to 0,5 μM of staurosporine for 4 hours, whereas this increase is only achieved in myotubes after a dose of 2 μM of staurosporine. The greatest significant difference in caspase-3 activity induction between myoblasts and myotubes is observed at a dose of 5 μM staurosporine, reaching an eight-fold induction in myoblasts, and only a two-fold induction in myotubes. These results indicate a significant difference of sensitivity to staurosporine between myoblasts and myotubes. As caspase-3 activation is considered to be an end-point in the apoptotic cascade involving either mitochondrial dependent and mitochondrial independent pathways, we next determined which was the myoblast and myotube responsiveness to staurosporine in terms of caspase-9 activation which is known to occur via mitochondrial pathways (1). As expected, no basal activation of caspase-9 was observed in untreated myoblasts and myotubes. Treatment with growing concentrations of staurosporine induced a significant activation of caspase-9 both in myoblasts and myotubes (Fig 2B). However, caspase-9 induction in response to 5 μM of staurosporine was greater in myoblast than in myotubes. These results demonstrate that staurosporine can induce apoptosis in both L6 myoblasts and myotubes through a mitochondrial-dependent pathway; and that myoblasts are more sensitive than myotubes to the induction of apoptosis via mitochondrial pathways.

Changes in ROS, GSH, and NFKappa B activation in myoblasts and myotubes in response to the apoptotic inducer, staurosporine.

We assessed oxidative stress in myoblasts and myotubes treated with staurosporine. As shown in Figure 3A, staurosporine induces an increase in intracellular ROS generation in a dose-dependent manner, in myoblasts and myotubes. Treatment with 2 μM staurosporine for 4 hours induces an increase of intracellular ROS generation of around two fold in myoblasts but only a 10 % increase was observed in myotubes. The highest increase in intracellular ROS generation is attained in myoblasts at 2 μM staurosporine. Such an increase requires 10 μM staurosporine in myotubes (150% of untreated control).

Staurosporine can also decrease the levels of intracellular GSH in a dose dependent manner, as shown in Fig 3B. Again, myoblasts respond with a more marked decrease in GSH and at lower concentrations of staurosporine than myotubes. The decrease in GSH in myotubes is observed only in treatments of staurosporine higher than 5 μM . However, in

myoblasts, the decrease in GSH is observed with staurosporine treatment from 0,1 to 5 μ M. On the contrary, higher concentrations of staurosporine, induced in myoblasts, an increase in intracellular GSH. Then GSH content has in both differentiating stages biphasic and opposite behaviour. We studied the staurosporine-induced activation of NFkappa B in myoblasts and myotubes. Basal NFkappa B activation is very low in myoblasts and in myotubes. We observed that staurosporine can activate NFkappa B in a dose dependent manner in myotubes (Fig 3C), with a maximum activation with 20 μ M staurosporine. In contrast, maximum activation is obtained in myoblasts at 5 μ M staurosporine. We conclude that staurosporine induces oxidative stress in myoblasts and in myotubes but the extent of response depends on differentiation stage, being higher in non-differentiated cells for any oxidative stress-related parameter tested.

Role of ROS scavengers on the apoptotic responsiveness of myoblasts to myotubes to staurosporine.

In order to establish whether the oxidative stress induced by staurosporine in myoblasts and myotubes is implicated in the apoptotic process, we used different approaches.

First, we observed that the pre-incubation of cells with ascorbic acid or trolox, two soluble ROS scavengers, could block the staurosporine induced-ROS production in myoblasts and myotubes (Fig 4A). However, ROS scavengers did not influence staurosporine-induced caspase-3 activity (Fig 4B). The same results were obtained for caspase-9 (data not shown). The staurosporine-induced activation of NFkappa B was also insensitive to antioxidants. Indeed, we observed (Fig 4C), that staurosporine-induced NFkappa B activation (at 5 μ M and 10 μ M of staurosporine) by ascorbic acid or trolox was even increased in both myotubes and myoblasts. These results show, that staurosporine induced-intracellular ROS are not involved in the apoptotic responsiveness to staurosporine neither in myoblasts nor in myotubes, and that NFkappa B activation induced by staurosporine is independent on ROS generation in both differentiation stages.

In order to determine the role of ROS to elicit apoptosis and NFkappaB activity, we studied the effect of hydrogen peroxide on caspase-3 induction and NFkappaB activation. H₂O₂ treatment alone for 1 hour can induce caspase-3 activation only at a low concentration (ranging from 0.1 to 0,5 mM) and again, mainly in myoblasts (Fig 5A). At higher concentrations (from 1mM to 2,5mM) H₂O₂ didn't induce caspase-3 activation, probably due to a direct toxic effect of hydrogen peroxide as is shown by a significant decrease in protein content on cellular extracts of these cells (Data not shown). In myotubes, H₂O₂ causes a minor activation of caspase 3, much lower than that attained in myoblasts. To determine

whether ROS induced during staurosporine treatment could play a protective role against apoptosis, we investigated the role of H₂O₂, on staurosporine-induced apoptosis in myoblasts and myotubes. Results (Fig 5B) demonstrate that H₂O₂, enhances staurosporine-induced caspase-3 activation in myoblasts. Whereas it doesn't have any effect on staurosporine-induced caspase-3 activity in myotubes.

We also investigated the role of H₂O₂ treatment on NFkappa B activation in myoblasts and myotubes. Results, show that H₂O₂ is able to induce NFkappa B activation in both myoblasts and myotubes, but the profile of activation is different between differentiation stages. Indeed, NFkappa B activation appears in myoblasts at 0,25 mM H₂O₂, whereas it is necessary to treat myotubes with at least 5mM H₂O₂ to obtain the same extent of NFkappa B activation observed in myoblasts at 0,25 mM H₂O₂. In conclusion, ROS themselves can induce apoptosis at least in non-differentiated cells and they are not in any case triggering any efficient protective response against staurosporine-induced cell death in spite of being efficient inducers of NF kappa B activation.

We tested the effect of GSH depletion on ROS production and activation of apoptotic pathways. For this purpose, we used buthionine sulfoximine which inhibits the "de novo" synthesis of GSH, by blocking the GSH synthase. Treatment of cells with 250 µM of buthionine sulfoximine overnight permits the reduction of at least 60% of intracellular GSH in myoblasts and in myotubes (Fig 6A). 10 µM staurosporine did not modify significantly GSH levels in myoblasts and reduce slightly in myotubes. However, in the presence of buthionine sulfoximine (BSO), levels of GSH were lowered when staurosporine was present in the medium to a similar extent than when staurosporine had not been added (Fig 6A). Figure 6 B shows that depletion of GSH neither affect basal levels of ROS nor the extent of induction of ROS in response to staurosporine in myoblasts and myotubes. Finally, we studied caspase-3 activation in myoblasts and myotubes treated with staurosporine, either in the presence or in the absence of buthionine sulfoximine. The results show (Fig 6C) that depletion of intracellular GSH doesn't enhance the staurosporine-induced caspase-3 activation, suggesting that neither ROS, nor GSH depletion are involved in staurosporine-induced apoptosis in myoblasts or myotubes.

Effect of UCP3 on the relationship between ROS and apoptotic responsiveness of myotubes

In order to analyse the effects of UCP3 in L6 muscle cells differentiated in culture, a recombinant adenoviral vector containing the full-length cDNA for the human UCP3 was used (AdCMV-UCP3). A time response of infection with this adenoviral vector AdCMV-UCP3 was performed (Fig 7) and compared with an adenoviral control AdCMV-LacZ, driving beta-Galactosidase (Lac Z-control). We show that UCP3 expression begins to be detected 12

hours after transduction, as shown in Fig 7, and reaches a maximum expression level 48h after transduction. Equal loading of mitochondrial proteins was assessed by parallel detection of the mitochondrial protein VDAC (Fig 7). The absence of significant changes in caveoline-3 detection allows us to confirm that transduction of the adenoviral vector didn't alter the normal differentiation process in L6 cells. Moreover, the levels of UCP3 obtained after 48 hours of transduction were in the range of physiological levels in skeletal muscle from high-fat treated rats (data not shown). The expression of high levels of UCP3 in L6 myotubes led to a significant reduction of about 37.1 ± 7.4 % $p \leq 0,05$ in $\Delta\Psi_m$ respect to cells transduced with the adenoviral vector control. $\Delta\Psi_{min}$ in UCP3-expressing myotubes was intermediate between the $\Delta\Psi_m$ of control cells and the $\Delta\Psi_m$ in cells treated with 5 μ M CCCP (about 4.8 ± 0.7 % of control $\Delta\Psi_m$, $p \leq 0,05$). Confocal microscopy examination of cultured myotubes after treatment with the $\Delta\Psi_m$ -sensitive compound JC-1 indicated a homogenous decrease in the $\Delta\Psi_m$ -dependent fluorescence (590/527 fluorescence ratio) in mitochondria from myotubes transduced with the AdCMV-UCP3 vector (data not shown). L6 myotubes expressing UCP3 were treated with growing concentrations of staurosporine for 4 hours. The presence of UCP3 didn't induce *per se* caspase-3 activation in myotubes. UCP3 didn't protect staurosporine-induced caspase-3 induction, but the opposite, it led to a moderate enhancement in the activation of caspase-3 by staurosporine (Fig 8A). Exposure of cells to 10 μ M CCCP overnight, followed by staurosporine treatment, didn't affect caspase-3 activation suggesting that the effect of UCP3 on apoptosis responsiveness doesn't involve $\Delta\Psi_m$ (Fig 8A). Moreover, UCP3 expression in L6 myotubes slightly increased the abundance of cleaved-caspase 9 in response to staurosporine in comparison to the levels achieved in cells transduced with LacZ adenoviral vector. These results indicate that UCP3 does not protect but sensitizes cells to staurosporine-induced apoptosis in myotubes. On the other hand, the presence of UCP3 neither decreased basal intracellular ROS generation (Fig 9A) nor modified staurosporine-induced intracellular ROS production. Moreover, we observed no significant changes due to the presence of UCP3 on staurosporine-induced NFkappa B activation (Fig 9B).

Effect of UCP3 on gene expression in myotubes

We investigated the effect of UCP3 transduction on the expression of mRNAs of genes potentially related to ROS metabolism and oxidative stress in differentiated L6 myotubes. We observed no major changes in any of the analyzed genes but for UCP2 expression that was significantly decreased (Table 1) due to the presence of UCP3.

We expanded our gene expression analysis to a more wide set of genes, and for this purpose we transduced C2C12 myotube cells with the same procedure previously detailed for L6 cells, to induce UCP3 expression. At a MOI of 100, UCP3 levels were in the same range as those obtained in L6 cells (data not shown). Neither genes corresponding to anti-oxidant machinery, nor UCPs, nor genes related to cellular stress were modified by the presence of high UCP3 levels. The only significant change observed was a near two-fold induction of mitochondrial carnitine palmitoyl transferase-1.

DISCUSSION

Present findings indicate that the responsiveness of apoptotic activation to staurosporine, an inducer of apoptosis involving mitochondrial pathways, is lowered in differentiated rat L6 muscle cells. This is consistent with the resistance to apoptosis occurring in muscle fibers "in vivo" (48) despite it is also known that numerous skeletal muscle myopathies and physiological processes such as ageing or exercise are associated with apoptosis in skeletal muscle (24; 25; 27; 49; 50). Present findings confirm that the appearance of resistance to activate apoptotic pathways occurs at the cellular level, in association with the acquisition of the differentiated status of the muscle cell, and it implicates apoptotic pathways elicited preferentially by mitochondrial-dependent mechanisms, such as caspase-9 activation. Multiple reasons for the resistance to apoptosis in differentiated muscle cells have been proposed, among them the high expression of anti-apoptotic proteins (21; 22). We attempted to establish the role of ROS production and signalling in the triggering of apoptosis in muscle cells, particularly when mitochondrial-dependent pathways are involved.

During myogenic differentiation of L6 cells, we observed that the basal levels of ROS are reduced only in initial stages of the differentiation process but not in fully differentiated myotubes. Our present data indicate that staurosporine increase ROS levels, but, similarly to apoptotic pathways, this induction is diminished in differentiated myotubes. Activation of NFkappaB, traditionally considered as a sensor of oxidative stress mediating transcriptional responses, was equally impaired in myotubes exposed to staurosporine. However, with the use of ascorbic acid or trolox, we demonstrate that NFkappa B activation due to staurosporine is independent of staurosporine-induced ROS in myoblasts and myotubes. It is known that the capacity of oxidative stress to activate NFkappa B depends on the type of cell or stimulus, and NFkappa B isn't always activated by ROS (51; 52) Moreover, staurosporine is known to induce apoptosis by acting on distinct cell processes, suggesting that different pathways could be responsible for NFkappa B activation in myoblasts and myotubes.

The status of myotubes respect to myoblasts in relation to the anti-oxidant system did not explain this refractoriness to increase ROS levels in response to staurosporine as both GSH content and gene expression for enzymes of the anti-oxidant system are down-regulated in myotubes respect to myoblasts. Thus, it is likely that it was the extent of ROS production itself what is impaired in response to staurosporine. The parallel impairment in ROS production and in apoptotic activation in myotubes suggests the possibility that it was the reduced ROS production the main mechanism explaining lowered apoptotic activation in myotubes. Direct assessment of this possibility did not support such statement. Blunting the

up-regulation of ROS levels in response to staurosporine by the use of anti-oxidants did not impair at all the activation of caspase-3 or caspase-9 neither in myoblasts nor in myotubes. Thus, it appears that in myogenic cells, regardless of their stage of differentiation, apoptotic activation by staurosporine did not require a rise in ROS levels. Another approach in the same direction, i.e. reduction of some of the anti-oxidant system by depletion of GSH, led to the same conclusion: no effect on the sensitivity of myoblasts and myotubes to the activation of apoptotic pathways. When cells were directly challenged with oxidative stress through the exposure to hydrogen peroxide, we could observe an activation of apoptotic pathways but myotubes showed also refractoriness to apoptotic activation in terms of caspase-3 and caspase-9 activation, thus indicating that resistance of myotubes to activate apoptosis occur also in response to a direct stimulus of oxidative stress. Similar observations have been reported in other myogenic cells lines (53). The additivity of the effects of staurosporine and hydrogen peroxide in eliciting apoptotic activation further supports that the mechanisms of activation of apoptosis in myogenic cells involve mechanisms other than an increase in ROS. In fact, agents other than staurosporine, like palmitate at high concentration, are capable of eliciting a rise in ROS levels in myotubes similar to that obtained with staurosporine, without leading to any activation of caspases (Duval, Camara and Villarroja, unpublished observations) thus indicating that a physiological induction of ROS is not enough to trigger apoptotic activation.

Current concepts on the role of UCP3 obtained from studies on isolated mitochondria indicate that a potential role for this mitochondrial protein could be to reduce ROS production and therefore it has been proposed that UCP3 could constitute a potential mechanism of protection against excessive ROS production in response to metabolic challenges or other stressor (36; 38; 54-56). UCP3 is preferentially expressed in skeletal muscle and such a role would be expected to be specifically relevant in skeletal muscle cells. Thus, UCP3 could constitute a system of protection for excessive ROS production, in this case behaving not as a scavenger of already produced ROS, like the chemical or enzymatic anti-oxidant systems, but acting as a modulator of the generation of ROS in mitochondria, due to its ability of mild uncoupling. However, no direct assessment of this proposal in muscle cells, has been reported to date. UCP3 gene expression is practically undetectable in myoblasts and its expression is associated with myogenic differentiation. However, the UCP3 levels attained in differentiated muscle cells either from myogenic cell lines or primary cultures of myoblasts differentiated into myotubes in culture are much lower than skeletal muscle *in vivo* (57; 58)). We induced UCP3 in mitochondrial from L6 myotubes at levels similar to those found in muscle "in vivo" by the use of an adenoviral vector, and we determined the behavior of the cells in relation to ROS production and apoptotic responsiveness in comparison with

myotubes transduced with a control vector. Results indicated that the presence of high levels of UCP3 caused a mild reduction in mitochondrial membrane potential, but had no significant consequences in patterns of gene expression for components of the antioxidant cellular system nor in gene markers of cell stress. The presence of UCP3 had no consequences on ROS levels in myotubes, neither in basal conditions nor in response to staurosporine. For apoptotic activation, UCP3 did not protect but the opposite, it caused a mild sensitization in the responsiveness of myotubes to staurosporine. These findings indicate that, despite UCP3 acts as a mitochondrial uncoupler, in the cellular context of myogenic cells, this does not modify significantly the ROS status. The sensitization effect observed for apoptotic activation is not likely to be related to ROS considering the lack of specific effects of UCP3 and, in general, the absence of a significant involvement of ROS in the activation of apoptotic pathways in myogenic cells described above. These findings are consistent with those already reported in 293-HEK cells induced to express UCP3 (40) and contrast with those reported in dorsal root ganglion neurons indicating a protective effect of UCP3 respect to apoptotic activation in response to hyperglycemia (33). It is possible that the specificity of cell environment or the type of stimuli led to opposite consequences of the presence of a high UCP3 activity in relation to the activation of cell death. This is similar to what has been reported to UCP2, which can favor or impair cell death depending on the cell context or type of stimulus (59-61).

As we have shown, UCP3 expression is increased along myogenic differentiation in L6 cells. On the other hand, UCP2 mRNA is decreased during L6 differentiation in a profile similar to that observed for anti-oxidant enzymes (SOD2, Gpx1, SOD1).

ACKNOWLEDGEMENT

This work was supported by grant SAF-2002-03648 from the Ministerio de Ciencia y Tecnología. Y. Camara was supported by the Spanish Ministry of Education. C Duval was supported by fellowships from the “Fondation pour la Recherche Médicale” and from the “Association Française contre les Myopathies”.

REFERENCES

1. Kuida K. Caspase-9. *Int J Biochem Cell Biol* 2000;32:121-124.
2. Fiordaliso F, Bianchi R, Staszewsky L, Cuccovillo I, Doni M, Laragione T, Salio M, Savino C, Melucci S, Santangelo F, Scanziani E, Masson S, Ghezzi P, Latini R. Antioxidant treatment attenuates hyperglycemia-induced cardiomyocyte death in rats. *J Mol Cell Cardiol* 2004;37:959-968.
3. Lyamzaev KG, Izyumov DS, Avetisyan AV, Yang F, Pletjushkina OY, Chernyak BV. Inhibition of mitochondrial bioenergetics: the effects on structure of mitochondria in the cell and on apoptosis. *Acta Biochim Pol* 2004;51:553-562.
4. McCarthy S, Somayajulu M, Sikorska M, Borowy-Borowski H, Pandey S. Paraquat induces oxidative stress and neuronal cell death; neuroprotection by water-soluble Coenzyme Q10. *Toxicol Appl Pharmacol* 2004;201:21-31.
5. Raha S, Robinson BH. Mitochondria, oxygen free radicals, and apoptosis. *Am J Med Genet* 2001;106:62-70.
6. Thirunavukkarasu C, Watkins S, Harvey SA, Gandhi CR. Superoxide-induced apoptosis of activated rat hepatic stellate cells. *J Hepatol* 2004;41:567-575.
7. Zhao Y, Oberley TD, Chaiswing L, Lin SM, Epstein CJ, Huang TT, St Clair D. Manganese superoxide dismutase deficiency enhances cell turnover via tumor promoter-induced alterations in AP-1 and p53-mediated pathways in a skin cancer model. *Oncogene* 2002;21:3836-3846.
8. Haendeler J, Tischler V, Hoffmann J, Zeiher AM, Dimmeler S. Low doses of reactive oxygen species protect endothelial cells from apoptosis by increasing thioredoxin-1 expression. *FEBS Lett* 2004;577:427-433.
9. Kim H, Kim YN, Kim H, Kim CW. Oxidative stress attenuates Fas-mediated apoptosis in Jurkat T cell line through Bfl-1 induction. *Oncogene* 2005;24:1252-1261.
10. Vaquero EC, Edderkaoui M, Pandol SJ, Gukovsky I, Gukovskaya AS. Reactive oxygen species produced by NAD(P)H oxidase inhibit apoptosis in pancreatic cancer cells. *J Biol Chem* 2004;279:34643-34654.
11. Fleury C, Mignotte B, Vayssiere JL. Mitochondrial reactive oxygen species in cell death signaling. *Biochimie* 2002;84:131-141.
12. Herrlich P, Bohmer FD. Redox regulation of signal transduction in mammalian cells. *Biochem Pharmacol* 2000;59:35-41.
13. Allen RG, Tresini M. Oxidative stress and gene regulation. *Free Radic Biol Med* 2000;28:463-499.

14. Karin M, Lin A. NF-kappaB at the crossroads of life and death. *Nat Immunol* 2002;3:221-227.
15. Prieto-Alamo MJ, Jurado J, Gallardo-Madueno R, Monje-Casas F, Holmgren A, Pueyo C. Transcriptional regulation of glutaredoxin and thioredoxin pathways and related enzymes in response to oxidative stress. *J Biol Chem* 2000;275:13398-13405.
16. Borisov AB, Carlson BM. Cell death in denervated skeletal muscle is distinct from classical apoptosis. *Anat Rec* 2000;258:305-318.
17. Tews DS, Goebel HH. DNA-fragmentation and expression of apoptosis-related proteins in muscular dystrophies. *Neuropathol Appl Neurobiol* 1997;23:331-338.
18. McArdle A, Maglara A, Appleton P, Watson AJ, Grierson I, Jackson MJ. Apoptosis in multinucleated skeletal muscle myotubes. *Lab Invest* 1999;79:1069-1076.
19. Cho DH, Hong YM, Lee HJ, Woo HN, Pyo JO, Mak TW, Jung YK. Induced inhibition of ischemic/hypoxic injury by APIP, a novel Apaf-1-interacting protein. *J Biol Chem* 2004;279:39942-39950.
20. Gustafsson AB, Tsai JG, Logue SE, Crow MT, Gottlieb RA. Apoptosis repressor with caspase recruitment domain protects against cell death by interfering with Bax activation. *J Biol Chem* 2004;279:21233-21238.
21. Koseki T, Inohara N, Chen S, Nunez G. ARC, an inhibitor of apoptosis expressed in skeletal muscle and heart that interacts selectively with caspases. *Proc Natl Acad Sci U S A* 1998;95:5156-5160.
22. Nagaraju K, Casciola-Rosen L, Rosen A, Thompson C, Loeffler L, Parker T, Danning C, Rochon PJ, Gillespie J, Plotz P. The inhibition of apoptosis in myositis and in normal muscle cells. *J Immunol* 2000;164:5459-5465.
23. Neuss M, Monticone R, Lundberg MS, Chesley AT, Fleck E, Crow MT. The apoptotic regulatory protein ARC (apoptosis repressor with caspase recruitment domain) prevents oxidant stress-mediated cell death by preserving mitochondrial function. *J Biol Chem* 2001;276:33915-33922.
24. Dalla LL, Sabbadini R, Renken C, Ravara B, Sandri M, Betto R, Angelini A, Vescovo G. Apoptosis in the skeletal muscle of rats with heart failure is associated with increased serum levels of TNF-alpha and sphingosine. *J Mol Cell Cardiol* 2001;33:1871-1878.
25. Fernandez-Sola J, Nicolas JM, Fatjo F, Garcia G, Sacanella E, Estruch R, Tobias E, Badia E, Urbano-Marquez A. Evidence of apoptosis in chronic alcoholic skeletal myopathy. *Hum Pathol* 2003;34:1247-1252.
26. Lee MJ, Lee JS, Lee MC. Apoptosis of skeletal muscle on steroid-induced myopathy in rats. *J Korean Med Sci* 2001;16:467-474.
27. Dirks A, Leeuwenburgh C. Apoptosis in skeletal muscle with aging. *Am J Physiol Regul Integr Comp Physiol* 2002;282:R519-R527.
28. Sandri M, Carraro U, Podhorska-Okolov M, Rizzi C, Arslan P, Monti D, Franceschi C. Apoptosis, DNA damage and ubiquitin expression in normal and mdx muscle fibers after exercise. *FEBS Lett* 1995;373:291-295.

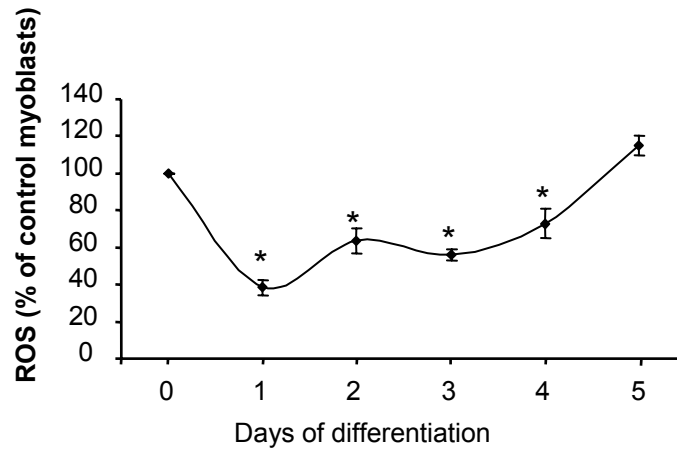
29. Sandri M, Podhorska-Okolow M, Geromel V, Rizzi C, Arslan P, Franceschi C, Carraro U. Exercise induces myonuclear ubiquitination and apoptosis in dystrophin-deficient muscle of mice. *J Neuropathol Exp Neurol* 1997;56:45-57.
30. Tidball JG, Albrecht DE, Lokensgard BE, Spencer MJ. Apoptosis precedes necrosis of dystrophin-deficient muscle. *J Cell Sci* 1995;108 (Pt 6):2197-2204.
31. Adhietty P.J., Hood D.A. Mechanisms of apoptosis in skeletal muscle. *Basic Applied Myology* 2003;13:171-179.
32. Nicholls DG, Rial E. A history of the first uncoupling protein, UCP1. *J Bioenerg Biomembr* 1999;31:399-406.
33. Vincent AM, Olzmann JA, Brownlee M, Sivitz WI, Russell JW. Uncoupling proteins prevent glucose-induced neuronal oxidative stress and programmed cell death. *Diabetes* 2004;53:726-734.
34. Bodrova ME, Dedukhova VI, Mokhova EN, Skulachev VP. Membrane potential generation coupled to oxidation of external NADH in liver mitochondria. *FEBS Lett* 1998;435:269-274.
35. Papa S, Skulachev VP. Reactive oxygen species, mitochondria, apoptosis and aging. *Mol Cell Biochem* 1997;174:305-319.
36. Vidal-Puig AJ, Grujic D, Zhang CY, Hagen T, Boss O, Ido Y, Szczepanik A, Wade J, Mootha V, Cortright R, Muoio DM, Lowell BB. Energy metabolism in uncoupling protein 3 gene knockout mice. *J Biol Chem* 2000;275:16258-16266.
37. Echtay KS, Esteves TC, Pakay JL, Jekabsons MB, Lambert AJ, Portero-Otin M, Pamplona R, Vidal-Puig AJ, Wang S, Roebuck SJ, Brand MD. A signalling role for 4-hydroxy-2-nonenal in regulation of mitochondrial uncoupling. *EMBO J* 2003;22:4103-4110.
38. Echtay KS, Roussel D, St Pierre J, Jekabsons MB, Cadenas S, Stuart JA, Harper JA, Roebuck SJ, Morrison A, Pickering S, Clapham JC, Brand MD. Superoxide activates mitochondrial uncoupling proteins. *Nature* 2002;415:96-99.
39. Leininger GM, Russell JW, van Golen CM, Berent A, Feldman EL. Insulin-like growth factor-I regulates glucose-induced mitochondrial depolarization and apoptosis in human neuroblastoma. *Cell Death Differ* 2004;11:885-896.
40. Dejean L, Camara Y, Sibille B, Solanes G, Villarroya F. Uncoupling protein-3 sensitizes cells to mitochondrial-dependent stimulus of apoptosis. *J Cell Physiol* 2004;201:294-304.
41. Dupuis L, di Scala F, Rene F, de Tapia M, Oudart H, Pradat PF, Meininger V, Loeffler JP. Up-regulation of mitochondrial uncoupling protein 3 reveals an early muscular metabolic defect in amyotrophic lateral sclerosis. *FASEB J* 2003;17:2091-2093.
42. Arnoult D, Parone P, Martinou JC, Antonsson B, Estaquier J, Ameisen JC. Mitochondrial release of apoptosis-inducing factor occurs downstream of cytochrome c release in response to several proapoptotic stimuli. *J Cell Biol* 2002;159:923-929.
43. Charlot JF, Pretet JL, Haughey C, Mouglin C. Mitochondrial translocation of p53 and mitochondrial membrane potential ($\Delta \Psi_m$) dissipation are early events in

- staurosporine-induced apoptosis of wild type and mutated p53 epithelial cells. *Apoptosis* 2004;9:333-343.
44. Tafani M, Minchenko DA, Serroni A, Farber JL. Induction of the mitochondrial permeability transition mediates the killing of HeLa cells by staurosporine. *Cancer Res* 2001;61:2459-2466.
 45. Negre-Salvayre A, Auge N, Duval C, Robbesyn F, Thiers JC, Nazzal D, Benoist H, Salvayre R. Detection of intracellular reactive oxygen species in cultured cells using fluorescent probes. *Methods Enzymol* 2002;352:62-71.
 46. Royall JA, Ischiropoulos H. Evaluation of 2',7'-dichlorofluorescein and dihydrorhodamine 123 as fluorescent probes for intracellular H₂O₂ in cultured endothelial cells. *Arch Biochem Biophys* 1993;302:348-355.
 47. Zamora M, Merono C, Vinas O, Mampel T. Recruitment of NF-kappaB into mitochondria is involved in adenine nucleotide translocase 1 (ANT1)-induced apoptosis. *J Biol Chem* 2004;279:38415-38423.
 48. Sandri M, Carraro U. Apoptosis of skeletal muscles during development and disease. *Int J Biochem Cell Biol* 1999;31:1373-1390.
 49. Podhorska-Okolow M, Sandri M, Zampieri S, Brun B, Rossini K, Carraro U. Apoptosis of myofibres and satellite cells: exercise-induced damage in skeletal muscle of the mouse. *Neuropathol Appl Neurobiol* 1998;24:518-531.
 50. Rasmussen UF, Krstrup P, Bangsbo J, Rasmussen HN. The effect of high-intensity exhaustive exercise studied in isolated mitochondria from human skeletal muscle. *Pflugers Arch* 2001;443:180-187.
 51. Hayakawa M, Miyashita H, Sakamoto I, Kitagawa M, Tanaka H, Yasuda H, Karin M, Kikugawa K. Evidence that reactive oxygen species do not mediate NF-kappaB activation. *EMBO J* 2003;22:3356-3366.
 52. Li N, Karin M. Is NF-kappaB the sensor of oxidative stress? *FASEB J* 1999;13:1137-1143.
 53. Catani MV, Savini I, Duranti G, Caporossi D, Ceci R, Sabatini S, Avigliano L. Nuclear factor kappaB and activating protein 1 are involved in differentiation-related resistance to oxidative stress in skeletal muscle cells. *Free Radic Biol Med* 2004;37:1024-1036.
 54. Brand MD, Pamplona R, Portero-Otin M, Requena JR, Roebuck SJ, Buckingham JA, Clapham JC, Cadenas S. Oxidative damage and phospholipid fatty acyl composition in skeletal muscle mitochondria from mice underexpressing or overexpressing uncoupling protein 3. *Biochem J* 2002;368:597-603.
 55. Murphy MP, Echtay KS, Blaikie FH, Asin-Cayuela J, Cocheme HM, Green K, Buckingham JA, Taylor ER, Hurrell F, Hughes G, Miwa S, Cooper CE, Svistunenko DA, Smith RA, Brand MD. Superoxide activates uncoupling proteins by generating carbon-centered radicals and initiating lipid peroxidation: studies using a mitochondria-targeted spin trap derived from alpha-phenyl-N-tert-butyl nitron. *J Biol Chem* 2003;278:48534-48545.
 56. Talbot DA, Lambert AJ, Brand MD. Production of endogenous matrix superoxide from mitochondrial complex I leads to activation of uncoupling protein 3. *FEBS Lett* 2004;556:111-115.

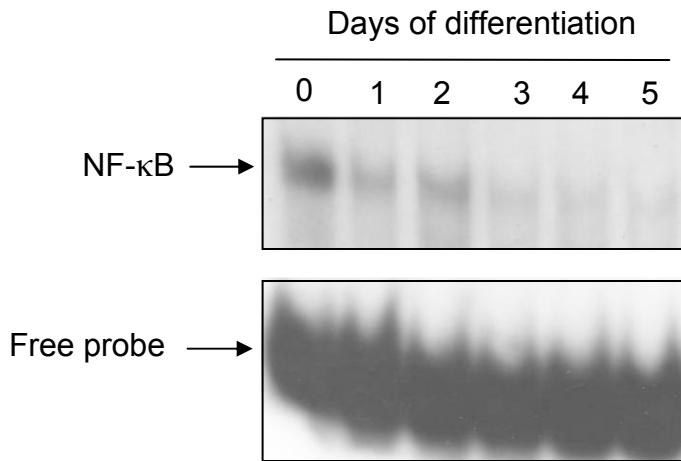
57. Garcia-Martinez C, Sibille B, Solanes G, Darimont C, Mace K, Villarroya F, Gomez-Foix AM. Overexpression of UCP3 in cultured human muscle lowers mitochondrial membrane potential, raises ATP/ADP ratio, and favors fatty acid vs. glucose oxidation. *FASEB J* 2001;15:2033-2035.
58. Solanes G, Pedraza N, Iglesias R, Giralt M, Villarroya F. The human uncoupling protein-3 gene promoter requires MyoD and is induced by retinoic acid in muscle cells. *FASEB J* 2000;14:2141-2143.
59. Teshima Y, Akao M, Jones SP, Marban E. Uncoupling protein-2 overexpression inhibits mitochondrial death pathway in cardiomyocytes. *Circ Res* 2003;93:192-200.
60. Mattiasson G, Shamloo M, Gido G, Mathi K, Tomasevic G, Yi S, Warden CH, Castilho RF, Melcher T, Gonzalez-Zulueta M, Nikolich K, Wieloch T. Uncoupling protein-2 prevents neuronal death and diminishes brain dysfunction after stroke and brain trauma. *Nat Med* 2003;9:1062-1068.
61. Mills EM, Xu D, Fergusson MM, Combs CA, Xu Y, Finkel T. Regulation of cellular oncosis by uncoupling protein 2. *J Biol Chem* 2002;277:27385-27392.

FIGURES

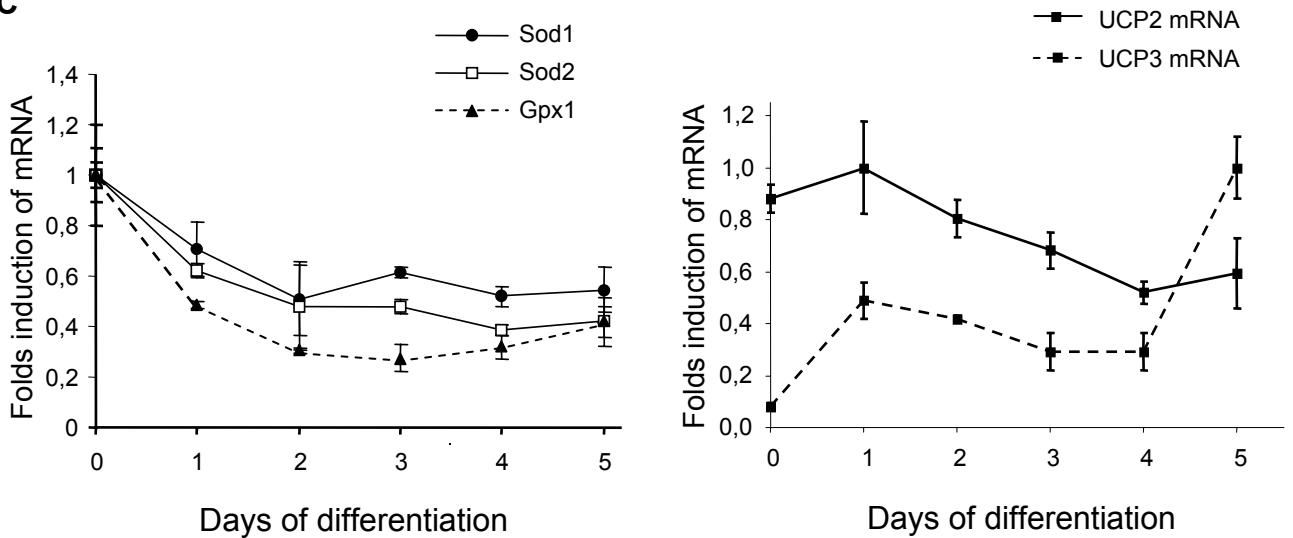
A



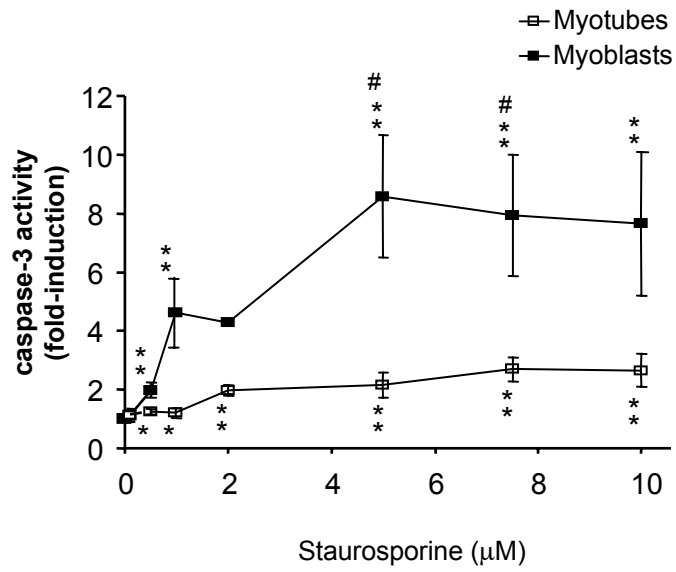
B



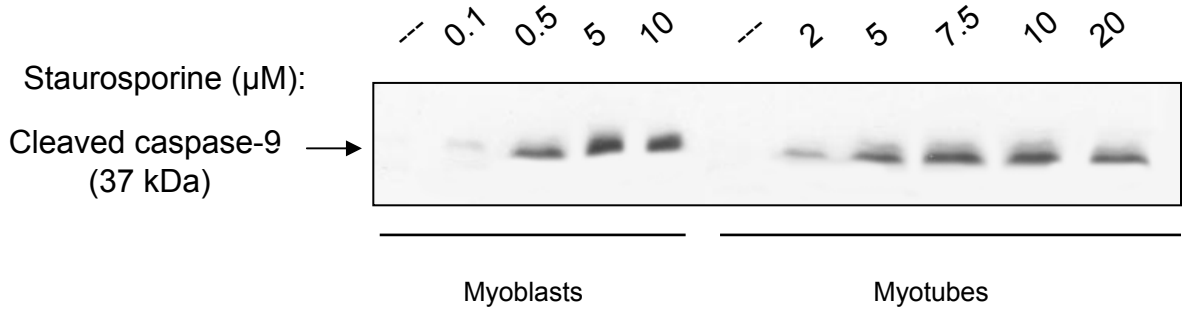
C



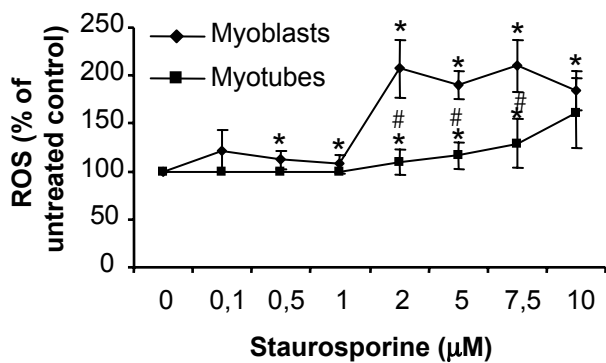
A



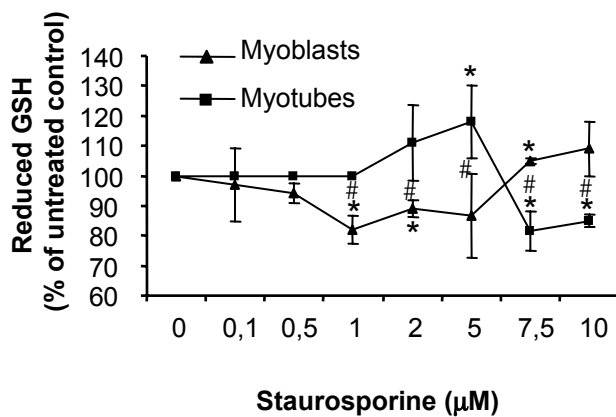
B



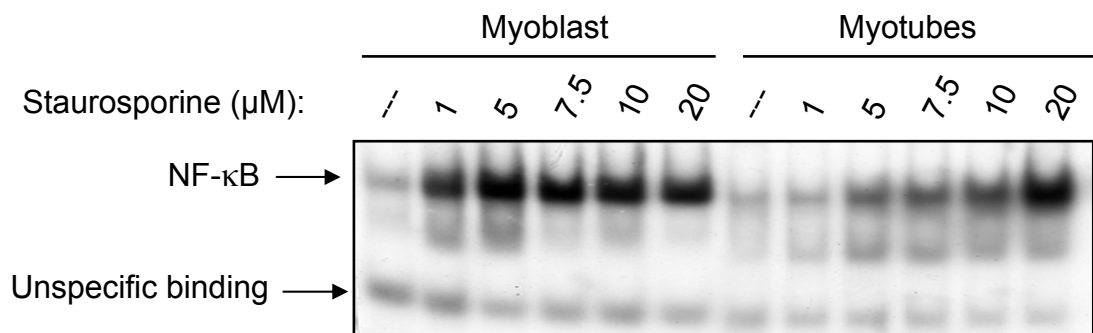
A



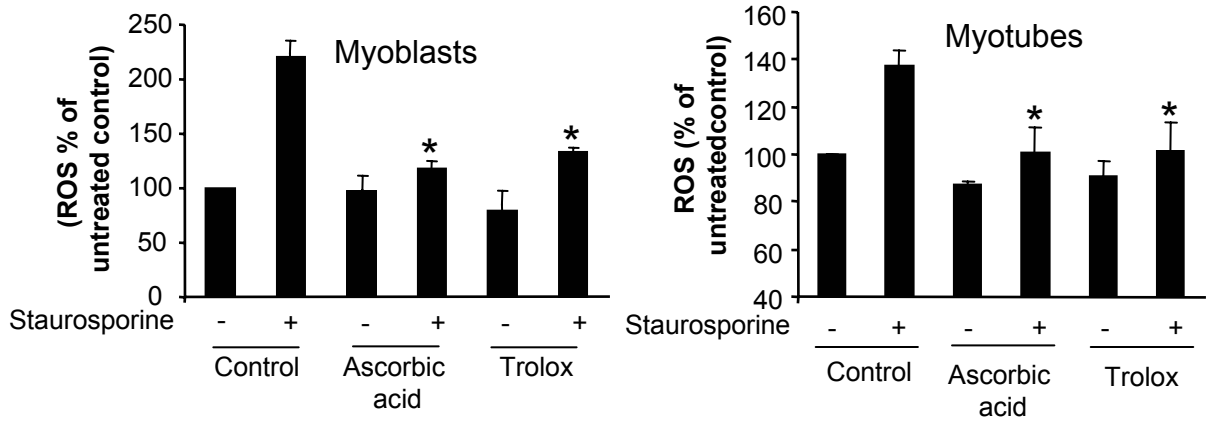
B



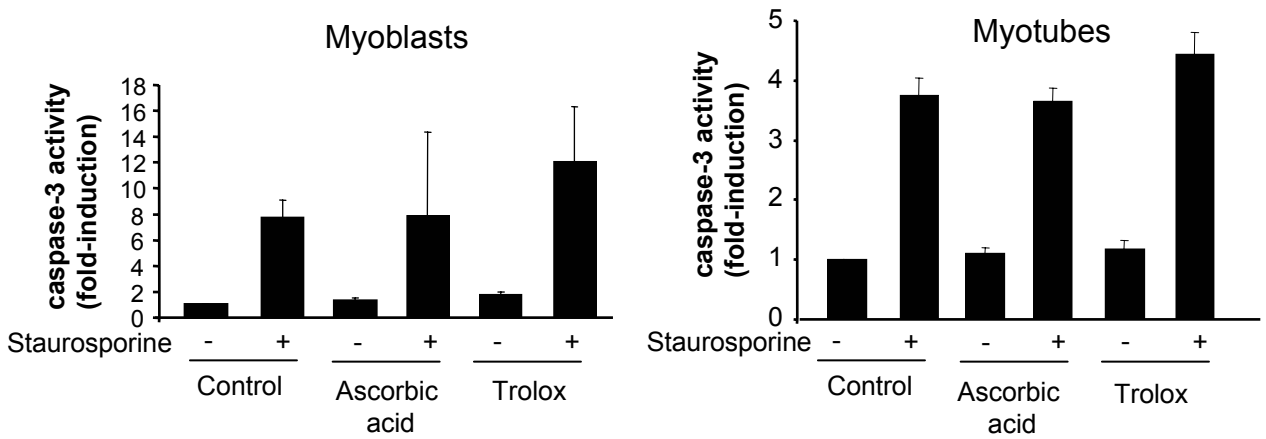
C



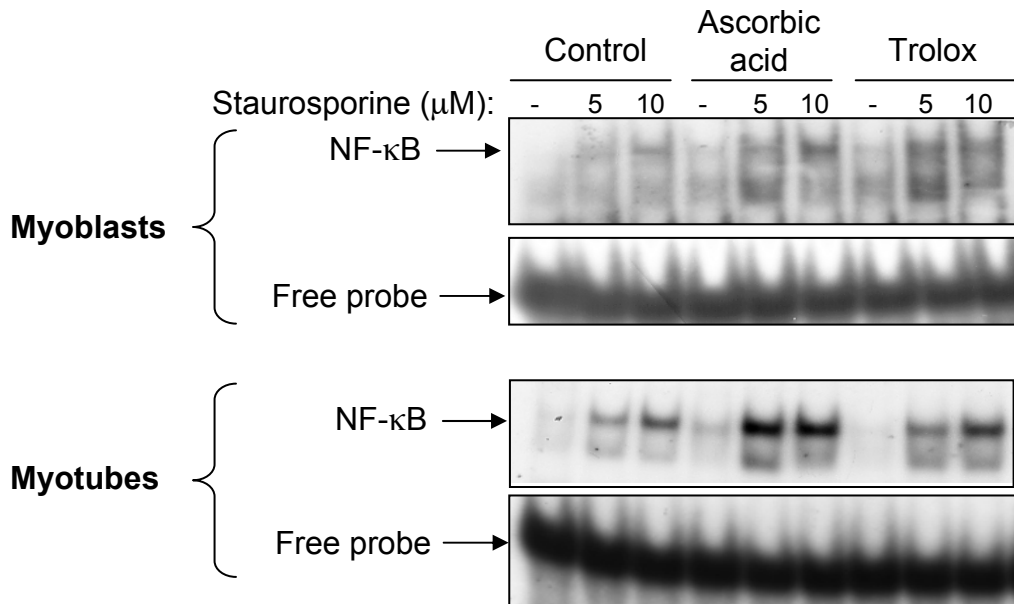
A



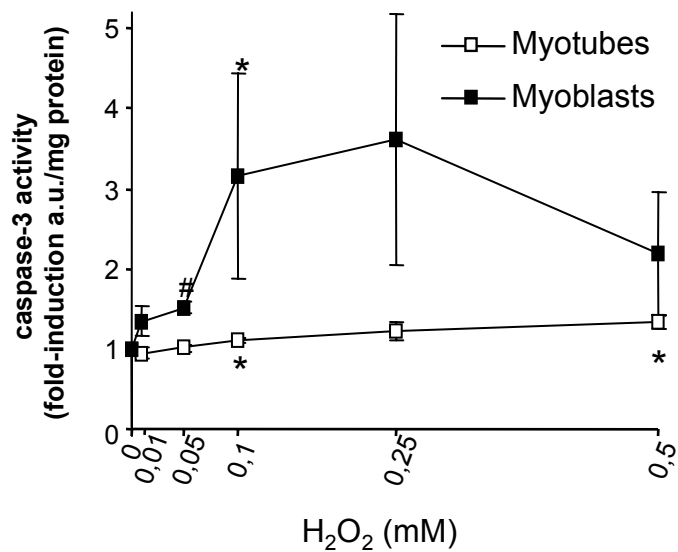
B



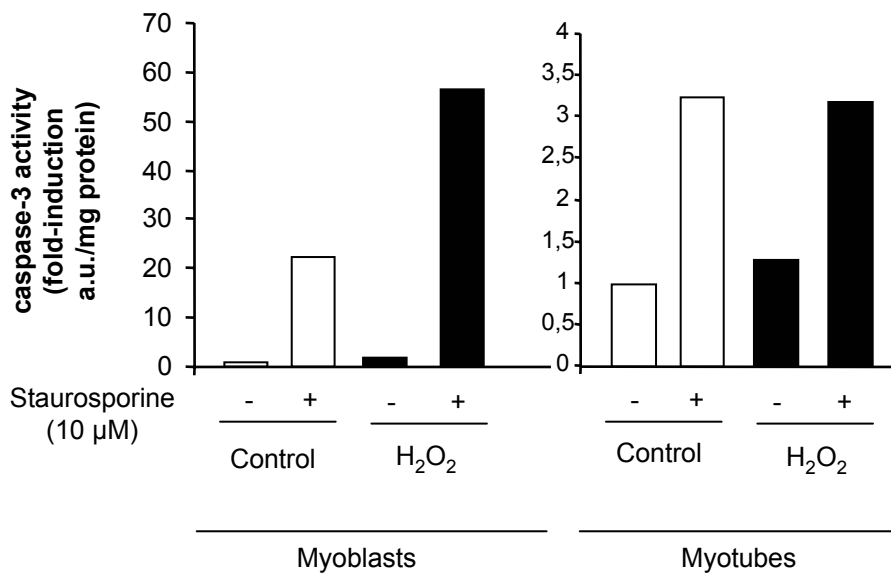
C



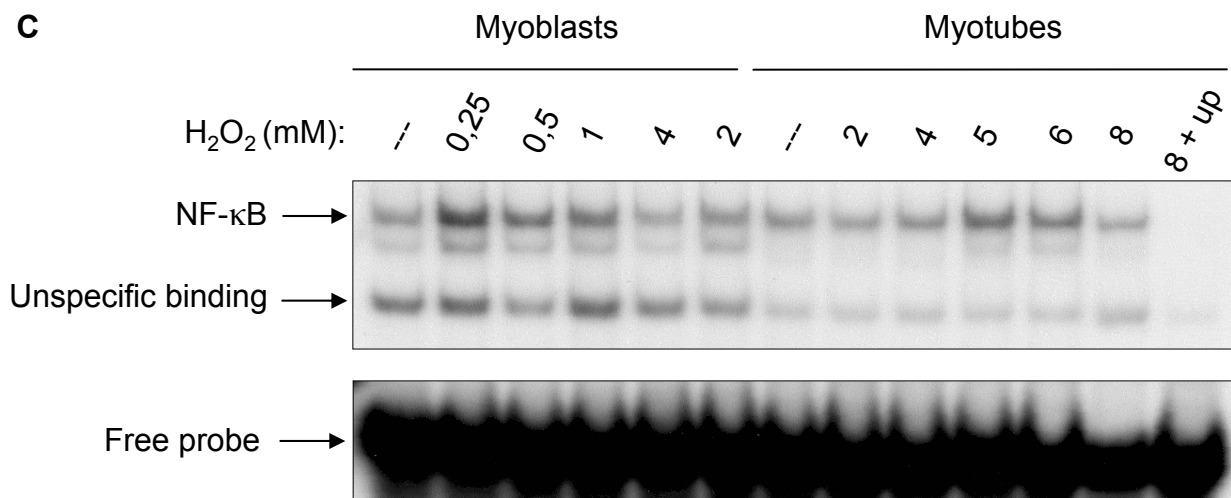
A



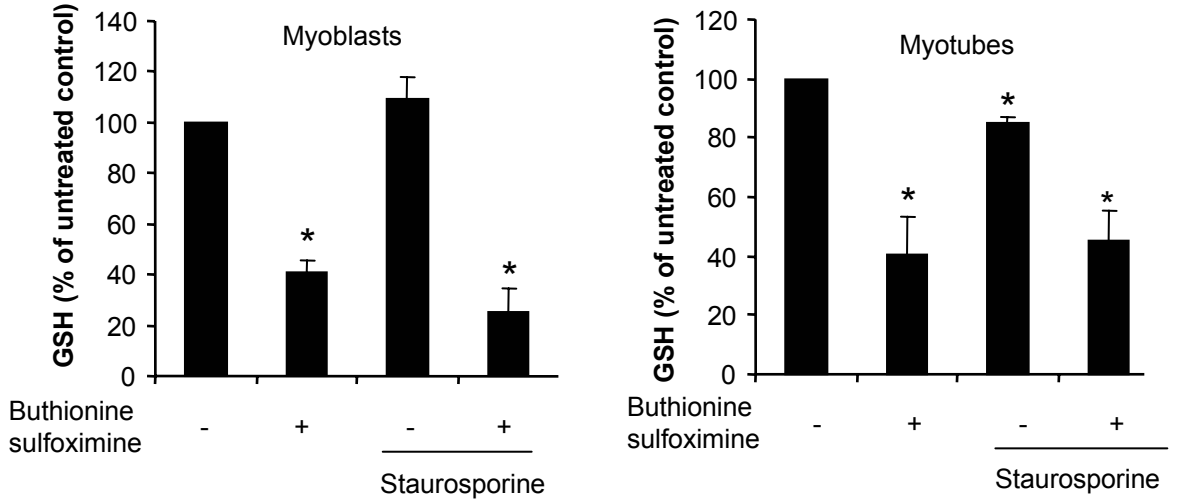
B



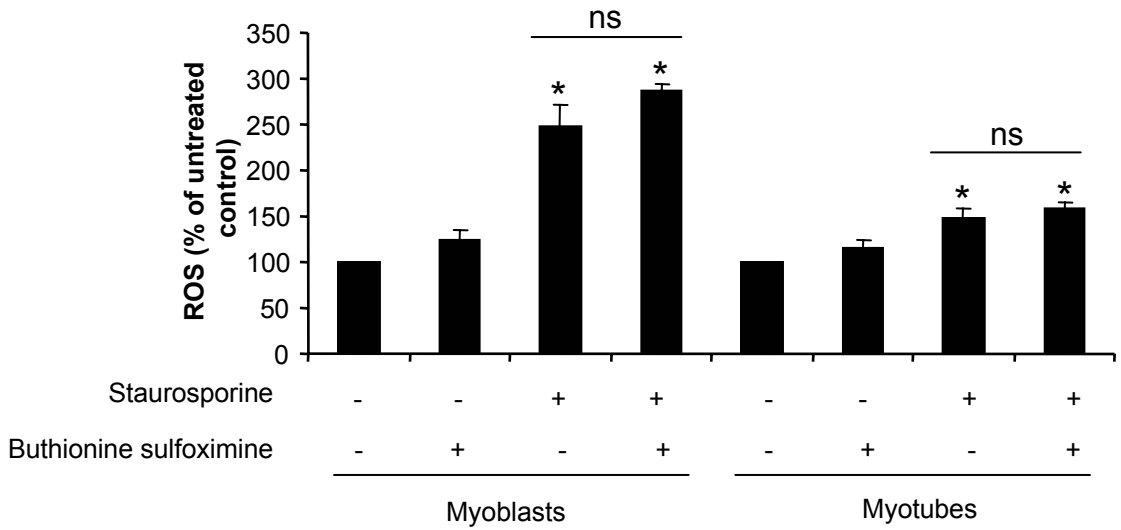
C



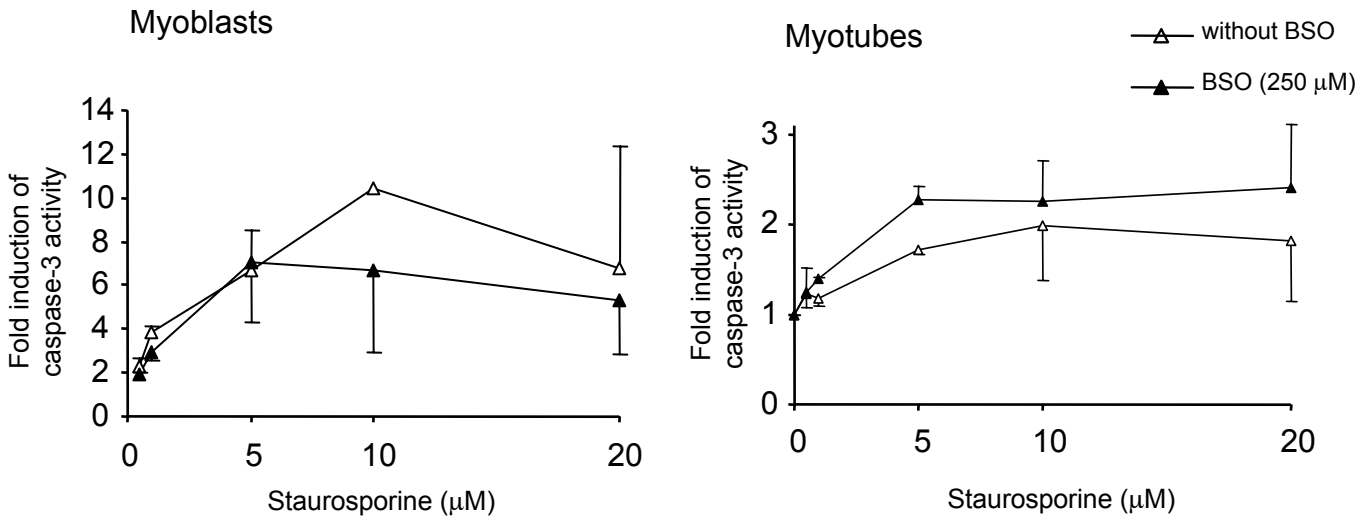
A

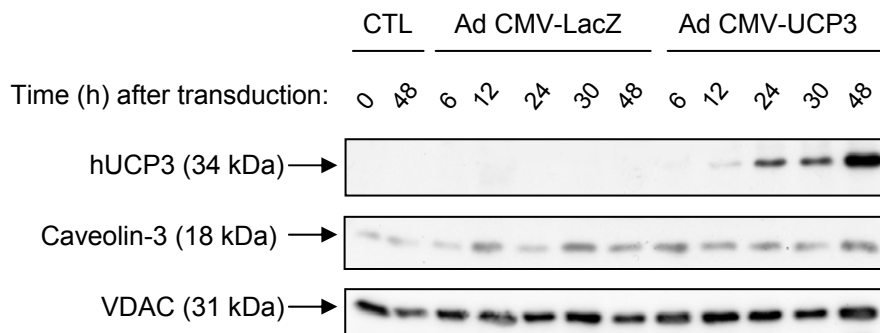


B

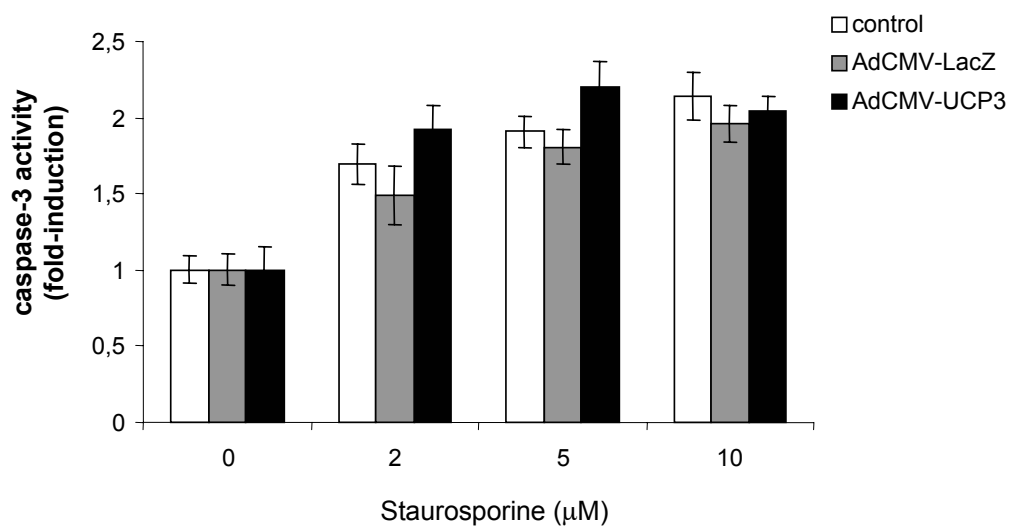


C

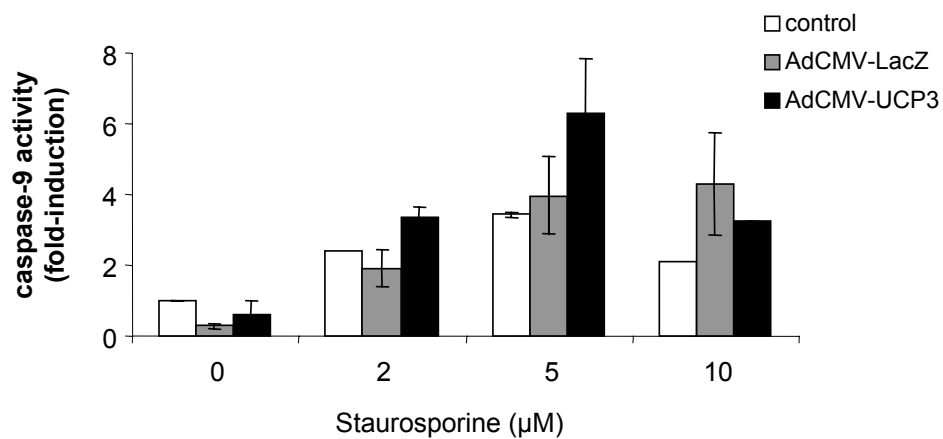
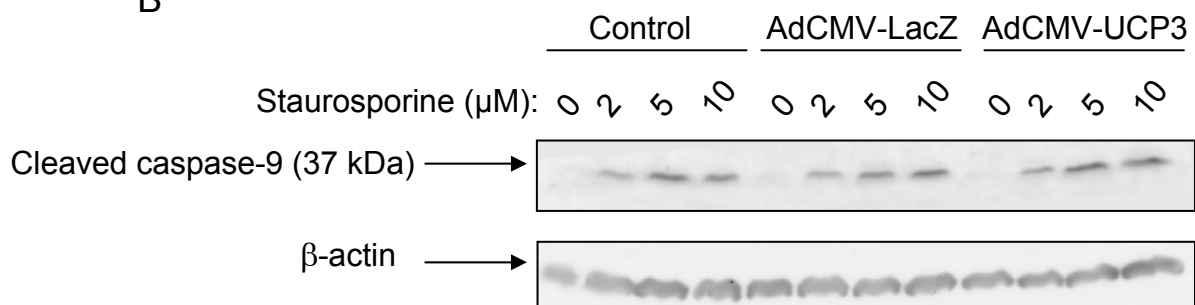




A



B



Gene	AdCMV-LacZ	AdCMV-UCP3
Superoxide dismutase 1	0.95 ± 0.06	0.86 ± 0.09
Superoxide dismutase 2	0.93 ± 0.05	0.77 ± 0.07
Glutathione peroxidase 1	0.95 ± 0.07	0.81 ± 0.06
Uncoupling protein 2	0.98 ± 0.08	0.61 ± 0.14 *
Uncoupling protein 3	0.99 ± 0.10	0.73 ± 0.13
m-TFB1	1.04 ± 0.14	0.87 ± 0.15
myogenin	0.99 ± 0.07	0.84 ± 0.06
m-CPT-1	0.92 ± 0.14	0.80 ± 0.12

Table 1: Gene expression in L6 cells expressing hUCP3. Results correspond to the fold-change for every mRNA respect to values in myotubes non transduced with adenoviral vectors, which were set to 1. Data are means ± SEM of 4-5 assays. Significant differences between AdCMV-LacZ and AdCMV-UCP3-treated cells are shown as *, $p \leq 0.05$.

LEGENDS TO FIGURES

Figure 1: Characterization of changes in ROS content, NFkappaB activity and oxidant-stress related gene expression in differentiating myogenic cells

A: Effect of myogenic differentiation of L6 cells on intracellular ROS content. Rat L6 cells were grown in Dulbecco's minimal essential medium (DMEM) containing 10% fetal bovine serum (FBS). To induce differentiation, L6 cells at 80% confluence were changed to DMEM containing 2% FBS. Cells, at indicated days of differentiation were loaded with the H₂-DCFDA 10 μ m, for 1h, to detect intracellular ROS. Data are expressed as a percentage of control myoblasts. Results are means \pm S.E.M. for at least 3 separate experiments. Statistical significance of differences between myotubes and control myoblasts are shown as *p<0,05.

B: NFkappa B binding activity of L6 cells along differentiation. Nuclear extracts from L6 myoblasts and myotubes at the indicated day of differentiation (see Materials and Methods) were subjected to EMSA assay to determine NFkappa B binding activity. Example of a representative experiment. Arrow in the left indicates the specific band corresponding to active NFkappa B.

C: Effect of myogenic differentiation on oxidative stress-gene expression (SOD1, SOD2 and GPx1) in L6 cells. Total RNA was extracted from L6 myoblasts and myotubes. Quantitative mRNA expression analysis was performed by a Real-time PCR procedure as explained in materials and methods.

Figure 2: Activation of caspase 3 and caspase 9 in response to the apoptotic inducer staurosporine, in myoblasts and myotubes.

A: Caspase-3 activity induction in L6 myoblasts and myotubes exposed to growing concentrations of staurosporine during 4 h. Data are expressed as fold induction of caspase-3 activity at any given concentration of staurosporine respect to values in untreated cells. Results are means \pm S.E.M. for at least 5 separate experiments. Statistical significance of differences between treated cells and untreated controls are shown as *p<0,05; **p<0,01. Statistical significance of differences between myoblasts and myotubes at any concentration of staurosporine are shown as #p<0,05.

B: Caspase-9 induction in myoblasts and myotubes in response to staurosporine. Example of immunodetection of the cleaved, active form of caspase-9 performed on cytosolic extracts from cell treated as in A.

Figure 3: Involvement of ROS in the responsiveness of myoblasts and myotubes to the apoptotic inducer: staurosporine.

A: Intracellular ROS generation in L6 myoblasts and myotubes, measure with H₂-DCFDA (for details see material and methods) in response to staurosporine. Data are expressed as a percentage of untreated control. Results are means ± S.E.M. for at least 3 separate experiments. Statistical significance of differences between cells and untreated controls are shown as *p<0,05. Statistical significance of differences between myoblasts and myotubes at any concentration of staurosporine are shown as #p<0,05.

B: Effect of staurosporine on intracellular GSH (for details see material and methods). Data are expressed as a percentage of untreated control. Results are means ± S.E.M. for at least 3 separate experiments. Statistical significance of differences between cells and untreated controls are shown as *p<0,05. Statistical significance of differences between myoblasts and myotubes at any concentration of staurosporine are shown as #p<0,05.

C: NFkappa B binding activity of L6 cells exposed to growing concentrations of staurosporine: Nuclear extracts from L6 myoblasts and myotubes stimulated with different concentrations of staurosporine were subjected to EMSA assay to determine NFkappa B binding activity. Arrow in the left indicates the specific band corresponding to active NFkappa B.

Figure 4: Effect of antioxidants on ROS and the responsiveness of myoblasts and myotubes to staurosporine

A: Effect of ascorbic acid and trolox pre-incubation (2 mM, overnight) on intracellular ROS generation, measured with H₂-DCFDA probe in L6 myoblasts and myotubes exposed to 10 μM staurosporine. Data are expressed as a percentage of untreated control. Results are means ± S.E.M. for at least 3 separate experiments. Statistical significance of differences between cells and untreated controls are shown as *p<0,05.

B: Effect of ascorbic acid and trolox on staurosporine induced caspase-3 activation in L6 myoblasts and myotubes. Cells were pre-incubated overnight with 2 mM of the indicated antioxidants and caspase-3 activation was measured fluorimetrically after 10 μM staurosporine treatment for 4 hours. Data are expressed as fold respect to untreated control. Results are means ± S.E.M. for at least 4 separate experiments.

C: Effect of ascorbic acid and trolox on staurosporine induced NFkappa B activation in L6 myoblasts and myotubes. Nuclear extracts from L6 myoblasts and myotubes pre-treated with antioxidants (2 mM, overnight) and stimulated with different concentrations of staurosporine for 4 hours, were subjected to EMSA assay to determine NFkappa B binding activity. Arrow in the left indicates the specific band corresponding to active NFkappa B.

Figure 5: Effect of H₂O₂ on caspase 3 and NFkappa B activity in myoblasts and myotubes .

A: H₂O₂ effect on caspase-3 activation in L6 myoblasts and myotubes. Myoblasts or myotubes were exposed to growing concentrations of H₂O₂ for one hour, and then caspase-3 activation was measured. Results are means \pm S.E.M. for at least 4 separate experiments. Statistical significance of differences between cells and untreated controls are shown as *p<0,05. Statistical significance of differences between myoblasts and myotubes at any concentration of staurosporine are shown as #p<0,05.

B: Effect of 0.25mM H₂O₂ on 10 μ M staurosporine induced caspase-3 activation in L6 myoblasts and myotubes. Cells at myoblast or myotube stage of differentiation were previously exposed to the indicated concentration of H₂O₂ for one hour. Caspase-3 activation was fluorimetrically measured after 4 hours treatment with staurosporine 10 μ M. Data are expressed as fold respect to untreated control.

C: Effect of H₂O₂ on NFkappa B activation in L6 myoblasts and myotubes. Nuclear extracts from L6 myoblasts and myotubes treated with the indicated concentrations of H₂O₂ for 1 hour were subjected to EMSA assay to determine NFkappa B binding activity. Arrow in the left indicates the specific band corresponding to active NFkappa B.

Figure 6: Effect of glutathione depletion on ROS and the apoptotic responsiveness of myoblasts to myotubes to staurosporine.

A: Buthionine sulfoximine effect on intracellular GSH in L6 myoblasts and myotubes. L6 myoblast and myotubes were treated with buthionine sulfoximine, at 250 μ M, overnight before 10 μ M staurosporine treatment for 4h and then GSH levels were determined using the probe monochlorobimane. Data are expressed as a percentage of untreated control myoblasts. Results are means of \pm S.E.M. for at least 3 separate experiments. Statistical significance of differences between cells and untreated controls are shown as *p<0,05.

B: Buthionine sulfoximine effect on staurosporine induced-intracellular ROS generation in L6 myoblasts and myotubes. L6 myoblast and myotubes were treated with buthionine sulfoximine, at 250 μ M, overnight, before 10 μ M staurosporine treatment for 4h and ROS

were evaluated with H₂-DCFDA. Data are expressed as a percentage of untreated control cells. Results are means of \pm S.E.M. for at least 3 separate experiments.

C: Buthionine sulfoximine effect on Staurosporine induced-caspase 3 activation in L6 myoblasts and myotubes. Results are means of \pm standard deviation of two independent experiments.

Figure 7: Induction of UCP3 in L6 myotubes using the adenoviral vector AdCMV-UCP3

Immunodetection of UCP3, VDAC and Caveolin-3 was performed on 30 μ g of whole homogenate protein (see Material and Methods) from myotubes at the indicated time after transduction.

Figure 8: Effect of UCP3 on the apoptotic responsiveness to staurosporine

A: Caspase-3 activation was fluorimetrically measured in cellular extracts from L6 myotubes previously transduced or not with AdCMV-LacZ or AdCMV-UCP3 as described in Material and Methods. Not infected myotubes were pre-treated or not with 10 μ M CCCP for 1h. All cells were then exposed to increasing concentrations of staurosporine for 4h. Points are the fold-induction of caspase-3 activation respect to basal activity present in each condition, and which was set to 1, and are means \pm SEM of 5-7 independent experiments.

B: Example of immunodetection using cytosolic extracts obtained as in A, of the active, cleaved-form, of rat caspase-9. β -actin detection was used to assure equal protein loading of samples.

Figure 9: Effect of UCP3 on staurosporine induced ROS production and NFkappa B activation.

A: Effect of UCP3 expression on staurosporine-induced intracellular ROS generation in myotubes L6. L6 myotubes were infected (day 3) with the AdCMV-UCP3 or the AdCMV-LacZ control. At day 5, they were exposed to staurosporine, at indicated concentrations for 4h. ROS were estimated using H₂-DCFDA. Data are expressed as a percentage of untreated control. Results are means of \pm S.E.M. for at least 3 separate experiments.

B: Effect of UCP3 on staurosporine induced NFkappa B activation in L6 myotubes, previously transduced or not with AdCMV-LacZ or AdCMV-UCP3. All cells were then exposed to different concentrations of staurosporine for 4h. Nuclear extracts were subjected to EMSA assay to determine NFkappa B binding activity. Arrow in the left indicates the specific band corresponding to active NFkappa B.

Reactive oxygen species production in response to fatty acids in skeletal muscle cells. Effects of the mitochondrial uncoupling protein-3.

Carine Duval*, Yolanda Cámara*, Brigitte Sibille[#] and Francesc Villarroya[†]

From the Departament de Bioquímica i Biologia Molecular. Universitat de Barcelona, 08028-Barcelona. Spain.

Running title: Effects of fatty acids on reactive oxygen species in muscle cells.

* These authors contributed equally to this work.

[#] Present address: Laboratoire de Physiologie des Régulations Énergétiques, Cellulaires et Moléculaires, Centre National de la Recherche Scientifique-Université Claude Bernard Lyon 1, Unité Mixte de Recherches 5123, Villeurbanne, France.

[†] To whom correspondence should be addressed: Department of Biochemistry and Molecular Biology. University of Barcelona, Diagonal 645, 08028-Barcelona, Spain. Tel: 34-3-4021525; Fax: 34-3-4021559, E-mail: fvillarroya@ub.edu

ABSTRACT

Fatty acids induce an increase in ROS and enhance NF- κ B activation in L6 myotubes differentiated in culture, being palmitate more effective than oleate in eliciting such effect. The induction of high levels of expression of the mitochondrial uncoupling protein-3 (UCP3) in L6 myotubes achieved through the use of an adenoviral vector, lead to a moderate reduction of mitochondrial membrane potential. However, the capacity of fatty acids to increase ROS is not reduced but the opposite, moderately enhanced, due to the presence of UCP3. The presence of UCP3 in mitochondria did not modify gene expression for the antioxidant enzymes superoxide dismutase-1 and – 2, and glutathione peroxidase-1, either in basal conditions or in the presence of palmitate. However, in the presence of UCP3, UCP2 mRNA expression was down-regulated in response to palmitate. It is concluded that, at the cellular level, UCP3 does not act as protective against the action of fatty acids increasing ROS in differentiated skeletal muscle cells.

INTRODUCTION

Uncoupling proteins (UCPs) belong to the family of mitochondrial anion carriers present in the inner membrane of mitochondria (1). The founder member of the family, UCP1 is only expressed in brown adipocytes and its physiological role is related to non-shivering thermogenesis (2). UCP1 uncouple respiratory chain function from ATP synthesis by catalysing a highly regulated proton leak across the inner mitochondrial membrane, thereby dissipating energy as heat (3). Its activity requires fatty acids and is specifically inhibited by GDP (4).

UCP3 is a member of the UCP family with preferential expression in skeletal muscle. It shares a 56% sequence identity with UCP1, and 72% with UCP2, another member of the UCP family expressed ubiquitously. Like UCP1, UCP3 can uncouple respiratory chain from oxidative phosphorylation, as confirmed by studies using heterologous yeast and mammalian cell expression systems (5-7). Over-expression of UCP3 in several cell and tissue systems has been reported to reduce mitochondrial membrane potential, whereas mitochondria from UCP3 gene-null mice show a high membrane potential (8; 9). Multiple evidences indicate also that fatty acids activate directly the proton conductance of UCP3 whereas the capacity of GDP to inhibit it has been shown in reconstituted systems or in permeabilized cells expressing UCP3, but not in heterologous yeast expression systems (7; 10; 11). However, from a physiological point of view, it appears that UCP3 is not particularly involved in mediating cold-induced or diet-induced thermogenesis and its involvement in heat production has only been demonstrated in relation to drug-induced hyperthermia (12; 13).

The transcription of the UCP3 gene is extremely sensitive to availability of free fatty acids to skeletal muscle. Thus, in multiple physiological or pathological situations (fasting, high-fat diets, lactation, exercise...) UCP3 mRNA and protein levels are dramatically modulated according to the changes in free fatty acids. This happens regardless of whether the source of circulating free fatty acids is diet or lipolysis in white fat depots. Experimental manipulations leading to increased levels of intracellular fatty acids in muscle, such as over-expression of lipoprotein lipase in the tissue, or inhibition of fatty acid oxidation by etomoxir treatment, lead to enhanced UCP3 gene expression (14). Despite all these observations did not provide any direct information on the physiological role of UCP3, they suggested that UCP3 function could be related to fatty acid metabolism in skeletal muscle. A high expression of UCP3 favours fatty acid versus glucose oxidation in skeletal muscle cells (15; 16) and some authors have

hypothesized that UCP3 could favour the export of fatty acid from mitochondria when its capacity of oxidation is exceeded by fatty acid availability (17-19)

Recent data on the biochemical behaviour of UCP3 has led to the proposal that the major role of its uncoupling activity is to reduce reactive oxygen production by mitochondria (20), similarly to what has been proposed for UCP2 (21-25). Thus, UCP3-null mice show enhanced ROS production in skeletal muscle mitochondria and accumulation of products resulting from oxidative stress in this tissue (9; 26). These findings would be consistent with former bioenergetic studies in mitochondria that led to the conclusion that “mild-uncoupling” is associated with a protection against ROS production (27-29) It has been also reported that ROS themselves, either directly or via the production of 4-OH-nonenal, act as positive regulators of the proton conductance mediated by UCP2 or UCP3 (30; 31), although other reports have questioned these observations (32).

Fatty acids are energy-rich substrates that, when metabolised in mitochondria, result in a high electron flow in the respiratory chain with the subsequent mitochondrial ROS generation (33). Thus, fatty acids could elicit intracellular events closely related to the expected functions of UCP3 as they can enhance ROS production during oxidation in mitochondria. A likely hypothesis for the role of UCP3 in skeletal muscle could be that, when high free fatty acids become available, UCP3 gene expression is induced as a protective mechanism to favour a higher capacity of oxidizing these fatty acids without excess ROS production. Such a hypothesis would link events such as fatty acid-dependent regulation of UCP3 gene and the control of ROS production. However, direct evidence for this scenario is lacking, and, for instance, there is no experimental data on the effects of fatty acids on ROS production specifically in skeletal muscle cells. It has been reported that fatty acid effects on ROS are highly variable and range from induction to inhibition depending on the cell type. Moreover, it is also unknown whether UCP3 levels influence ROS production in skeletal muscle cells specifically in response to a high availability of fatty acids.

In the present work we have analyzed the effects of fatty acids on ROS generation in differentiated L6 muscle cells as well as on NF- κ B activity, a sensor of the ROS exposure of cells mediating some of the cellular effects of ROS. We have analyzed how the presence of UCP3 in muscle cell mitochondria influences fatty acids-induced ROS generation.

We show that fatty acids induce ROS production and NF- κ B activity in differentiated skeletal muscle cells but UCP3, despite lowering membrane potential, does not act as protective for this effects.

MATERIAL AND METHODS

Chemicals and reagents

DMEM with Glutamax[®], phenol red free RPMI-1640, and fetal bovine serum (FBS) were purchased from GIBCO (Grand Island, N.Y.). The ROS-sensitive fluorescent probe 6-carboxy-2', 7'-dichlorodihydrofluorescein diacetate, diacetoxymethyl-ester (H₂-DCFDA; DCF, 2', 7' -dichlorodihydrofluorescein) and the 5,5', 6,6'-tetrachloro-1, 1', 3, 3'-tetraethylbenzimidazole carbocyanide iodide (JC-1) were purchased from Molecular Probes (Eugene, OR, U.S.A) and dissolved in DMSO. Etomoxir, carbonyl cyanide m-chlorophenylhydrazone (CCCP), fatty acids, and fatty-acid-free BSA (FAF-BSA) were purchased from Sigma-Aldrich. Other reagents and chemicals were obtained from Sigma-Aldrich, Merck and Roche.

Cell Culture and adenoviral-mediated gene transfer

Rat L6 cells (ATCC Rockville, MD, USA) were grown in Dulbecco's minimal essential medium (DMEM) containing 10% fetal bovine serum (FBS). To induce differentiation, L6 cells at 80% confluence were changed to DMEM containing 2% FBS. Then L6 were maintained for 5 days in these conditions of culture to acquire myotube morphology. After 3 days of differentiation, L6 myotubes were infected with adenoviral vectors at a multiplicity of infection of 500, after 2 h. This treatment led to an efficiency of transduction of about 90%. Analyses (ROS levels, NF- κ B activation, real time PCR, and western blot) were performed 2 days after transduction. Recombinant adenovirus expressing the human UCP3 cDNA (AdCMV-UCP3) or *E.coli* betagalactosidase (AdCMV-LacZ) under the control of the cytomegalovirus promoter (CMV) were obtained and handed as reported elsewhere (15).

Fatty acids treatment

Oleate and palmitate salts were prepared immediately before use by dissolving the fatty acid in deionized water containing 1.2 equivalents of NaOH at 70°C, and 95°C respectively until obtaining an optically clear dispersion. The fatty acid salt solution was immediately added to DMEM medium containing fatty acid free bovine serum albumin (BSA) (Sigma) with continuous agitation to avoid precipitation. After 1h of conjugation at 37°C this medium was added to the cells. The FA: BSA molar ratio was 5:1.

Determination of intracellular ROS

The probe H₂-DCFDA was used to estimate the generation of intracellular ROS as reported elsewhere (34; 35). After incubation with the probe at 10 μ M for 1h, cells were washed twice with PBS and scraped into water. After sonication, the fluorescence of H₂-DCFDA stained cells was measured fluorimetrically (excitation wavelength 493 nm, emission wavelength 527 nm).

Determination of mitochondrial membrane potential ($\Delta\Psi_m$)

$\Delta\Psi_m$ was estimated by using the probe JC-1, and following previously established procedures as indicated by the supplier. JC-1 is a fluorescent compound (excitation maximum 490nm) that exists as a monomer at low concentrations and fluoresce red (emission, 527 nm); whereas at high concentrations it forms aggregates and its fluorescence is green (emission, 590 nm). JC-1 aggregates with red fluorescence are formed in mitochondria due to membrane potential-dependent uptake of the dye. L6 Myotubes 2 days after being transduced with the adenoviral vectors, and L6 myotubes treated with CCCP (5 μ M, 40min) were rinsed in serum-free medium and incubated with 5 μ M JC-1 at 37°C in a 5% CO₂ incubator for 15min in the dark. After rinsing the cells with serum-free culture medium the cell plates were analyzed by using a confocal microscope. The ratio of the reading at 590 nm to the reading at 527 nm (590:527 ratios) was taken as the relative $\Delta\Psi_m$ value.

Cell fractionation

Cells were harvested with a buffer containing 7.5 mM tri-sodium citrate 2-hydrate, 7 mM KCl, pH 7.4 and centrifuged at 400 x g for 2 min. The cell pellets were washed once with PBS and then resuspended in 1 ml of homogenization buffer (250 mM Sucrose, 1 mM EGTA, 10 mM Hepes, pH 7.4, 1 mM PMSF, 1 mM DTT, Complete-Mini Protease Inhibitor cocktail tablets (Roche)). After chilling on ice for 1 min, cells were disrupted by 50 strokes in a glass homogenizer. The homogenate was centrifuged once at 1500 x g for 10 min at 4°C to remove unbroken cells, plasmatic membranes and nuclei. The mitochondria-enriched fraction (heavy membrane fraction) was then pelleted by centrifugation at 10.000 x g for 10 min. For controls using mitochondria from tissue, mitochondria-enriched extracts were prepared from gastrocnemius muscles obtained from Wistar rats fed a regular chow or a high-fat diet (80% fat/20%protein) for three months, as described elsewhere (36). Protein

concentration of subcellular fractions was measured using the BCA Protein Assay kit (Pierce) in the presence of 0.1% TritonX-100 (Boehringer Mannheim).

Western blot analysis

Samples of homogenates or mitochondria were separated by SDS-PAGE on 12.8% and transferred to polyvinylidene fluoride membranes (PVDF membranes) (Immobilon-P, Millipore). These were incubated with antibodies against UCP3 (Chemicon AB3046 (1:1000)) or voltage-dependent anion carrier or porin (VDAC) (Calbiochem Anti-Porin 31HL (1:1000)). VDAC detection was used to ensure equal loading of mitochondrial protein and correct cell fractionation. The binding of antibodies was detected with a horseradish peroxidase-coupled anti-mouse (Bio-Rad 170-6516 (1:3000)) or anti-rabbit (Santa Cruz sc-2004 (1:3000)) secondary antibody, and an enhanced chemiluminescence (ECL) detection kit (Amersham).

Nuclear extract preparation

Extracts were prepared as reported elsewhere (37). For the isolation of nuclear protein extracts of L6 myotubes, 2 plates of 58.1 cm² cells were washed twice with ice-cold PBS and scrapped off the plates in 400 μ l of buffer A (10 mM Hepes, pH 7.9, 10 mM KCl, 0.1 mM EDTA, 0.1 mM EGTA, 1 mM dithiothreitol, 0.5 mM PMSF, and protease inhibitors (5 μ g/ml each of aprotinin, leupeptin, and pepstatin)). Cells were allowed to swell on ice for 15 min; then 25 μ l of Nonidet P-40 (0.5%) was added, and the suspension was thoroughly mixed for 10 s. The homogenate was centrifuged (16,000 x g, 4°C, 60 s.), and the nuclear pellet was resuspended in 50 μ l of ice-cold buffer C (20 mM Hepes, pH 7.9, 0.4 M NaCl, 1 mM EDTA, 1 mM EGTA, 1 mM dithiothreitol, 1 mM PMSF, and protease inhibitors (5 μ g/ml each of aprotinin, leupeptin, and pepstatin)). Nuclear lysates were maintained on ice for 15 min with occasional mixing. The nuclear extract was cleared (16,000 x g, 4°C, 5 min), and the supernatant containing the proteins from the nuclear extract was transferred to a fresh tube and stored at -80°C. Proteins concentrations were determined by the Bradford assay (Bio-Rad).

Electrophoretic Mobility Shift Assay

Nuclear extracts from L6 myotubes were used in electrophoretic mobility shift assays. A double stranded oligonucleotide corresponding to a consensus NF- κ B DNA binding site (5'-TCT AGA GTT GAG GGG ACT TTC CCA G-3', obtained from Roche

Applied Science) was end-labeled using [α -³²P]dCTP and Klenow enzyme. Nuclear protein extracts (10 μ g) were incubated for 30 min at room temperature with binding buffer (25 mM Hepes, pH 7.6, 0.5 dithiothreitol, 12.5 mM ZnSO₄, 50 mM KCl, 1 mg/ml bovine serum albumin, 5% glycerol, 0.1% Nonidet P-40, and 2.5 μ g of poly(dI-dC) (deoxyinosinic-deoxycytidylic- acid)). The DNA probe (30,000 cpm) was added and incubated for 20 min at room temperature. Samples were run on 5% non-denaturing polyacrilamide gels in 0.5 X Tris-borate-EDTA at 130 V and 4°C for 60 min. Specific NFkappa B activity was assessed in competition tests. In these assays, random samples were pre-incubated with 100-fold molar excess of unlabeled double-stranded oligonucleotides before the addition of the DNA probe to compete specific NFkappa B binding.

Real time PCR

Total RNA was extracted from cells with the method of the Tripure Isolation Reagent (Boehringer Mannheim). Quantitative mRNA expression analysis was done in a two-step reaction: first, 1 μ g of total RNA was transcribed into cDNA by means of RT-PCR (real time reverse transcriptase chain reaction) on the GeneAmp PCR system 2400 (Applied Biosystems, USA), and then, a Real-Time PCR was performed on the ABI PRISM 7700HT sequence detection (Applied Biosystems, U.S.A). The RT-PCR was done in a final volume of 50 μ l using TaqMan[®] Reverse Transcription Reagents (Applied Biosystems, U.S.A), which contains MultiScribe[™] Reverse Transcriptase, RNase inhibitor, dNTP Mixture, Random Hexamers, 10X RT buffer, and MgCl₂ solution. TaqMan[®] Real-Time PCR reaction was performed in a final volume of 25 μ l using TaqMan[®] Universal PCR Master Mix, and gene expression probes (Applied Biosystems, U.S.A): 18S ribosomal RNA (Hs99999901_s1), glutathione peroxidase-1 (Rn00577994_g1), uncoupling protein-2 (Rn00571166_m1), uncoupling protein-3 (Rn00565874_m1), superoxide dismutase-2 (Rn00566942_g1), and superoxide dismutase-1 (Rn00584772_m1).

Appropriate controls with no RNA, primers, or reverse transcriptase were included in each set of experiments. Each sample was run in duplicate, and the mean value of the duplicate was used to calculate the mRNA expression of the gene of interest. The quantity of the gene of interest in each sample was normalized to that of the endogenous control using comparative ($2^{-\Delta CT}$) method according to manufacturer's instructions (Applied Biosystems, U.S.A). 18S ribosomal RNA was used as endogenous control.

Statistical analysis

Data, shown as means \pm SEM, were analyzed with Student's t-test for determination of the significance of differences, which were considered to be significant at a P value of less than 0.05.

RESULTS

Gene transfer delivery of UCP3 to L6 myotubes. Effects on $\Delta\Psi_m$.

To deliver UCP3 to L6 rat muscle cells differentiated in culture, a recombinant adenoviral vector containing the full-length cDNA for the human UCP3 was used. Fig 1A shows that UCP3 protein was not detectable in differentiated L6 myotubes. This is in agreement with the very low expression of UCP3 mRNA in skeletal muscle cells in culture respect to skeletal muscle in vivo (38). There was a dose-dependent increase in the presence of UCP3 in mitochondria from myotubes treated with increasing amounts of AdCMV-UCP3, as shown by the appearance of a single band of around 34 kDa in immunoblot analysis. Parallel assays were performed using mitochondrial fractions from gastrocnemius muscle of control rats and rats fed a high-fat, carbohydrate-free, diet, a known inducer of UCP3 gene expression in muscle. Equal loading of mitochondrial proteins was assessed by parallel detection of the mitochondrial protein VDAC. Results indicated that the induction of UCP3 protein expression in mitochondria attained using the m.o.i. 500 transduction dose of AdCMV-UCP3 was in the range of physiological levels in muscle from the high-fat treated rats. The induction of UCP3 protein levels in mitochondria was also time-dependent, and time course studies using the m.o.i indicated a maximum 48h after the transduction with the adenoviral vector (data not shown). Immunoblot analysis of cytosolic or nuclear fractions of myotubes transduced with AdCMV-UCP3 did not show any specific band, thus indicating a correct delivery of the mitochondria to the mitochondrial fraction (data not shown).

The expression of high levels of UCP3 in L6 cells led to a significant reduction in $\Delta\Psi_m$ respect to cells transduced with a control adenoviral vector driving beta-galactosidase (LacZ, control) (Fig 1B). However, there was no collapse of $\Delta\Psi_m$, as evidenced by a higher levels respect to cells treated with the chemical uncoupler CCCP. Confocal microscopy examination of cultured myotubes after treatment with the $\Delta\Psi_m$ -sensitive compound JC-1 indicated a homogeneous decrease in the $\Delta\Psi_m$ -dependent fluorescence (590/527 fluorescence ratio) in mitochondria from myotubes transduced with the AdCMV-UCP3 vector.

Intracellular ROS generation in L6 myotubes treated with fatty acids. Effects of UCP3.

Dose-response analysis of the effects of two types of fatty acid, palmitate and oleate, on ROS production estimated as H₂-DCFDA fluorescence is shown in Fig 2A. Oleate had a low but significant effect on ROS production, with a maximum of around 20% induction respect to control cells (BSA-treated) that was attained at 0.1 mM. No effect was observed at lower concentrations. Palmitate causes a much higher effect on ROS production, with a maximum of 80% induction at 0.5 mM. The levels of ROS induction by palmitate were higher than those induced by equivalent amounts of oleate except at the low dose of 0,1mM fatty acid. The addition of 40μM etomoxir 1h before the treatment with fatty acids, increases ROS production induced by palmitate 1mM (three-fold induction, data not shown).

Basal levels of ROS in myotubes expressing high levels of UCP3 were not significantly different from cells treated with equivalent amounts of a control adenoviral vector (Fig 2B). When these cells were treated with palmitate, the induction of ROS was higher in myotubes expressing UCP3.

High concentrations of palmitate are known to trigger apoptosis in some cell types (39; 40) but we did not observe an induction of caspase-3 or caspase-9 activity after exposing cells expressing or not UCP3 to any of the palmitate concentrations tested (0.1 mM; 0.5 mM; 1 mM) neither in the absence or the presence of UCP3.

Effects of fatty acids on NF-κB activity in L6 myotubes. Effects of UCP3.

L6 myotubes were treated with increasing amounts of oleate or palmitate and the activation of NF-κB was determined through an electrophoretic mobility shift assay. Results indicated that oleate elicited a moderate dose-dependent increase in the levels of the specific NF-κB band whereas palmitate led to a much more robust effect, with a maximal induction of about 2-fold respect to controls at 1 mM (Fig 3).

Results on the effects of palmitate on L6 myotubes that had been induced to express high levels of UCP3 in mitochondria are shown in Fig 4. UCP3 expression did not cause any significant effect on NF-κB activity in comparison with L6 myotubes with no treatment or transduced with the control adenoviral vector. Addition of palmitate elicited a significant induction of NF-κB activity in L6 myotubes that was higher in cells showing a high expression of UCP3.

Gene expression in L6 myotubes in response to palmitate. Effects of UCP3.

The effects of palmitate on the expression of mRNAs of genes potentially related to ROS and oxidative stress were determined in L6 myotubes that had been treated with the control adenoviral vector or transduced with the vector leading to high UCP3 protein levels (Fig 5). Palmitate treatment did not modify significantly the mRNA levels for SOD1, SOD2 and GPx1 in control cells, but led to an increase in UCP2 mRNA. The high UCP3 expression achieved with the adenoviral vector caused a reduction in UCP2 mRNA both in basal and palmitate-treated myotubes but did not alter SOD1, SOD2, and GPx1 mRNA neither in basal conditions nor in response to palmitate.

DISCUSSION

The current concepts on the biochemical behavior of UCP3 in isolated mitochondria suggest that the reduction in mitochondrial membrane potential elicited by its proton conductance activity, especially in the presence of fatty acids, could be protective for ROS. However, our results indicate that, in skeletal muscle cells in culture, high levels of UCP3 did reduce ROS neither in basal conditions nor in response to palmitate.

Exposure of differentiated muscle cells to fatty acids results in an increase in intracellular ROS, much more pronounced for palmitate than for oleate. This was observed both by direct assessment using a ROS-sensitive fluorescent probe, and indirectly by the analysis of NF- κ B activation, a sensor of ROS-mediated stress in cells. The induction of ROS production and NF- κ B in skeletal muscle myotubes in response to fatty acids is similar to that observed in cardiomyocytes (41) or beta-cells (42) but contrasts with reports in other cells systems, such as endothelial cells, in which fatty acids reduce ROS (43). The rise in ROS in response to fatty acids is consistent with the enhancement in mitochondrial oxidative pathways when fatty acids act as fuel substrates. The highest effects of palmitate have been attributed in other cell systems to the activation of ceramide synthesis pathways as well as to the activation of non-mitochondrial pathways of ROS production such as NAD(P)H oxidase activities (44).

Transduction of skeletal muscle myotubes with an adenoviral vector leading to high levels of UCP3 protein in mitochondria, in the range of those present in muscle mitochondria from rats under a high-fat diet, cause a reduction in mitochondrial membrane potential, that, similarly to what has been already reported in human myotubes (15), is much less than the overall collapse elicited by chemical uncouplers. In these conditions, the presence of high levels of UCP3, did not reduce but even enhanced somewhat ROS production when myotubes were exposed to fatty acids. The lack of protective effect and even some enhancement in ROS production in response to fatty acids in myotubes expressing UCP3 was evidenced by the extent of activation of the oxidative stress-sensitive transcription factor NF- κ B, a distinct event respect to ROS production itself but indicative of oxidative stress experienced by cells. These findings were surprising, despite previous works in other cell systems have already reported the association between lowered mitochondrial membrane potential and enhanced ROS production in the presence of palmitate (42). Several hypothesis can

be proposed to explain such an effect. When muscle cells express high levels of UCP3, fatty acid oxidation is enhanced (15; 16). The potential effect that mild uncoupling due to UCP3 might have in the reduction of ROS production can be compensated by this enhancement of oxidative activity of fatty acids in mitochondria and subsequent increase in ROS production.

On the other hand, distinct mechanisms for the action of UCP3 may be considered. Enhancement of ROS production when palmitate oxidation is blocked by etomoxir suggests that palmitate oxidation does not lead to a higher ROS production but the opposite, high concentrations of palmitate inside the cells elicited by impaired oxidation promote other pathways of ROS production not associated to palmitate oxidation itself. Among them, production of ceramide is a previously recognized mechanism (40). It has been described that ceramide can inhibit respiratory complex III and, similarly to pharmacological agents such as antimycin A, favor ROS production in this way (45; 46). It is also known that the combination of complex III inhibition and uncoupling may lead to maximal production of ROS (47) and this could explain the enhancement of ROS production by UCP3 in the presence of palmitate. Experimental research is under way to establish this possibility.

Another mechanism by which UCP3 activity could enhance ROS production could be indirectly, via its effects on UCP2 gene expression in response to fatty acids. UCP2 and UCP3 are similar proteins and UCP2 has been also proposed to be protective from ROS production (21-25). We could observe that UCP2 gene expression is up-regulated in response to palmitate in myotubes, in agreement with previous reports indicating that fatty acids activate the UCP2 gene promoter (48). However, we observed that the up-regulation of UCP2 in response to palmitate is lowered by the presence of high levels of UCP3. Again, this effect can be related to the enhancement of palmitate oxidation due to the presence of UCP3 because this would result in an enhanced removal of fatty acids as activators of UCP2 gene transcription via their oxidation. If UCP2 was more effective than UCP3 in the reduction of ROS production, the down-regulation observed could contribute to the enhancement in ROS production elicited by UCP3 in muscle cells.

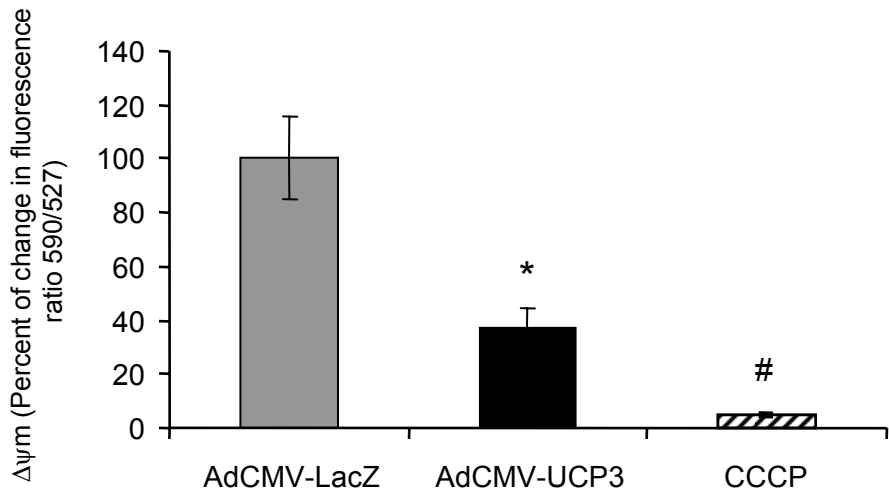
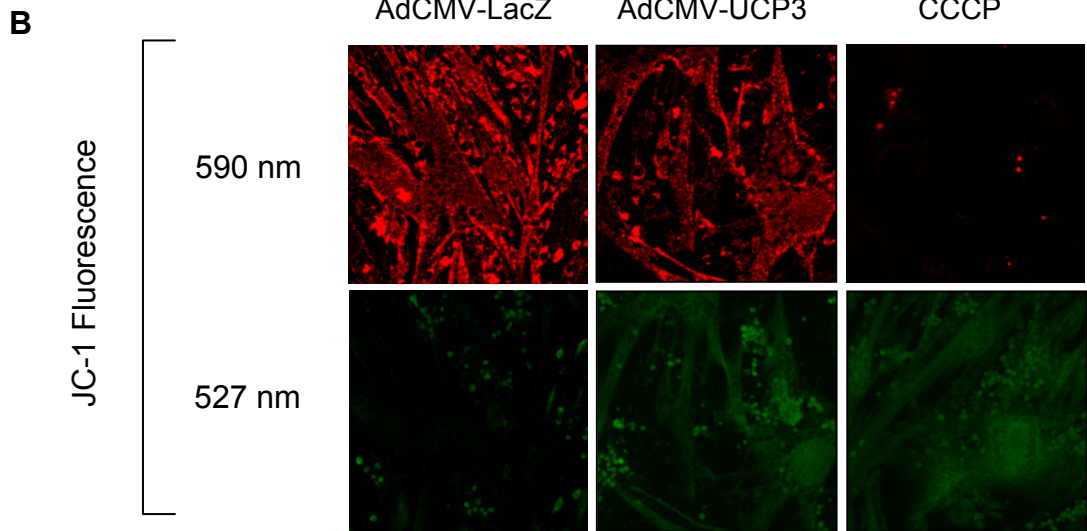
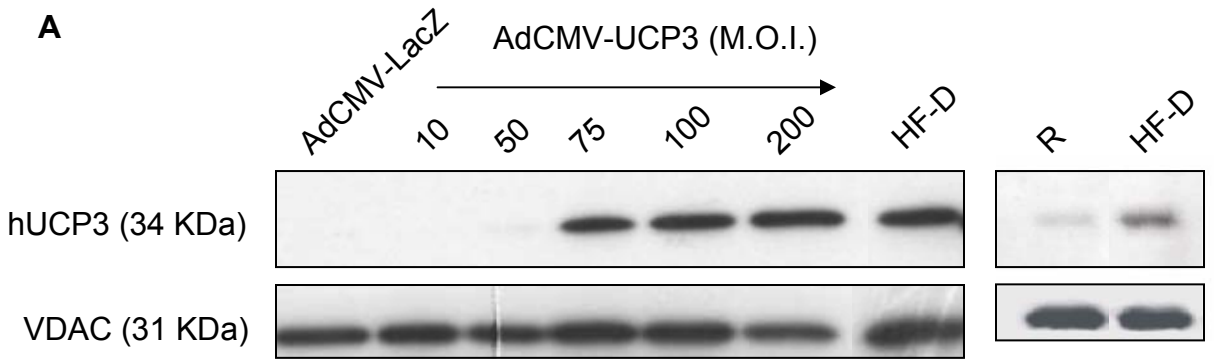
In summary, present findings indicate that, at the cellular level, fatty acids promote ROS in differentiated muscle cells, and the activity of UCP3, including lowering of mitochondrial membrane potential, does not result in protection against ROS production.

ACKNOWLEDGEMENTS

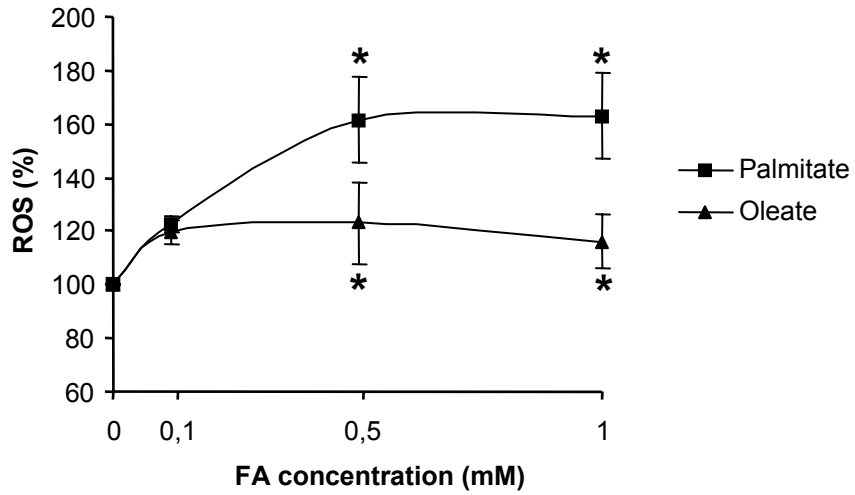
This work was supported by grant SAF2002-03648 from
Ministerio de Ciencia y Tecnología.

C. Duval was supported by fellowship from the “Fondation pour la Recherche
Médicale” and from the “Association Française contre les Myopathies”.

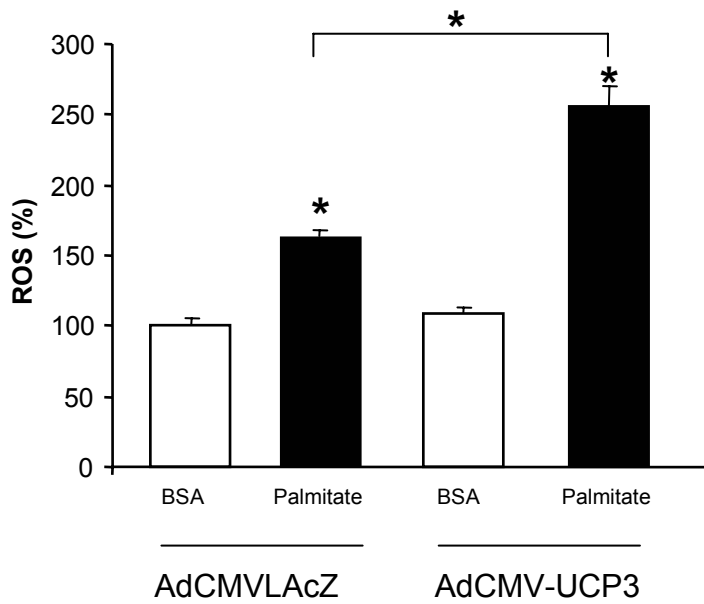
Y. Camara is supported by the Spanish Ministry of Education.

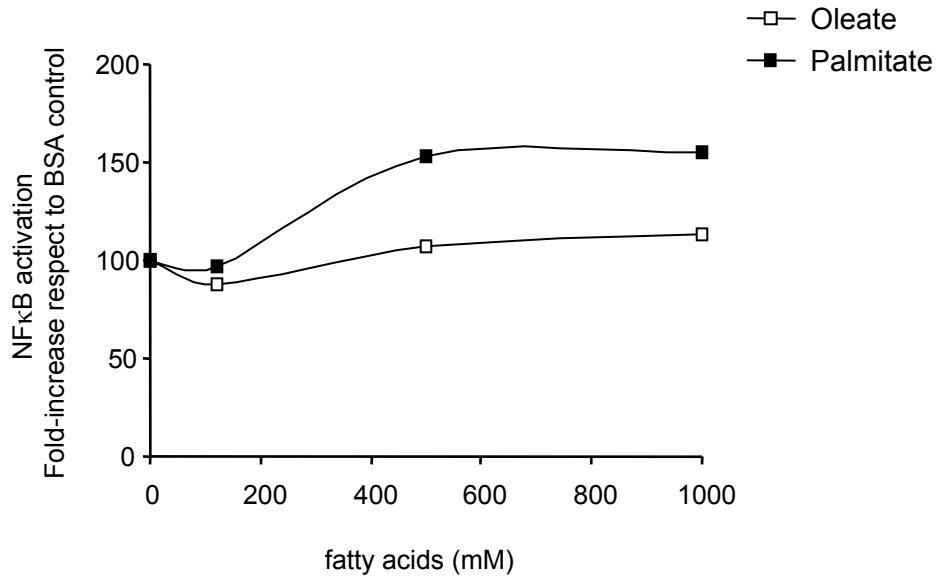
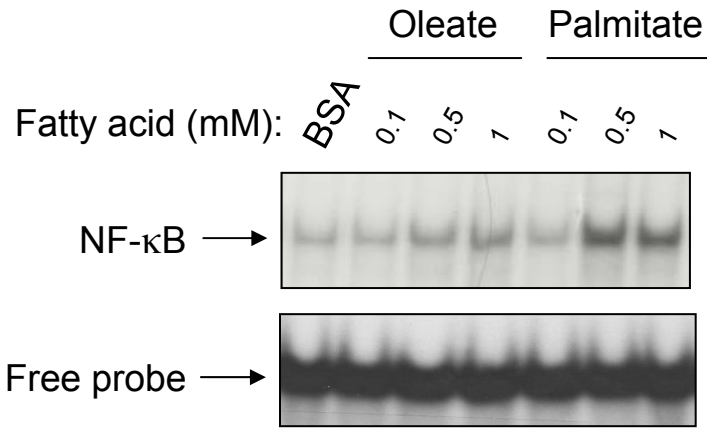


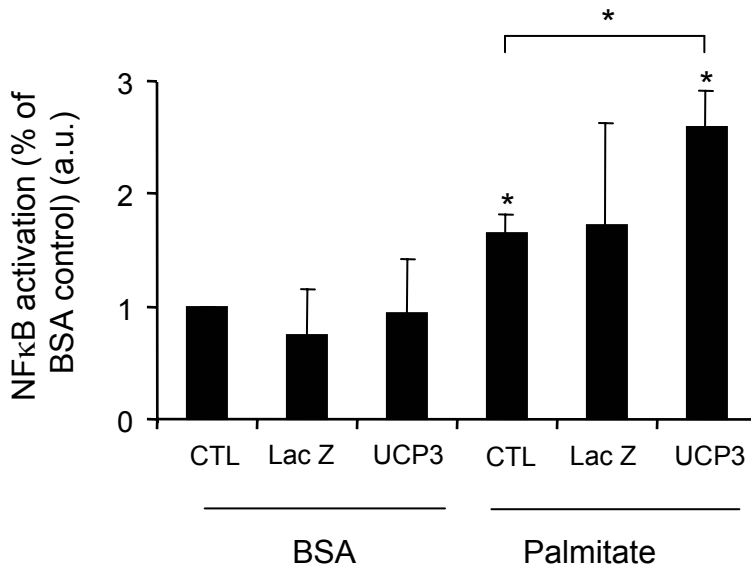
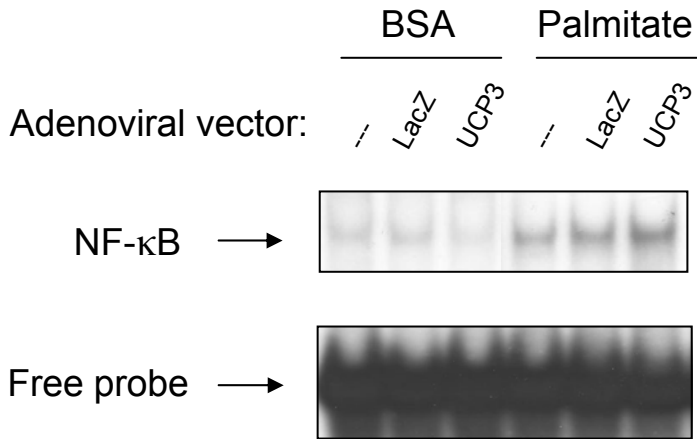
A

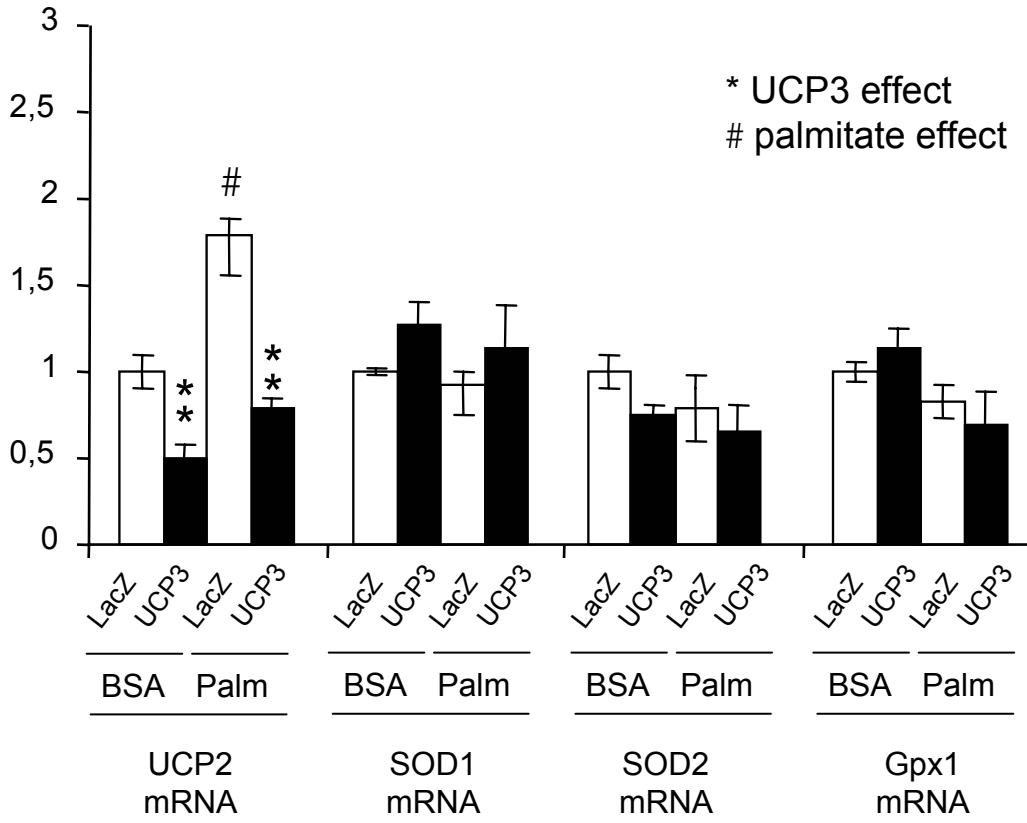


B









LEGENDS TO FIGURES

Figure 1: Characterization of adenoviral-mediated UCP3 overexpression on L6 myotubes.

A: Comparison of mitochondrial UCP3 levels in L6 myotubes transduced with AdCMV-UCP3 at the indicated MOI and AdCMV-LacZ (MOI 200) versus mitochondrial fraction of the skeletal muscle from rats fed a normal diet (R) or a high-fat diet (HF-D). Immunodetections of UCP3 and VDAC were performed on 30 μ g of mitochondrial protein (see Material and Methods).

B: Relative membrane potential ($\Delta\Psi_m$) was estimated on cells transduced with either AdCMV-LacZ or AdCMV-UCP3 by the fluorescence ratio 590/527 after treatment with JC-1 (see Materials and Methods). On the top: Confocal microscopy photographs of cells loaded with JC1, expressing or not UCP3, or incubated with CCCP. In the bottom: results expressed as percentages of change with respect to the control cells (AdCMV-LacZ) that was set to 100. Cells were treated under standard conditions of culture. As a positive control for $\Delta\Psi_m$ reduction, nontransduced cells were treated with 5 mM CCCP 4h before determination and the expected collapse of $\Delta\Psi_m$ was observed. Bars are means \pm SE of three experiments performed in triplicate dishes. The significance of the differences between controls and UCP-overexpression is * $p < 0.001$. The significance of the differences between CCCP and UCP-overexpression is # $p < 0.001$.

Figure 2: Intracellular ROS generation in L6 myotubes treated with FA, effect of UCP3 expression

A: Dose effect of BSA-conjugated palmitate or oleate during 24h on intracellular ROS generation in L6 myotubes. ROS generation is measured as explained in materials and methods. Data are expressed as a percentage of BSA control. Results are means \pm S.E.M. for at least 3 separate experiments. Statistical significance of differences between palmitate treated and controls are shown as * $p < 0, 05$.

B: Effect of UCP3 expression on FA induced-intracellular ROS generation in L6 myotubes. L6 myotubes previously transduced with AdCMV-LacZ or AdCMV-UCP3 were exposed to 1 mM BSA-conjugated palmitate for 24h. Data are expressed as a

percentage of the control AdCMV-LacZ treated with BSA. Results are means \pm S.E.M. for at least 3 separate experiments. Statistical significance of differences between palmitate treated and controls BSA are shown as $*p < 0, 05$.

Figure 3: Effect of FA treatment on NF- κ B binding activity of L6 myotubes.

Nuclear extracts from L6 myotubes treated with different concentrations of BSA-conjugated Oleate or Palmitate (see Materials and Methods) were subjected to EMSA assay to determine NF- κ B binding activity.

Figure 4: Effect of UCP3 overexpression on palmitate-induced NF- κ B activation in L6 myotubes.

L6 myotubes were transduced or not with AdCMV-LacZ or AdCMV-UCP3 and were subsequently treated with 1 mM of BSA-conjugated palmitate (see Materials and Methods) 48h after infection with adenoviral vectors. Nuclear extracts from these cells were subjected to EMSA assay to determine NF- κ B binding activity.

Figure 5: Effect of FA and UCP3 overexpression on oxidative stress-gene expression in L6 myotubes.

L6 myotubes previously transduced with AdCMV-LacZ or AdCMV-UCP3 were exposed to 1 mM BSA-conjugated palmitate for 24h. Then total RNA was extracted from cells. Quantitative mRNA expression analysis was done in a two-step reaction, as explained in materials and methods.

FIGURES

REFERENCES

1. Ricquier D, Bouillaud F. The uncoupling protein homologues: UCP1, UCP2, UCP3, StUCP and AtUCP. *Biochem J* 2000;345 Pt 2:161-179.
2. Himms-Hagen J. Brown adipose tissue thermogenesis: interdisciplinary studies. *FASEB J* 1990;4:2890-2898.
3. Enerback S, Jacobsson A, Simpson EM, Guerra C, Yamashita H, Harper ME, Kozak LP. Mice lacking mitochondrial uncoupling protein are cold-sensitive but not obese. *Nature* 1997;387:90-94.
4. Nicholls DG, Rial E. A history of the first uncoupling protein, UCP1. *J Bioenerg Biomembr* 1999;31:399-406.
5. Jaburek M, Varecha M, Gimeno RE, Dembski M, Jezek P, Zhang M, Burn P, Tartaglia LA, Garlid KD. Transport function and regulation of mitochondrial uncoupling proteins 2 and 3. *J Biol Chem* 1999;274:26003-26007.
6. Guerini D, Prati E, Desai U, Nick HP, Flammer R, Gruninger S, Cumin F, Kaleko M, Connelly S, Chiesi M. Uncoupling of protein-3 induces an uncontrolled uncoupling of mitochondria after expression in muscle derived L6 cells. *Eur J Biochem* 2002;269:1373-1381.
7. Hinz W, Faller B, Gruninger S, Gazzotti P, Chiesi M. Recombinant human uncoupling protein-3 increases thermogenesis in yeast cells. *FEBS Lett* 1999;448:57-61.
8. Gong DW, Monemdjou S, Gavriloova O, Leon LR, Marcus-Samuels B, Chou CJ, Everett C, Kozak LP, Li C, Deng C, Harper ME, Reitman ML. Lack of obesity and normal response to fasting and thyroid hormone in mice lacking uncoupling protein-3. *J Biol Chem* 2000;275:16251-16257.
9. Vidal-Puig AJ, Grujic D, Zhang CY, Hagen T, Boss O, Ido Y, Szczepanik A, Wade J, Mootha V, Cortright R, Muoio DM, Lowell BB. Energy metabolism in uncoupling protein 3 gene knockout mice. *J Biol Chem* 2000;275:16258-16266.
10. Rial E, Gonzalez-Barroso M, Fleury C, Iturrizaga S, Sanchis D, Jimenez-Jimenez J, Ricquier D, Goubern M, Bouillaud F. Retinoids activate proton transport by the uncoupling proteins UCP1 and UCP2. *EMBO J* 1999;18:5827-5833.
11. Zhang CY, Hagen T, Mootha VK, Sliker LJ, Lowell BB. Assessment of uncoupling activity of uncoupling protein 3 using a yeast heterologous expression system. *FEBS Lett* 1999;449:129-134.
12. Mills EM, Banks ML, Sprague JE, Finkel T. Pharmacology: uncoupling the agony from ecstasy. *Nature* 2003;426:403-404.

13. Mills EM, Rusyniak DE, Sprague JE. The role of the sympathetic nervous system and uncoupling proteins in the thermogenesis induced by 3,4-methylenedioxymethamphetamine. *J Mol Med* 2004;82:787-799.
14. Kratky D, Strauss JG, Zechner R. Tissue-specific activity of lipoprotein lipase in skeletal muscle regulates the expression of uncoupling protein 3 in transgenic mouse models. *Biochem J* 2001;355:647-652.
15. Garcia-Martinez C, Sibille B, Solanes G, Darimont C, Mace K, Villarroya F, Gomez-Foix AM. Overexpression of UCP3 in cultured human muscle lowers mitochondrial membrane potential, raises ATP/ADP ratio, and favors fatty acid vs. glucose oxidation. *FASEB J* 2001;15:2033-2035.
16. Bezaire V, Spriet LL, Campbell S, Sabet N, Gerrits M, Bonen A, Harper ME. Constitutive UCP3 overexpression at physiological levels increases mouse skeletal muscle capacity for fatty acid transport and oxidation. *FASEB J* 2005;19:977-979.
17. Himms-Hagen J, Harper ME. Physiological role of UCP3 may be export of fatty acids from mitochondria when fatty acid oxidation predominates: an hypothesis. *Exp Biol Med (Maywood)* 2001;226:78-84.
18. Schrauwen P, Saris WH, Hesselink MK. An alternative function for human uncoupling protein 3: protection of mitochondria against accumulation of nonesterified fatty acids inside the mitochondrial matrix. *FASEB J* 2001;15:2497-2502.
19. Schrauwen P, Hoeks J, Schaart G, Kornips E, Binas B, Van De Vusse GJ, van Bilsen M, Luiken JJ, Coort SL, Glatz JF, Saris WH, Hesselink MK. Uncoupling protein 3 as a mitochondrial fatty acid anion exporter. *FASEB J* 2003;17:2272-2274.
20. Echtay KS, Roussel D, St Pierre J, Jekabsons MB, Cadenas S, Stuart JA, Harper JA, Roebuck SJ, Morrison A, Pickering S, Clapham JC, Brand MD. Superoxide activates mitochondrial uncoupling proteins. *Nature* 2002;415:96-99.
21. Arsenijevic D, Onuma H, Pecqueur C, Raimbault S, Manning BS, Miroux B, Couplan E, Alves-Guerra MC, Goubern M, Surwit R, Bouillaud F, Richard D, Collins S, Ricquier D. Disruption of the uncoupling protein-2 gene in mice reveals a role in immunity and reactive oxygen species production. *Nat Genet* 2000;26:435-439.
22. Duval C, Negre-Salvayre A, Dogilo A, Salvayre R, Penicaud L, Casteilla L. Increased reactive oxygen species production with antisense oligonucleotides directed against uncoupling protein 2 in murine endothelial cells. *Biochem Cell Biol* 2002;80:757-764.
23. Lee FY, Li Y, Zhu H, Yang S, Lin HZ, Trush M, Diehl AM. Tumor necrosis factor increases mitochondrial oxidant production and induces expression of uncoupling protein-2 in the regenerating mice [correction of rat] liver. *Hepatology* 1999;29:677-687.
24. Negre-Salvayre A, Hirtz C, Carrera G, Cazenave R, Trolly M, Salvayre R, Penicaud L, Casteilla L. A role for uncoupling protein-2 as a regulator of mitochondrial hydrogen peroxide generation. *FASEB J* 1997;11:809-815.

25. Pecqueur C, Alves-Guerra MC, Gelly C, Levi-Meyrueis C, Couplan E, Collins S, Ricquier D, Bouillaud F, Miroux B. Uncoupling protein 2, in vivo distribution, induction upon oxidative stress, and evidence for translational regulation. *J Biol Chem* 2001;276:8705-8712.
26. Brand MD, Pamplona R, Portero-Otin M, Requena JR, Roebuck SJ, Buckingham JA, Clapham JC, Cadenas S. Oxidative damage and phospholipid fatty acyl composition in skeletal muscle mitochondria from mice underexpressing or overexpressing uncoupling protein 3. *Biochem J* 2002;368:597-603.
27. Boveris A, CHANCE B. The mitochondrial generation of hydrogen peroxide. General properties and effect of hyperbaric oxygen. *Biochem J* 1973;134:707-716.
28. Okuda M, Lee HC, Kumar C, CHANCE B. Comparison of the effect of a mitochondrial uncoupler, 2,4-dinitrophenol and adrenaline on oxygen radical production in the isolated perfused rat liver. *Acta Physiol Scand* 1992;145:159-168.
29. Skulachev VP. Uncoupling: new approaches to an old problem of bioenergetics. *Biochim Biophys Acta* 1998;1363:100-124.
30. Echtay KS, Murphy MP, Smith RA, Talbot DA, Brand MD. Superoxide activates mitochondrial uncoupling protein 2 from the matrix side. Studies using targeted antioxidants. *J Biol Chem* 2002;277:47129-47135.
31. Echtay KS, Esteves TC, Pakay JL, Jekabsons MB, Lambert AJ, Portero-Otin M, Pamplona R, Vidal-Puig AJ, Wang S, Roebuck SJ, Brand MD. A signalling role for 4-hydroxy-2-nonenal in regulation of mitochondrial uncoupling. *EMBO J* 2003;22:4103-4110.
32. Couplan E, Mar Gonzalez-Barroso M, Alves-Guerra MC, Ricquier D, Gubern M, Bouillaud F. No evidence for a basal, retinoic, or superoxide-induced uncoupling activity of the uncoupling protein 2 present in spleen or lung mitochondria. *J Biol Chem* 2002;277:26268-26275.
33. Cocco T, Di Paola M, Papa S, Lorusso M. Arachidonic acid interaction with the mitochondrial electron transport chain promotes reactive oxygen species generation. *Free Radic Biol Med* 1999;27:51-59.
34. Negre-Salvayre A, Auge N, Duval C, Robbesyn F, Thiers JC, Nazzal D, Benoist H, Salvayre R. Detection of intracellular reactive oxygen species in cultured cells using fluorescent probes. *Methods Enzymol* 2002;352:62-71.
35. Royall JA, Ischiropoulos H. Evaluation of 2',7'-dichlorofluorescein and dihydrorhodamine 123 as fluorescent probes for intracellular H₂O₂ in cultured endothelial cells. *Arch Biochem Biophys* 1993;302:348-355.
36. Pedraza N, Solanes G, Carmona MC, Iglesias R, Vinas O, Mampel T, Vazquez M, Giralt M, Villarroya F. Impaired expression of the uncoupling protein-3 gene in skeletal muscle during lactation: fibrates and troglitazone reverse lactation-induced downregulation of the uncoupling protein-3 gene. *Diabetes* 2000;49:1224-1230.

37. Zamora M, Merono C, Vinas O, Mampel T. Recruitment of NF-kappaB into mitochondria is involved in adenine nucleotide translocase 1 (ANT1)-induced apoptosis. *J Biol Chem* 2004;279:38415-38423.
38. Solanes G, Pedraza N, Iglesias R, Giralt M, Villarroya F. The human uncoupling protein-3 gene promoter requires MyoD and is induced by retinoic acid in muscle cells. *FASEB J* 2000;14:2141-2143.
39. Listenberger LL, Schaffer JE. Mechanisms of lipoapoptosis: implications for human heart disease. *Trends Cardiovasc Med* 2002;12:134-138.
40. Unger RH, Orci L. Lipoapoptosis: its mechanism and its diseases. *Biochim Biophys Acta* 2002;1585:202-212.
41. Hickson-Bick DL, Sparagna GC, Buja LM, McMillin JB. Palmitate-induced apoptosis in neonatal cardiomyocytes is not dependent on the generation of ROS. *Am J Physiol Heart Circ Physiol* 2002;282:H656-H664.
42. Carlsson C, Borg LA, Welsh N. Sodium palmitate induces partial mitochondrial uncoupling and reactive oxygen species in rat pancreatic islets in vitro. *Endocrinology* 1999;140:3422-3428.
43. Duval C, Auge N, Frisach MF, Casteilla L, Salvayre R, Negre-Salvayre A. Mitochondrial oxidative stress is modulated by oleic acid via an epidermal growth factor receptor-dependent activation of glutathione peroxidase. *Biochem J* 2002;367:889-894.
44. Inoguchi T, Li P, Umeda F, Yu HY, Kakimoto M, Imamura M, Aoki T, Etoh T, Hashimoto T, Naruse M, Sano H, Utsumi H, Nawata H. High glucose level and free fatty acid stimulate reactive oxygen species production through protein kinase C--dependent activation of NAD(P)H oxidase in cultured vascular cells. *Diabetes* 2000;49:1939-1945.
45. Gudz TI, Tserng KY, Hoppel CL. Direct inhibition of mitochondrial respiratory chain complex III by cell-permeable ceramide. *J Biol Chem* 1997;272:24154-24158.
46. Di Paola M, Cocco T, Lorusso M. Ceramide interaction with the respiratory chain of heart mitochondria. *Biochemistry* 2000;39:6660-6668.
47. Lyamzaev KG, Izyumov DS, Avetisyan AV, Yang F, Pletjushkina OY, Chernyak BV. Inhibition of mitochondrial bioenergetics: the effects on structure of mitochondria in the cell and on apoptosis. *Acta Biochim Pol* 2004;51:553-562.
48. Hatakeyama Y, Scarpace PJ. Transcriptional regulation of uncoupling protein-2 gene expression in L6 myotubes. *Int J Obes Relat Metab Disord* 2001;25:1619-1624.

La expresión ectópica de UCP3 en mitocondrias de hígado sensibiliza a la apertura del poro de transición en la permeabilidad mitocondrial (MPTP)

INTRODUCCIÓN

Las proteínas desacopladoras mitocondriales (UCPs) son miembros de la familia de transportadores localizados en la membrana mitocondrial interna. UCP2 y UCP3 son similares al primer miembro descrito de la familia, UCP1, que se expresa exclusivamente en tejido adiposo marrón donde media la termogénesis no asociada a temblor gracias a su capacidad para desacoplar la respiración de la fosforilación oxidativa (1).

Los niveles de expresión de los miembros de la familia UCP en hígado son bajos. La expresión de UCP2, cuya expresión es bastante ubicua en el organismo, es baja en el hígado. De hecho, estudios de inmunocitoquímica, revelaron que, en condiciones basales, su expresión en hígado, está restringida a las células de Kupffer, y no está presente por tanto, en hepatocitos (2). Sin embargo, otros estudios indicaron que bajo el estrés inducido por LPS (3), o en respuesta a estímulos que conlleven elevados niveles de catabolismo lipídico (dieta rica en grasas, tratamiento con fibratos...), aparecen niveles substanciales de UCP2 en hepatocitos (4; 5). Patologías asociadas a una alteración del metabolismo lipídico en el hígado, como la esteatosis hepática no asociada a alcoholismo, están también asociadas a una elevada expresión de UCP2 en el hígado (6).

UCP3 tiene un patrón de expresión tisular más restringido que UCP2, expresándose en elevados niveles en músculo esquelético, tejido adiposo marrón, y en menor medida también en corazón, tejido adiposo blanco y algunos tipos específicos de neuronas (7-11) no se expresa en el hígado, pero datos recientes muestran que en situaciones de máxima actividad del catabolismo de ácidos grasos en hígado (por ejemplo con una dieta rica en grasas más un tratamiento con bezafibrato), se induce la expresión de elevados niveles de UCP3 en hígado (12). La capacidad de los ácidos grasos para inducir la expresión de UCP3 en tejidos periféricos, como el tejido adiposo o el hígado, parece estar mediada por la activación de elementos de respuesta a PPAR localizados en el promotor del gen UCP3, por lo menos en lo que se refiere a células musculares (13-15). Los mecanismos moleculares que sostienen la represión de la expresión de UCP3 en hepatocitos, cualesquiera que sean, parecen

ser evitados tan sólo por tratamientos que conllevan una presencia extremadamente elevada de ácidos grasos y un elevado catabolismo lipídico en el hígado.

La importancia funcional de una elevada expresión de UCP2 o UCP3 en hígado no es totalmente comprendida actualmente. La hipótesis actual sobre la función fisiológica de dichas proteínas, sugiere un papel como favorecedoras de la oxidación y/o transporte de ácidos grasos, así como un papel en la protección contra una elevada producción de especies reactivas de oxígeno. Recientemente, las UCPs han sido relacionadas con la regulación de la muerte celular programada (11; 16-19) o de los eventos críticos en la muerte celular programada regulada por vías mitocondriales, es la permeabilización de la membrana mitocondrial externa, que puede estar mediada por la apertura de un canal multiproteico que respondería a ciertos estímulos aumentando la conductancia de la membrana a moléculas de hasta 1,5 kDa, conocido como MPTP o *mitochondrial permeability transition pore*. El MPTP puede abrirse en respuesta a diferentes estímulos, entre los que aparecen por ejemplo, una disminución de potencial, o una concentración elevada de calcio o atractilato (20). En un trabajo realizado como parte de esta tesis doctoral, se muestra como la expresión de UCP3 en células HEK-293, sensibilizaba al MPTP al estímulo del calcio (21), por lo que al disponer de mitocondrias funcionales de hígado, nos propusimos determinar también si UCP3 puede actuar como modulador de la actividad del MPTP. Para profundizar en estos aspectos, desarrollamos un modelo ectópico de expresión de elevados niveles de UCP3 a través de la transferencia *in vivo*, usando un vector adenovírico para la expresión de la forma humana de UCP3. En el presente estudio determinamos las consecuencias de una elevada expresión de UCP3 en hígado, sobre la función mitocondrial y el metabolismo global del organismo.

MATERIAL Y MÉTODOS

Inducción de la Expresión de UCP3 en el hígado de ratones

Los ratones utilizados eran de la cepa C57Bl6/J (Harlan Interfauna) y fueron mantenidos hasta el momento de su sacrificio en el estabulario de la Facultad de Biología (Universidad de Barcelona), en condiciones estándar de iluminación (ciclos de 12h luz/oscuridad) y temperatura (21 ± 1 °C). Fueron alimentados con una dieta estándar compuesta por un 72% de carbohidratos, 6% grasas, 22% proteína (% energía bruta) (B.K. Universal, España). Los experimentos se realizaron con ratones macho de 6.5 semanas de edad que fueron inyectados por la vena lateral de la cola, con 10^9 pfu de un vector adenovírico para la expresión de la β -galactosidasa (AdCMV-LacZ) o de la forma humana de UCP3 (AdCMV-UCP3). En estudios preliminares

determinamos que 72h después de la inyección se lograba un nivel óptimo de expresión del transgen, con lo que éste fue el tiempo utilizado en todos los experimentos posteriores. Los grupos experimentales sometidos a ayuno, lo fueron durante las 36h previas a su sacrificio.

Aislamiento de la Fracción Mitocondrial de Músculo

El músculo gastrocnemio de ratones fue inmediatamente homogenizado con un politrón tras su extracción, en un tampón de homogenización conteniendo 440 mM Sacarosa, 20 mM Na⁺/MOPS pH 7.2, 1 mM EDTA, y 0.1 mM PMSF. Todo el proceso se realizó a 4°C. Se centrifugó el homogenado a 1000g durante 10 minutos a 4°C. El sobrenadante se centrifugó de nuevo a 1000g durante 10 minutos a 4°C. El sobrenadante recuperado se centrifugó a 10.000 g durante 10 minutos a 4°C. El sedimento se resuspende en unos 400 µl de tampón de homogenización y constituye la fracción mitocondrial de músculo. La valoración de la concentración de proteína se realizó sobre un volumen de muestra conteniendo un 0.1% final de Tritón X-100, a fin de solubilizar completamente todas las membranas.

Inmunodetección o Análisis *Western blot*

Para la detección de citocromo c y UCP3, muestras de la fracción mitocondrial de músculo o hígado de ratón se separaron en una electroforesis en gel de acrilamida desnaturizante (SDS-PAGE) al 12,8%. Posteriormente fueron transferidas a membranas de *polyvinylidene fluoride* (PVDF membranes, Immobilon-P, Millipore). Éstas fueron posteriormente incubadas con anticuerpos contra UCP3 (Chemicon AB3046 (1:1000)) y contra el citocromo c (Pharmingen clone 7H8.2C12 (1:500)) que se utilizó para determinar la corrección tanto de la carga de proteína como del fraccionamiento mitocondrial. La unión de anticuerpos se detectó con un anticuerpo secundario anti-ratón (Bio-Rad 170-6516 (1:3000)) o anti-conejo (Santa Cruz sc-2004 (1:3000)), ambos asociados a la peroxidasa de rábano, mediante el kit de detección quimioluminiscente enhanced chemiluminescence (ECL, Amersham).

Valoración de la Concentración de Metabolitos Circulantes

La valoración de metabolitos circulantes en plasma se ha realizado con los lectores *Accu-Chek® Sensor* (Roche) para la Glucosa, *AccuTrend®GCT* (Roche) para los triacilglicéridos y *AccuTrend®Lactate* para el Lactato según las indicaciones del fabricante. Los cuerpos cetónicos y NEFA en plasma fueron valorados mediante los

kits colorimétricos *β -hydroxybutyrate Liquid Color®* (Stanbio), y *NEFA C ACS-ACOD Method* (Wako).

Obtención de mitocondrias funcionales de hígado

El hígado extraído de los ratones fue inmediatamente homogenizado en un tampón de homogenización conteniendo 250 mM Sacarosa desionizada, 1 mM EDTA, 50 mM KCl y 25 mM Tris, con la ayuda de un homogenizador de vidrio. El homogenizado se centrifugó a 700g durante 10 min y a 4°C. El sobrenadante resultante, se centrifugó a 7000g durante 10 min y a 4°C. El precipitado que se resuspendió en un pequeño volumen (aproximadamente 400 μ l) de tampón de homogenización corresponde a la fracción mitocondrial del hígado. Es importante realizar todo el proceso a 4°C y/o en contacto con hielo. Recuperaremos una pequeña parte de la fracción mitocondrial para su análisis por *western blot*. Centrifugamos a 10.000g a 4°C, y resuspendemos en tampón homogenización suplementado con 2 mM PMSF, 2 μ g/ml de leupeptina, pepstatina, aprotinina y 2 mM de Benzamidina. La valoración de la concentración de proteína de las muestras se realiza tras diluir las muestras 1/10 en tampón de homogenización con un 0,3% Tritón mediante el método *BCA Protein Assay (PIERCE)*.

Ensayos de Consumo de Oxígeno

Las tasas de respiración de la fracción mitocondrial obtenida de hígado de ratón, fueron determinadas polarográficamente a 25°C utilizando un electrodo de oxígeno de Clark (Rank Brothers, Ltd.) conectado a un micro-computador que permite una lectura continua de la concentración de oxígeno en el medio. El medio en el que se realizaron las medidas contenía 250 mM Sacarosa desionizada, 1 mM EDTA, 50 mM KCl, 25 mM Tris, 5 mM KH_2PO_4 , y 0.3% BSA delipidada (Sigma).

Las mediciones del consumo de oxígeno en estado 4 se realizaron utilizando como substrato 6 mM de glutamato/malato o 6 mM de succinato (en presencia de 5 μ M de rotenona). El consumo de oxígeno en respuesta a 1 mM de ADP se consideró como la respiración en estado 3. El índice del control respiratorio se calculó en base a la relación estado 3/estado 4 para cada una de las muestras.

Sobre la respiración en estado 4 (succinato 6 mM; 5 μ M rotenona; 10 μ g/ml oligomicina), se determinó el efecto de la adición secuencial de 300 μ M de palmitato y 1 mM de GDP.

Análisis de la Expresión Génica mediante PCR a Tiempo Real

El RNA total fue extraído de las muestras de hígado de ratón con el kit *Rneasy* (Qiagen). El análisis cuantitativo de la expresión de los mRNA se llevó a cabo en una reacción de PCR en dos pasos: en primer lugar, 1µg del RNA total se retrotranscribió a cDNA mediante una RT-PCR (*reverse transcriptase polymerase chain reaction*) en el GeneAmp PCR system 2400 (Applied Biosystems, USA), y seguidamente, una Real-Time PCR se llevó a cabo en el ABI PRISM 7700HT sequence detection (Applied Biosystems, U.S.A). La RT-PCR se realizó en un volumen final de 50µl utilizando el *kit* TaqMan® Reverse Transcription Reagents (Applied Biosystems, U.S.A), que contiene la Transcriptasa Reversa MultiScribe™, un inhibidor de RNasas, una mezcla de dNTP, *Random Hexamers*, tampón 10X para la RT, y una solución de MgCl₂. La reacción de PCR a tiempo real se realizó en un volumen final de 25µl utilizando la *TaqMan*® *Universal PCR Master Mix*, y las sondas para expresión génica TaqMan® diseñadas por Applied Biosystems (U.S.A): *18S ribosomal RNA* (Hs99999901_s1), *uncoupling protein 2* (Mm00495907_g1), *PGC-1α* (Mm00447183_m1), *glutathione peroxidase 1* (Mm00656767_g1), *glutathione peroxidase 4* (Mm00515041_m1), *heme oxygenase 1* (Mm00516004_m1), *superoxide dismutase 2* (Mm00449726-m1), *sequestosome 1* (Mm00448091_m1), *Transformation related protein 53* (Mm00441964_g1), *c-fos* (Mm00487425_m1), *c-jun* (Mm00495062_s1), *Nfκb1 (p105)* (Mm00476361_m1), *acetyl-Coenzyme A dehydrogenase, medium chain* (Mm00431611_m1), *peroxisome proliferator activated receptor α* (Mm00440939_m1), y *peroxisome proliferator activated receptor α* (Mm00803186_g1).

Se incluyó un control sin RNA, mix de reacción o transcriptasa reversa en cada serie experimental. Cada muestra se analizó por duplicado, y la media de los valores de cada duplicado se utilizó para determinar el nivel de expresión de cada mRNA a estudio. La cantidad del gen de interés contenido en cada muestra se normalizó en relación a un control endógeno utilizando el método de comparación de ($2^{-\Delta CT}$) de acuerdo a las instrucciones del fabricante (Applied Biosystems, USA). En nuestro caso, el RNA ribosómico 18S se utilizó como control endógeno.

Determinación del Swelling en Mitocondrias de Hígado

Determinamos el *swelling* o hinchamiento mitocondrial valorando el descenso de la absorbancia a 540 nm y 25°C de una solución de mitocondrias (22). Las mitocondrias de hígado fueron obtenidas según el procedimiento descrito previamente, pero resuspendiendo el último precipitado correspondiente a la fracción mitocondrial, en un tampón 213 mM manitol, 71 mM sacarosa, y 5 mM HEPES/Tris pH 7,8. Se

incubaron 0,25 mg/ml de solución mitocondrial en un tampón 250 mM Sacarosa desionizada, 5 mM succinato, 10 μ M EGTA, 2 μ M rotenona, 1 mM KH₂PO₄ y 10 mM TrisMOPS pH 7,4, a 25°C. En este momento se añadió 5 μ M de CsA (Ciclosporina A) cuando se requería. Transcurridos 2 minutos, se realizó una lectura continua de la absorbancia a 540 nm durante 6 minutos, con el programa cinético del espectrofotómetro Shimadzu- UV-160A. Los reactivos requeridos, a la concentración indicada, se añadieron y mezclaron por inversión con la solución mitocondrial justo antes de iniciar la lectura. El atractilato y Ciclosporina A fueron adquiridos de Sigma.

Análisis Estadístico

Los datos se muestran como media \pm error estándar, y fueron analizados con el Test de la *T-Student* para la determinación de diferencias significativas que se consideraron significativas para p-valores inferiores a 0.05.

RESULTADOS

Establecimiento de la expresión ectópica de UCP3 en hígado de ratón

La expresión ectópica de UCP3 en las mitocondrias de hígado proporciona una herramienta única para analizar el impacto de UCP3 en la bioenergética: UCP3 aparece en un contexto prácticamente “libre de UCPs” y es posible estudiar su actividad en mitocondrias altamente acopladas, gracias a la facilidad para obtener mitocondrias funcionales y en suficiente cantidad para realizar análisis bioenergéticos. La transferencia génica mediada por vectores adenovíricos *in vivo*, permite la expresión de elevados niveles de UCP3 en las mitocondrias del hígado, mayores que los presentes en el músculo esquelético, entorno natural de expresión de la proteína (Figura 1B). Comprobamos además que UCP3 se dirigía correctamente a la mitocondria (no detectábamos expresión de la proteína en núcleos o citosol) y que la máxima expresión se lograba a 72h de la inyección del vector en nuestro modelo experimental (Datos no mostrados).

La expresión ectópica de UCP3 en hígado no provoca una alteración en los niveles de metabolitos circulantes

La presencia de elevados niveles de UCP3 en el hígado de ratones inyectados con el vector adenovírico, no provocó una alteración significativa en la concentración de ninguno de los metabolitos circulantes analizados (Glucosa, NEFA, Lactato, Triglicéridos, o β -hidroxibutirato) (Tabla 1).

Tras someter a los ratones inyectados a ayuno durante las 36h previas al sacrificio, los parámetros circulantes respondieron de la forma esperada (descenso en los niveles de glucosa, aumento en los niveles de β -hidroxibutirato). Sin embargo, los niveles de NEFA no sufrían cambios significativos (Tabla 1). En los ratones ayunados, la expresión de UCP3 tampoco supuso ninguna modificación de los metabolitos circulantes.

La presencia de elevados niveles de UCP3 en hígado no provoca una alteración del índice de control respiratorio ni la respiración en estado 4

Niveles elevados de inducción de UCP3 no supusieron una modificación de la tasa respiratoria en estado 3 o estado 4, en presencia de ninguno de los sustratos utilizados: Glutamato/malato (que aporta los electrones al complejo I de la cadena respiratoria) o Succinato (que aporta los electrones directamente al complejo II) (Figura 2A). Igualmente, el control respiratorio o relación entre las tasas de consumo de oxígeno en estado 3 respecto a las de estado 4, no sufrió alteraciones en presencia de UCP3 para ninguno de los sustratos utilizados. (Figura 2B)

La tasa de respiración en estado 4 se estimulaba en presencia de 300 μ M de palmitato, de igual forma en presencia o ausencia de UCP3. Igualmente, la posterior adición de 1 mM de GDP no revertía el desacoplamiento inducido por el ácido graso, ya fuera en presencia o ausencia de UCP3 (Figura 2C).

Efecto de UCP3 sobre la expresión de genes relacionados con el metabolismo lipídico y estrés celular

Se determinaron las consecuencias de la expresión de UCP3 sobre la expresión génica en hígado. Se determinó que los genes codificantes para los componentes de la maquinaria antioxidante celular (superóxido dismutasa, glutatión peroxidasa...) están inalterados en presencia de UCP3. Sin embargo, la expresión de c-fos y Trp53 se induce con la expresión de la proteína. (Figura 3B).

El ayuno de los ratones durante 36h, provoca a su vez, un incremento en los genes que codifican para proteínas implicadas en el control del estrés oxidativo, como la glutatión peroxidasa 4, la superóxido dismutasa 2 o la sqtm 1, así como la expresión de genes implicados en el metabolismo lipídico (Mcad, PGC-1 α). De hecho, la expresión de UCP3 en ratones ayunados durante 36h, favorece la inducción de la expresión de estos genes implicados en el metabolismo lipídico (Figura 3).

La presencia de UCP3 afecta también de forma positiva a la expresión de genes relacionados con la fase aguda de la respuesta celular al estrés, como son Trp53 y c-fos. En presencia de UCP3, existe también cierta tendencia a inducir la

expresión de UCP2, aunque la inducción no llega a ser significativa estadísticamente. (Figura 3B).

La expresión ectópica de UCP3 en hígado favorece la apertura del MPTP

Las mitocondrias aisladas tienen la propiedad de hincharse o sufrir un *swelling* ante un aumento de la permeabilidad de la membrana mitocondrial externa, fenómeno que puede detectarse como el descenso en la absorbancia a 540 nm de una muestra de mitocondrias y que, en tanto que inhibible por ciclosporina A, es un índice de la apertura del MPTP. Las mitocondrias aisladas de hígado de ratón inyectado con UCP3 mostraron un mayor *swelling*, o descenso más rápido de absorbancia ya en estado basal. Igualmente, observamos como respondían repetidamente con una mayor pendiente, mayor *swelling* a concentraciones crecientes de dos conocidos inductores de la apertura del MPTP (Calcio (Figura 4A) y atractilato (Figura 4B). El descenso en la absorbancia era revertido en cualquier caso en presencia de CsA, con lo que podemos asegurar que el fenómeno era dependiente de la apertura del MPTP.

DISCUSIÓN

UCP3 se expresa preferencialmente en músculo esquelético y TAM. De hecho, el hígado constituye en condiciones basales, un entorno libre de UCPs, ya que la expresión de UCP2 se cree que está restringida a las células de Kupffer (2), aunque pueda inducirse su expresión en determinadas situaciones (3-6) Por ello, la expresión de UCP3 en el hígado resulta un modelo ideal para el estudio de las propiedades bioquímicas de la proteína. Por otro lado, se sabe que UCP3 puede llegar a expresarse en hígado ante una situación de estrés metabólico como la que supone una dieta hiperlipídica asociada al tratamiento con fibratos (12).

La inyección de vectores adenovíricos por la vena lateral de la cola del ratón, nos permitió una expresión eficiente de UCP3, que además quedaba restringida al hígado, como demuestra el hecho de que no se produzca variación en los niveles de la proteína en el músculo esquelético de los ratones inyectados. Los niveles de expresión que inducimos en hígado, son muy superiores a los que se dan en el músculo, sin embargo, esta elevada expresión no está asociada a ninguna alteración en la tasa de consumo de oxígeno en estado 4, con lo que podemos descartar la existencia de un desacoplamiento inespecífico como se ha descrito en otros modelos de sobre-expresión de UCP3 (23; 24). De hecho, los elevados niveles de UCP3 no parecen afectar de forma general al metabolismo del organismo, que no muestra ninguna alteración significativa en la concentración de metabolitos circulantes.

Actualmente existe un intenso debate sobre si la actividad desacoplante que se describió para UCP3 *in vitro* constituye o forma parte de su función fisiológica. La falta de una alteración en la tasa de respiración en estado 4, parece contradecir el que UCP3 tenga una actividad desacoplante *in vivo*. Algunos autores consideran que dicha actividad desacoplante tiene lugar únicamente en presencia de cofactores como los ácidos grasos, y que es sensible a GDP, como fue descrito anteriormente para UCP1 (1). No obstante, no observamos ninguna alteración significativa del consumo de oxígeno tras la adición de un ácido graso como el palmitato, ni tampoco un reacomplamiento inducido por GDP. Dado que este órgano no es el entorno natural de expresión de UCP3, es posible que carezca de algún cofactor necesario para que la proteína desarrolle dicha actividad.

La expresión de UCP3 en músculo esquelético correlaciona con el nivel de ácidos grasos libres y se induce en situaciones de estrés como la sepsis (25), caquexia (26) y el ayuno (7; 27)... Datos obtenidos del estudio de UCP2 y de ratones deficientes para la expresión de UCP3, sugieren que la proteína tendría un papel fundamental en la limitación de la producción de ROS, gracias a su capacidad para acelerar el consumo de oxígeno (28). Recientemente se ha propuesto además, que el propio estrés oxidativo estaría regulando la actividad de la proteína (29; 30). El ayuno comporta un aumento en la disponibilidad de ácidos grasos para el metabolismo hepático, y un acúmulo de estos ácidos grasos, puede resultar perjudicial, debido a la posibilidad de formación de metabolitos reactivos como los lipoperóxidos o las ceramidas, que podrían dañar estructuras y funciones celulares. En nuestro caso, sorprendentemente, no detectamos el aumento esperado en el nivel de NEFA con el ayuno, sin embargo, el aumento en los niveles de β -hidroxibutirato, indican que efectivamente, se está produciendo una activación del catabolismo lipídico en el hígado. Los ácidos grasos pueden inducir la producción de ROS (31; 32). De hecho, observamos como 36h de ayuno, eran suficientes para inducir significativamente la expresión de diversos genes relacionados con el control de los ROS, como las enzimas antioxidantes SOD2, y Gpx4 y la proteína Sqtm1, sugiriendo que se estaba creando una situación de estrés oxidativo que requiere de la expresión de dichos productos génicos. Así mismo, y como esperábamos, el ayuno inducía la expresión de genes implicados en el metabolismo lipídico, como son la Mcad (*Acil-CoA deshidrogenase medium chain*) y PGC-1 α , potencial coactivador transcripcional de PPARs, a fin de acelerar la oxidación de los ácidos grasos y reducir su acumulación.

El modelo de ayuno, nos permitía, exponer a UCP3, a un entorno proclive a su activación. Por ello, utilizamos el modelo de ayuno combinado con la inducción de la expresión de la proteína en hígado. Pudimos observar que la expresión de UCP3 no

afecta de forma generalizada a la expresión de genes relacionados con el estrés oxidativo, ni siquiera en una situación de ayuno. Sin embargo, en presencia de UCP3, se produce una inducción de proteínas implicadas en mecanismos de estrés celular, como son la p53 y c-fos (33). También existe cierta tendencia a la inducción de la expresión de UCP2, aunque no de forma estadísticamente significativa. Se considera que UCP2 podría jugar un papel en el control de la generación de ROS, (34; 35), sugiriendo que UCP3 contribuye a crear un entorno que requiere de la presencia de UCP2 y apuntando de nuevo a la generación de un estrés celular por parte de UCP3. Recientemente, se ha descrito la capacidad de UCP3 para proteger a células neuronales de la apoptosis, mediante su capacidad para limitar la producción de ROS (11). Sin embargo, trabajos previos de nuestro grupo, mostraban la capacidad de la proteína para sensibilizar a células de riñón frente a un estímulo pro-apoptótico dependiente de regulación mitocondrial (21). Uno de los mecanismos a través de los cuales, UCP3 podría estar afectando a la regulación de la muerte celular, es a través de su influencia sobre el MPTP, ya sea gracias a su actividad desacoplante o debido a una interacción con proteínas implicadas en la regulación del proceso. De hecho, en el modelo celular de células HEK-293, observábamos como el MPTP presentaba una mayor sensibilidad a la apertura en respuesta a un conocido inductor como es el calcio. En el presente estudio, y utilizando una metodología y aproximación experimental totalmente distintas, observamos, como las mitocondrias respondían a conocidos inductores de la apertura del MPTP, como son el calcio y el atractilato (20), con un mayor *swelling* o hinchamiento. Además, en ausencia de la adición de inductores, las mitocondrias que contenían UCP3, mostraban un nivel de *swelling* superior. El *swelling*, puede deberse a una inestabilidad de las membranas mitocondriales, pero en nuestro caso, era revertido por la adición de un inhibidor específico del MPTP, como es la ciclosporina A (36). La apertura del MPTP es un evento estrechamente relacionado con la muerte celular dependiente de vías reguladas a nivel mitocondrial (37). No obstante, tanto el aspecto macroscópico del hígado, como los datos de consumo de oxígeno, metabolitos circulantes y expresión génica, sugieren que no se está produciendo una mortalidad celular en el tejido. De hecho, la apertura del MPTP en condiciones basales, podría deberse a la presencia de trazas de inductores de la apertura (posiblemente calcio) en el tampón de ensayo. Así, de nuevo la expresión de UCP3, parece sensibilizar al MPTP ante sus inductores. Además, la acción sensibilizadora de la apertura del MPTP por parte de UCP3 se da con independencia del tipo de estímulo inductor, ya que el mecanismo de acción de atractilato y calcio sobre el MPTP es diferente (20).

Por otro lado, la presencia de UCP3 tiende a favorecer la expresión de genes relacionados con la oxidación de ácidos grasos, como es la Mcad, y PGC-1 α (aunque no de forma significativa en este último caso), ambos en una situación de ayuno, y por tanto, proclive a la activación de UCP3. Estos datos sugieren, que UCP3 podría estar favoreciendo la oxidación de ácidos grasos como ya se ha descrito en diversos modelos *in vitro* (38; 39).

Posiblemente, la acción de la proteína UCP3 dependa del tipo celular, el estímulo y la intensidad del mismo, pudiendo afectar a diferentes procesos celulares, como son la oxidación de ácidos grasos y la modulación de la muerte celular programada.

BIBLIOGRAFÍA

1. Nicholls DG, Rial E. A history of the first uncoupling protein, UCP1. *J Bioenerg Biomembr* 1999;31:399-406.
2. Larrouy D, Laharrague P, Carrera G, Viguerie-Bascands N, Levi-Meyrueis C, Fleury C, Pecqueur C, Nibbelink M, Andre M, Casteilla L, Ricquier D. Kupffer cells are a dominant site of uncoupling protein 2 expression in rat liver. *Biochem Biophys Res Commun* 1997;235:760-764.
3. Ruzicka M, Skobisova E, Dlaskova A, Santorova J, Smolkova K, Spacek T, Zackova M, Modriansky M, Jezek P. Recruitment of mitochondrial uncoupling protein UCP2 after lipopolysaccharide induction. *Int J Biochem Cell Biol* 2005;37:809-821.
4. Nakatani T, Tsuboyama-Kasaoka N, Takahashi M, Miura S, Ezaki O. Mechanism for peroxisome proliferator-activated receptor-alpha activator-induced up-regulation of UCP2 mRNA in rodent hepatocytes. *J Biol Chem* 2002;277:9562-9569.
5. Tsuboyama-Kasaoka N, Takahashi M, Kim H, Ezaki O. Up-regulation of liver uncoupling protein-2 mRNA by either fish oil feeding or fibrate administration in mice. *Biochem Biophys Res Commun* 1999;257:879-885.
6. Baffy G. Uncoupling protein-2 and non-alcoholic fatty liver disease. *Front Biosci* 2005;10:2082-2096.
7. Boss O, Samec S, Paoloni-Giacobino A, Rossier C, Dulloo A, Seydoux J, Muzzin P, Giacobino JP. Uncoupling protein-3: a new member of the mitochondrial carrier family with tissue-specific expression. *FEBS Lett* 1997;408:39-42.
8. Matsuda J, Hosoda K, Itoh H, Son C, Doi K, Tanaka T, Fukunaga Y, Inoue G, Nishimura H, Yoshimasa Y, Yamori Y, Nakao K. Cloning of rat uncoupling protein-3 and uncoupling protein-2 cDNAs: their gene expression in rats fed high-fat diet. *FEBS Lett* 1997;418:200-204.

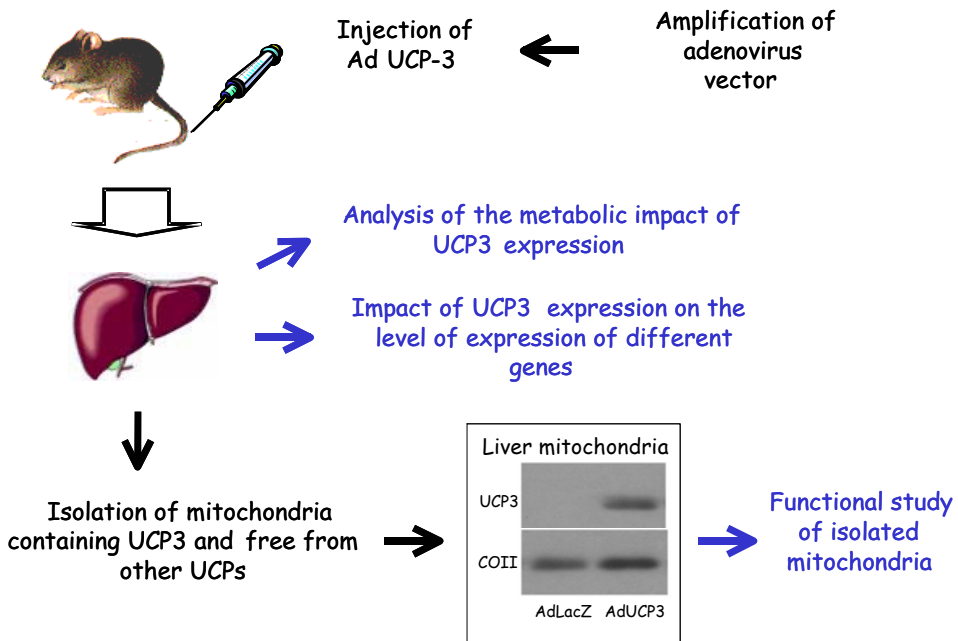
9. Vidal-Puig A, Solanes G, Grujic D, Flier JS, Lowell BB. UCP3: an uncoupling protein homologue expressed preferentially and abundantly in skeletal muscle and brown adipose tissue. *Biochem Biophys Res Commun* 1997;235:79-82.
10. Yoshitomi H, Yamazaki K, Tanaka I. Cloning of mouse uncoupling protein 3 cDNA and 5'-flanking region, and its genetic map. *Gene* 1998;215:77-84.
11. Vincent AM, Olzmann JA, Brownlee M, Sivitz WI, Russell JW. Uncoupling proteins prevent glucose-induced neuronal oxidative stress and programmed cell death. *Diabetes* 2004;53:726-734.
12. Lanni A, Mancini F, Sabatino L, Silvestri E, Franco R, De Rosa G, Goglia F, Colantuoni V. De novo expression of uncoupling protein 3 is associated to enhanced mitochondrial thioesterase-1 expression and fatty acid metabolism in liver of fenofibrate-treated rats. *FEBS Lett* 2002;525:7-12.
13. Brun S, Carmona MC, Mampel T, Vinas O, Giralt M, Iglesias R, Villarroya F. Activators of peroxisome proliferator-activated receptor- α induce the expression of the uncoupling protein-3 gene in skeletal muscle: a potential mechanism for the lipid intake-dependent activation of uncoupling protein-3 gene expression at birth. *Diabetes* 1999;48:1217-1222.
14. Pedraza N, Solanes G, Carmona MC, Iglesias R, Vinas O, Mampel T, Vazquez M, Giralt M, Villarroya F. Impaired expression of the uncoupling protein-3 gene in skeletal muscle during lactation: fibrates and troglitazone reverse lactation-induced downregulation of the uncoupling protein-3 gene. *Diabetes* 2000;49:1224-1230.
15. Young ME, Patil S, Ying J, Depre C, Ahuja HS, Shipley GL, Stepkowski SM, Davies PJ, Taegtmeyer H. Uncoupling protein 3 transcription is regulated by peroxisome proliferator-activated receptor (α) in the adult rodent heart. *FASEB J* 2001;15:833-845.
16. Mattiasson G, Shamloo M, Gido G, Mathi K, Tomasevic G, Yi S, Warden CH, Castilho RF, Melcher T, Gonzalez-Zulueta M, Nikolich K, Wieloch T. Uncoupling protein-2 prevents neuronal death and diminishes brain dysfunction after stroke and brain trauma. *Nat Med* 2003;9:1062-1068.
17. Teshima Y, Akao M, Jones SP, Marban E. Uncoupling protein-2 overexpression inhibits mitochondrial death pathway in cardiomyocytes. *Circ Res* 2003;93:192-200.
18. Diano S, Matthews RT, Patrylo P, Yang L, Beal MF, Barnstable CJ, Horvath TL. Uncoupling protein 2 prevents neuronal death including that occurring during seizures: a mechanism for preconditioning. *Endocrinology* 2003;144:5014-5021.
19. Leininger GM, Russell JW, van Golen CM, Berent A, Feldman EL. Insulin-like growth factor-I regulates glucose-induced mitochondrial depolarization and apoptosis in human neuroblastoma. *Cell Death Differ* 2004;11:885-896.
20. Zoratti M, Szabo I. The mitochondrial permeability transition. *Biochim Biophys Acta* 1995;1241:139-176.

21. Dejean L, Camara Y, Sibille B, Solanes G, Villarroya F. Uncoupling protein-3 sensitizes cells to mitochondrial-dependent stimulus of apoptosis. *J Cell Physiol* 2004;201:294-304.
22. Notario B, Zamora M, Vinas O, Mampel T. All-trans-retinoic acid binds to and inhibits adenine nucleotide translocase and induces mitochondrial permeability transition. *Mol Pharmacol* 2003;63:224-231.
23. Cadenas S, Echtay KS, Harper JA, Jekabsons MB, Buckingham JA, Grau E, Abuin A, Chapman H, Clapham JC, Brand MD. The basal proton conductance of skeletal muscle mitochondria from transgenic mice overexpressing or lacking uncoupling protein-3. *J Biol Chem* 2002;277:2773-2778.
24. Guerini D, Prati E, Desai U, Nick HP, Flammer R, Gruninger S, Cumin F, Kaleko M, Connelly S, Chiesi M. Uncoupling of protein-3 induces an uncontrolled uncoupling of mitochondria after expression in muscle derived L6 cells. *Eur J Biochem* 2002;269:1373-1381.
25. Sun X, Wray C, Tian X, Hasselgren PO, Lu J. Expression of uncoupling protein 3 is upregulated in skeletal muscle during sepsis. *Am J Physiol Endocrinol Metab* 2003;285:E512-E520.
26. Bing C, Brown M, King P, Collins P, Tisdale MJ, Williams G. Increased gene expression of brown fat uncoupling protein (UCP)1 and skeletal muscle UCP2 and UCP3 in MAC16-induced cancer cachexia. *Cancer Res* 2000;60:2405-2410.
27. Gong DW, He Y, Karas M, Reitman M. Uncoupling protein-3 is a mediator of thermogenesis regulated by thyroid hormone, beta3-adrenergic agonists, and leptin. *J Biol Chem* 1997;272:24129-24132.
28. Vidal-Puig AJ, Grujic D, Zhang CY, Hagen T, Boss O, Ido Y, Szczepanik A, Wade J, Mootha V, Cortright R, Muoio DM, Lowell BB. Energy metabolism in uncoupling protein 3 gene knockout mice. *J Biol Chem* 2000;275:16258-16266.
29. Echtay KS, Roussel D, St Pierre J, Jekabsons MB, Cadenas S, Stuart JA, Harper JA, Roebuck SJ, Morrison A, Pickering S, Clapham JC, Brand MD. Superoxide activates mitochondrial uncoupling proteins. *Nature* 2002;415:96-99.
30. Echtay KS, Esteves TC, Pakay JL, Jekabsons MB, Lambert AJ, Portero-Otin M, Pamplona R, Vidal-Puig AJ, Wang S, Roebuck SJ, Brand MD. A signalling role for 4-hydroxy-2-nonenal in regulation of mitochondrial uncoupling. *EMBO J* 2003;22:4103-4110.
31. Hickson-Bick DL, Sparagna GC, Buja LM, McMillin JB. Palmitate-induced apoptosis in neonatal cardiomyocytes is not dependent on the generation of ROS. *Am J Physiol Heart Circ Physiol* 2002;282:H656-H664.
32. Carlsson C, Borg LA, Welsh N. Sodium palmitate induces partial mitochondrial uncoupling and reactive oxygen species in rat pancreatic islets in vitro. *Endocrinology* 1999;140:3422-3428.
33. Herr I, Debatin KM. Cellular stress response and apoptosis in cancer therapy. *Blood* 2001;98:2603-2614.

34. Negre-Salvayre A, Hirtz C, Carrera G, Cazenave R, Trolly M, Salvayre R, Penicaud L, Casteilla L. A role for uncoupling protein-2 as a regulator of mitochondrial hydrogen peroxide generation. *FASEB J* 1997;11:809-815.
35. Arsenijevic D, Onuma H, Pecqueur C, Raimbault S, Manning BS, Miroux B, Couplan E, Alves-Guerra MC, Goubern M, Surwit R, Bouillaud F, Richard D, Collins S, Ricquier D. Disruption of the uncoupling protein-2 gene in mice reveals a role in immunity and reactive oxygen species production. *Nat Genet* 2000;26:435-439.
36. Crompton M, Ellinger H, Costi A. Inhibition by cyclosporin A of a Ca²⁺-dependent pore in heart mitochondria activated by inorganic phosphate and oxidative stress. *Biochem J* 1988;255:357-360.
37. Zamzami N, Kroemer G. The mitochondrion in apoptosis: how Pandora's box opens. *Nat Rev Mol Cell Biol* 2001;2:67-71.
38. Bezaire V, Spriet LL, Campbell S, Sabet N, Gerrits M, Bonen A, Harper ME. Constitutive UCP3 overexpression at physiological levels increases mouse skeletal muscle capacity for fatty acid transport and oxidation. *FASEB J* 2005;19:977-979.
39. Garcia-Martinez C, Sibille B, Solanes G, Darimont C, Mace K, Villarroya F, Gomez-Foix AM. Overexpression of UCP3 in cultured human muscle lowers mitochondrial membrane potential, raises ATP/ADP ratio, and favors fatty acid vs. glucose oxidation. *FASEB J* 2001;15:2033-2035.

Figura 1

A



B

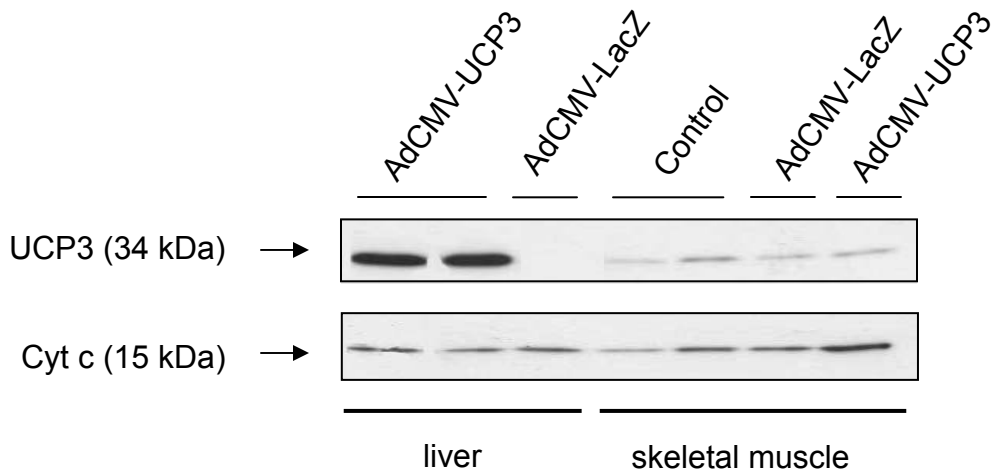


Figura 1: Inducción de la expresión de UCP3 en las mitocondrias de hígado de ratón mediada por un vector adenovírico. **A.** Esquema del planteamiento experimental **B.** Análisis por *western blot* de 30 μ g de proteína mitocondrial proveniente del hígado (*liver*) o el músculo esquelético (*skeletal muscle*) de ratones control o inyectados con un vector adenovírico para la expresión de la β -galactosidasa (AdCMV-LacZ) o UCP3 (AdCMV-UCP3). La obtención de las muestras tubo lugar 72 h después de inyectar los vectores adenovíricos. Inmunodetección con anticuerpos específicos contra el citocromo c o UCP3.

Tabla 1

Tabla 1: Concentración plasmática de metabolitos circulantes en presencia de UCP3 y en respuesta al ayuno

Metabolite	AdCMV-LacZ		AdCMV-UCP3	
	Fed	Fasted	Fed	Fasted
Glucose (mg/dl)	18.9 ± 0.5	11.2 ± 1.5 **	17.1 ± 0.1	12.2 ± 0.8 *
Lactate (mg/dl)	1.5 ± 0.26	---	1.7 ± 0.8	---
Triglycerides (mg/dl)	374.5 ± 61.4	---	445.8 ± 32.1	287.5 ± 73.5
NEFA (μM)	1615.6 ± 247.5	863.2 ± 140.9	1642.3 ± 268.4	1063.9 ± 200.9
β-hidroxybutirate (μM)	162.2 ± 40.4	1516.6 ± 297.4 **	153.4 ± 19.0	1293.2 ± 724.9 **

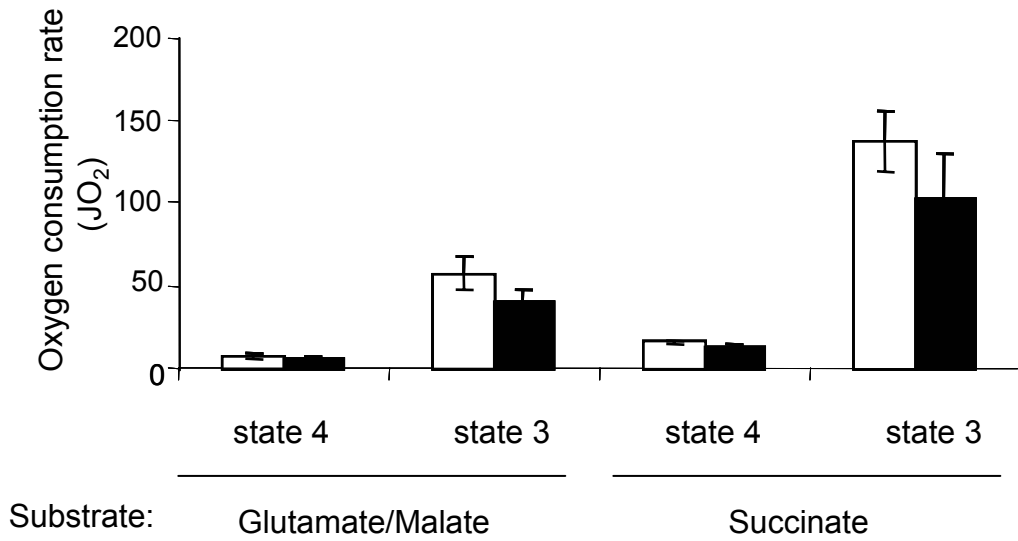
La concentración plasmática de los indicados metabolitos circulantes se estimó en ratones inyectados con AdCMV-LacZ o AdCMV-UCP3, sometidos (fasted) o no (fed) a 36h de ayuno antes del sacrificio. Los resultados son medias ± error estándar de 3-6 experimentos independientes. Las diferencias significativas debidas al ayuno se muestran como *p<0,05; ** p<0,01. NEFA: ácidos grasos libres.

Figure 2: Efecto de UCP3 sobre la tasa de respiración mitocondrial. Efecto sobre el control respiratorio y la respuesta a palmitato y GDP. Se obtuvieron mitocondrias funcionales del hígado de ratones 72 después de la inyección con los AdCMV-LacZ o AdCMVUCP y se valoró el consumo de oxígeno en diferentes condiciones según lo descrito en el Material y Métodos. **A.** Determinación de la tasa de consumo de oxígeno en estado 4 y 3 (en presencia de 1 mM ADP), utilizando como sustrato succinato 6 mM (en presencia de 5 μ M de rotenona) o una mezcla de Glutamato/Malato 6 mM. **B.** Índice de Control respiratorio (relación estado3/estado 4) utilizando las mismas condiciones que en A. **C.** Determinación de la tasa de consumo de oxígeno en estado 4 (succinato 6 mM; rotenona 5 μ M; y 10 μ g/ml de oligomicina) tras la adición secuencial de 300 μ M de palmitato, 1 mM GDP y 3 μ M de CCCP.

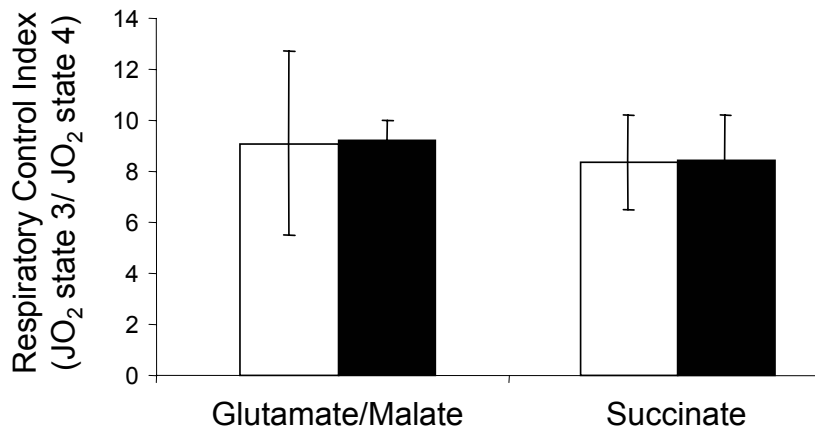
Figura 2

□ AdCMV-LacZ
■ AdCMV-UCP3

A



B



C

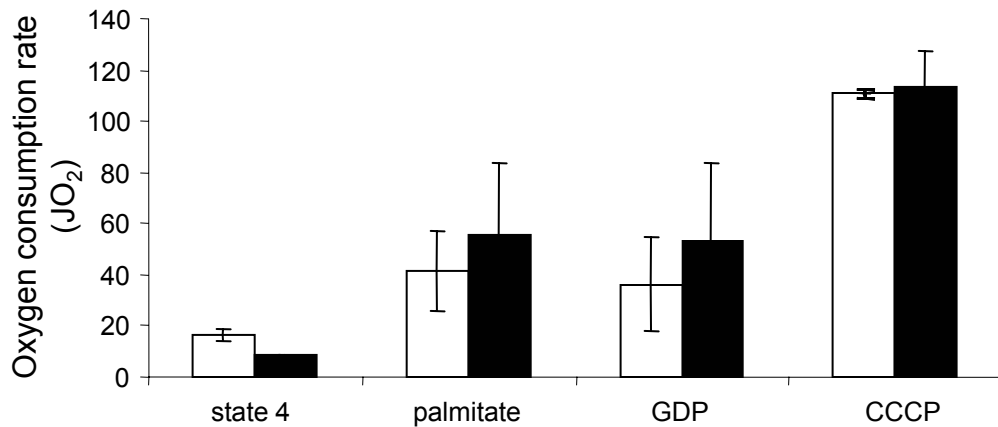
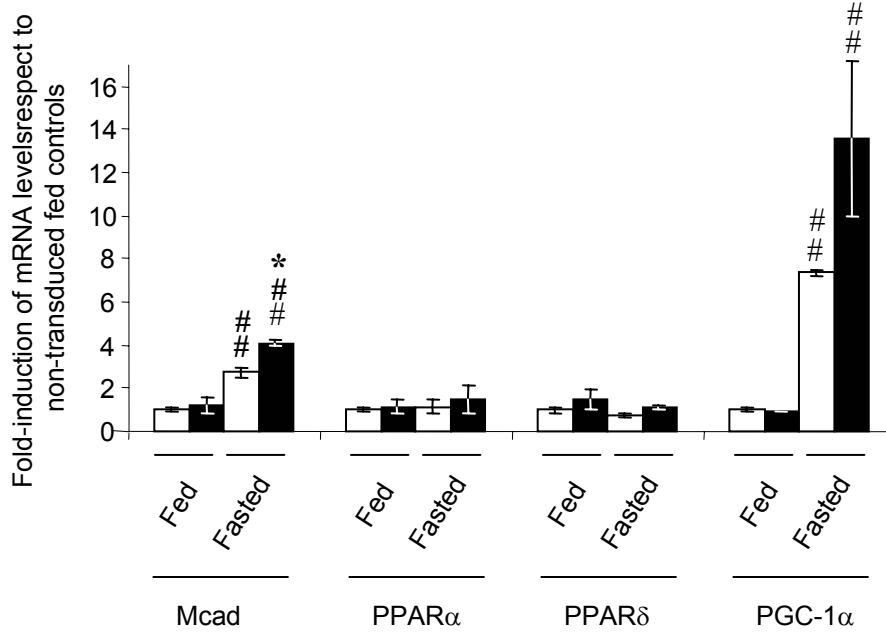


Figure 3: Efecto de UCP3 sobre la expresión de genes relacionados con estrés celular y metabolismo lipídico en el hígado. Ratones C57Bl6/J fueron inyectados con un vector adenovírico que induce la expresión de la β -galactosidasa (AdCMV-LacZ) o de UCP3 (AdCMV-LacZ). Un grupo de los ratones inyectados se mantuvo ayunado (fasted) durante las 36 h previas al sacrificio. 72 h después de la inyección se sacrificaron los animales y se obtuvo el RNA total del hígado. Se cuantificó la expresión de los genes indicados mediante *Real-time* PCR. **A.** Análisis cuantitativo de genes implicados en el metabolismo hepático **B.** Análisis cuantitativo de genes relacionados con estrés celular. Los resultados representan las veces de inducción/represión de un determinado mRNA en un grupo experimental, respecto al nivel de dicho mRNA en ratones transducidos con el AdCMV-LacZ. Las diferencias significativas debidas a la presencia de UCP3 se muestran como * $p < 0,05$. Las diferencias significativas debidas al ayuno se muestran como # $p < 0,05$ o ## $p < 0,01$.

Figura 3

AdCMV-LacZ
AdCMV-UCP3

A



B

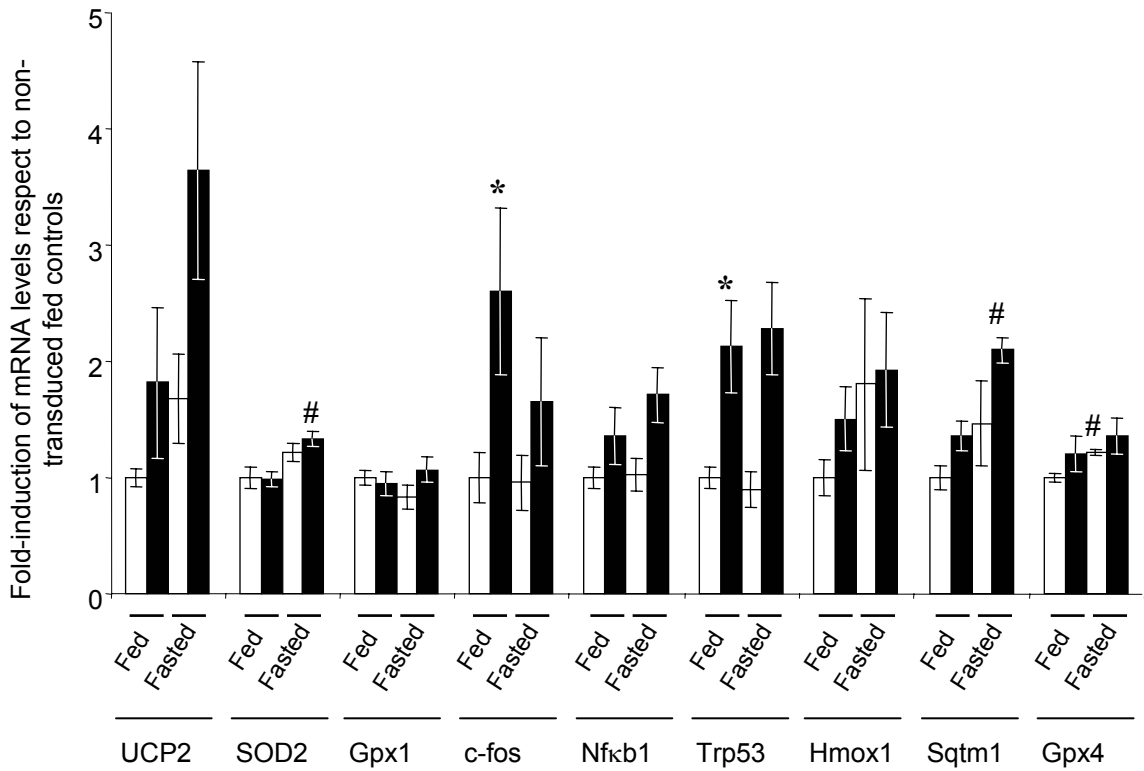
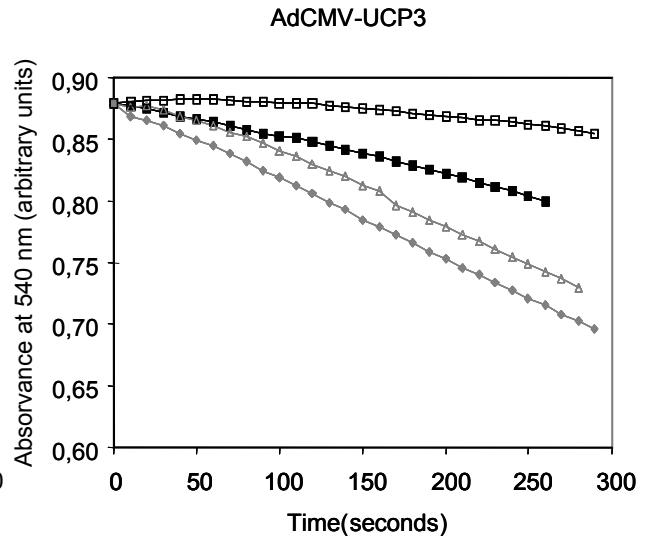
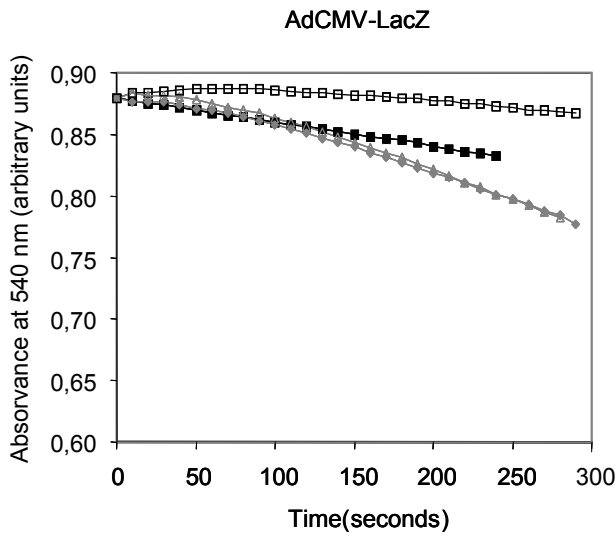


Figure 4: Efecto de UCP3 sobre la apertura del MPTP. Mitocondrias aisladas del hígado de ratones inyectados con vectores adenovíricos para la expresión de la β -galactosidasa (AdCMV-LacZ) o de UCP3 (AdCMV-UCP3), fueron analizadas para determinar el nivel de *swelling* mitocondrial en respuesta a diferentes compuestos. En la figura se muestra un ejemplo de un ensayo en el que se valoró el descenso en la absorbancia a 540 nm y 25°C de las soluciones mitocondriales, tras la adición de las concentraciones indicadas de **A.** CaCl_2 y **B.** Atractilato. La CsA se añadió dónde se indica, a una concentración de 5 μM , 2 minutos antes de iniciarse la lectura.

Figura 4

A

- Control
- △ 100 μM CaCl_2
- ◆ 200 μM CaCl_2
- 200 μM CaCl_2 + CsA



B

- Control
- × 150 μM Atractylate
- 300 μM Atractylate

